Aalborg Universitet

Wind Farms: Modeling and Control

Soleimanzadeh, Maryam

Publication date:
2012

Document Version
Early version, also known as pre-print

[Link to publication from Aalborg University](#)

Citation for published version (APA):
Soleimanzadeh, M. (2012). Wind Farms: Modeling and Control.

Maryam Soleimanzadeh

Wind Farms:
Modeling and Control

Wind Farms: Modeling and Control
Ph.D. thesis

Contents

CONTENTS

Paper C: An Optimization Framework for Load and Power Distribution in Wind Farms   79

Paper D: A distributed optimization framework for wind farms   97

Preface and Acknowledgements

This thesis is submitted as a collection of papers in partial fulfillment of the requirements for a Doctor of Philosophy in Automation and Control at Department of Electronic Systems, Aalborg University, Denmark. The work has been carried out in the period from November 2008 to November 2011 under supervision of Professor Rafael Wisniewski.

During the last three years, I had the pleasure to work at Automation and Control section with very nice and supportive colleagues, and I want to thank all of them. Foremost, I would like to express my gratitude to my supervisor Professor Rafael Wisniewski not only for being my advisor, but also for being a good teacher and a nice friend. His patience, motivation and his support during this period is greatly appreciated.

I also like to extend my thanks to staff at Energy Research Center of the Netherlands, especially Arno J. Brand, Stoyan Kanev, Huseyin Ozdemir and the others for being extremely helpful during my half a year stay at their research center. I also want to thank Justin Rice and Jan-willem van Wingerden for their great help on my last work.

My deepest thanks go to my family; I appreciate my parents sending me inspiration half way across the world, and I am grateful of my husband Mojtaba, whose love and encouragement has been my greatest strength. Thank you very much.

Abstract

The primary purpose of this work is to develop control algorithms for wind farms to optimize the power production and augment the lifetime of wind turbines in wind farms.

In this regard, a dynamical model for wind farms was required to be the basis of the controller design. In the first stage, a dynamical model has been developed for the wind flow in wind farms. The model is based on the spatial discretization of the linearized Navier-Stokes equation combined with the vortex cylinder theory. The spatial discretization of the model is performed using the Finite Difference Method (FDM), which provides the state space form of the dynamic wind farm model. The model provides an approximation of the behavior of the flow in wind farms, and obtains the wind speed in the vicinity of each wind turbine.

The control algorithms in this work are mostly on the basis of the developed wind farm model. The wind farm control algorithms provide reference signals for the controller of each wind turbine as commands. The reference signals are provided such that the demanded power from the whole farm is satisfied and also the structural loads on wind turbines are minimized. Three different control strategies have been addressed in this work, two centralized controller with two different strategies and one distributed controller. In the fist strategy for centralized control, the reference signal is determined for individual wind turbines such that the load acting on wind turbines in low frequencies is minimized. The controller is practically feasible. Yet, the results on load reduction in this approach are not very significant.

In the second strategy, the wind farm control problem has been divided into below rated and above rated wind speed conditions. In the above rated wind speed pitch angle and power reference signals are provided by the wind farm controller, whereas in below rated, the rotor speed reference signals are determined for maximum power production and load reduction. The structural loads in this strategy are dynamic loads, the tower fore-aft and side-to-side motion of the single wind turbines which change persistently with the wind speed variations. Therefore, the controller has to perform all the computations in a relatively fast sampling rate which makes it difficult to implement practically. However, the controller has a very satisfactory results in terms of covering the required total power and load reduction.

The third approach is distributed control of wind farm using the wind farm intrinsic distributed structure; where, the wind turbines are counted as subsystems of the distributed system. The coupling between the subsystems is the wind flow and the power demand of the wind farm. Distributed controller design commences with formulating the problem, where a structured matrix approach has been put in to practice. Afterwards, an H_2 control problem is implemented to obtain the controller dynamics for a wind farm such that the structural loads on wind turbines are minimized.

Synopsis

Det primære formål med dette arbejde var, at udvikle reguleringsalgoritmer til vindmølleparker. I denne forbindelse var en dynamisk model af vindmølleparken påkrævet, for at muliggøre regulatordesignet. Først blev en dynamisk model udviklet, der beskriver vind dynamik i vindmølleparken. Vindmølleparkmodellen er dannet på basis af en lineariseret Navier-Stokes ligning kombineret med moment teori. Ydermere er Finite Difference Metoden (FDM) blevet benyttet til stedsdiskretisering af ligningerne. Denne model giver en tilnærmet viden om, hvad der sker bag vindmølleparken, og er repræsenteret i form af ordinære differentialligninger, der er anvendt i vindmøllepark-reguleringsalgoritmerne.

De designede reguleringsalgoritmer er baserede på den udviklede vindmøllepark model. Vindmøllepark reguleringen giver referencesignaler til de enkelte vindmøllers regulatorer. Referencesignalerne er udregnet, således den samlede energiproduktion for vindmølleparken er overholdt, mens belastningen på vindmøllerne er minimeret. Der er udviklet tre forskellige reguleringsstrategier, to centraliserede regulatorer og en distribueret regulator.

I den første reguleringsstrategi får vindmølleparkregulatoren en effektreference, og styrer statiske belastninger på vindmøllen. Belastningsreduktionen er dog ikke særlig stor med denne reguleringsstrategi.

I den anden strategi er reguleringsproblemet opdelt i to: under nominel vindhastighed og over nominel vindhastighed. Over nominel vindhastighed er pitchvinklen og effektreferencen givet af vindmølleparkregulatoren. Under nominel vindhastighed sikrer referencen for rotorhastigheden, at energiproduktionen maksimeres, samt at belastningerne reduceres. Belastningerne er her dynamiske belastninger, der oprinder fra sideværts og frem og tilbage bevægelser for de enkelte vindmøller. Regulatoren har vist tilfredsstillende resultater med hensyn til både maksimering af energiproduktionen og reduktion af belastninger. Dog er det er ikke praktisk i nutidens teknologi, at sende andre reference signaler end effektreference.

Den tredje reguleringsstrategi er distribueret regulering af vindmølleparken ved hjælp af en struktureret matrix tilgang. Denne regulering sætter effektreferencesignalerer, og resultater viser en tilfredsstillende belastningsreduktion.

1 | Introduction

One of the most significant current discussions in wind energy production is to reduce the cost of energy and to raise the quality of power. Motivated by this fact, this thesis provides a solution to optimize the power production in wind farms and augment the lifetime of wind turbines in the farm.

In this work we focus on developing optimal control algorithms for wind farms on the basis of a dynamical model for wind flow in the farms. The aim of optimal control methods is to provide the demanded power and reduce the structural loads on the individual turbines in the wind farm.

This chapter describes the background and motivation for developing a dynamical model and control for wind farms, and provides an outline of the state-of-the-art within wind flow models and wind farm control methods.

1.1 Motivation

The existence of wind-mills has been known since thousands of years ago. The first record of using wind-mills as a provider of useful mechanical power, dates back to 3000 years ago in Persia. The Persian wind-mill was a vertical axis turbine illustrated in Figure 1.1. Since then, various types of wind-mills have been invented, and one of the most popular types was the horizontal axis European wind-mills. The European wind-mills were in use for centuries for most of the mechanical task, including water pumping, grinding grain and many others [Spera 94].

The first horizontal axis wind-mill that used for electricity production was constructed in the United states in 1887. It was a 12-kW turbine with 144 blades made of cedar wood, each with a rotating diameter of 17 meters illustrated in Figure 1.2. In Denmark, by 1900, more than 2500 wind turbines were installed with an estimated power capacity of 30 MW. Afterwards, the first modern wind turbine was built in Denmark around 1956 named Gedser turbine, shown in Figure 1.3a.

Nowadays, mostly wind turbines are installed in groups to form small or large wind farms. Grouping the turbines help to save the space and reduce the cost of installation and maintenance. However, the wake interaction between upstream and downstream wind turbines decreases the total produced power in compare to an equal number of stand-alone turbines [Pao 09].

In large wind farms, the upwind turbines extract most of the power from wind and increase the turbulence intensity in the wake reaching other turbines. Thus, the fluctuations and vibrations of the downwind turbines are greater than upwind turbines and results in
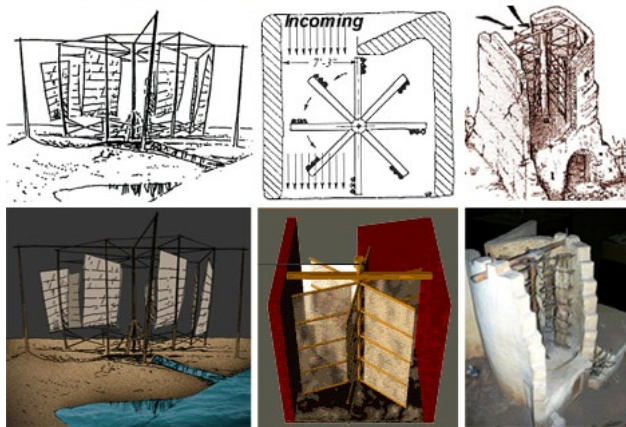
Figure 1.1: Persian vertical-axis wind-mill, 3000 years ago
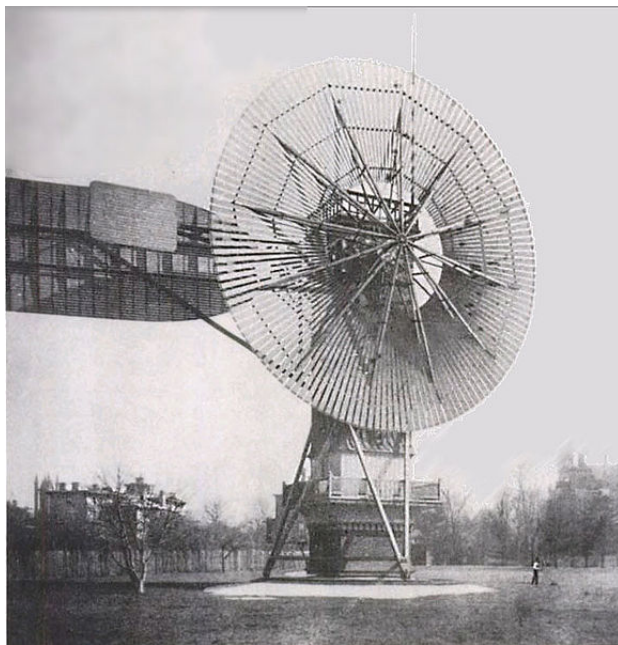
Figure 1.2: The first electricity-producing wind turbine, 1887

(a) Gedser turbine 1956   (b) A 2MW wind turbine
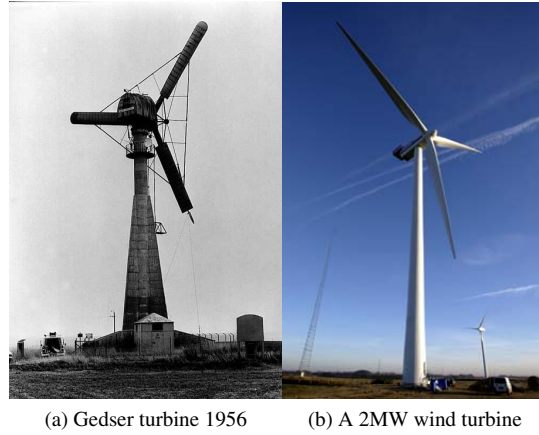
Figure 1.3: First Modern wind turbine in 1956 and a 2MW wind turbine

Figure 1.4: The wake of upwind turbines on downwind turbines in HornsRev wind farm.

more fatigue loads on them [Adams 96]. Therefore, the lifetimes of turbines that most frequently are in the downwind location are shortest, which results in reduction of the effective lifetime of the whole farm.

Design of controllers for wind farms presents a challenge to prognosticate the effect of the wake formed behind a wind turbine on the other wind turbines. This challenge originates in the significant decrement in mean wind speed reaching downwind turbines, and the increment in turbulence which has been shown in a picture (Figure 1.4) from Horns-Rev wind farm. Considering this fact that by changing the power demand of a wind turbine, the generated wake of the turbine can be modified, the power reference signal for each wind turbine is chosen as the control command. Even tough the wakes can also be affected by changing the pitch angle or rotor speed of a turbine, mostly in wind farm controller design, the control input is the power set point of the individual turbines.

In this regard, the focus of this thesis is to develop wind farm controllers, which improve the power set-point distribution among wind turbines and control the structural loads to optimize the energy production. To reach these goals, a wind farm flow model that can be used in control methods is an imperative requirement [Fernandez 09,

Rethore 07]. Thus, the first aim of the work is to establish a dynamical model for the wind farm. Afterwards, wind farm control algorithms are developed on the basis of the dynamical model.

1.2   State of the Art and Background

Wind energy is one way of electrical generation from renewable sources that uses wind turbines to convert the energy contained in flowing air into electrical energy. Wind power is a very fast growing energy source, this growth has been achieved by concentrating a large number of wind turbines in wind farms for a better utilization of regions with good wind resources. As a result of increasing wind farms penetration in power systems, development of accurate wind farms models to improve the planning and their exploitation is a requirement. The recent development of large wind farms has initiated the development of advanced, automatic wind farm controllers. A wind farm controller has access to extensive information from the controllers of the individual wind turbines. Moreover, the farm controller is provided with the information from the wind flow model of the entire farm. This information could be used by the wind farm controller to adjust the power reference for each wind turbine. In this regard, the controller may consider other vital parameters like structural loads on the turbines to increase the farm efficiency and the life time of the wind turbines.

 This section expounds the state of the art of wind flow models in wind farms and also the wind farm control methods. The emphasis in this section is on the dynamical models that provide information to be used in wind farm controller design.

Wind farm model

The penetration of wind energy into the power networks is more and more increasing, and wind turbine farms with hundreds of MW capacity are being built all over the world. Therefore the power networks are being more dependent on, and vulnerable to, the wind and wind turbine sites [Hansen 02]. Thus, the wind farms in the power networks should be controllable, and in this regard, it is necessary to know the dynamic characteristics and the interactions of wind turbines in the farms.

 Deriving a proper wind farm model including wind speed model for a wind farm location is a complicated process. Regarding modeling the wind speed, in some research papers the model consists of two elements: a slowly varying mean wind speed of hourly average and a rapidly varying turbulence component, where mean wind speed is considered constant throughout the observation period. The component is modeled by a normal distribution with a null mean value and a standard deviation that is proportional to the current value of the mean wind speed [Suvire 08, Nichita 02].

 [Crespo 99] has conducted a thorough review on wind farm and wind turbine wake models up to year 1999. One of the approaches to the problem of modeling wind farms addressed in [Crespo 99], assumes that when an area contains a large number of wind turbines, they play a role as distributed roughness elements, so the ambient atmospheric flow will be modified. An important issue in wind farm modeling is the interaction of several wakes and the way in which the velocity deficits and turbulence created by each machine accumulate at locations where several wakes meet [Crespo 99]. Furthermore, some engineering models presently applied for calculating production losses due to wake

effects from neighboring wind turbines are based on the local momentum equations, disregarding the interaction with the atmosphere.

A large and growing body of literature has modeled wind farms with either the purpose of farm layout optimization [Ozturk 04, Lackner 07, Elkinton 08], or power quality improvement [Akhmatov 03, Kazachkov 03, Trujillo 07, Rodriguez-Amenedo 08].

A common wind speed model for modeling wind farms, uses time-series auto regressive and moving average model. The method requires actual hourly wind speed data collected over a long period of time for the particular geographic location to construct a wind speed simulation model for the specific site [Billinton 96]. This model can reflect the true probabilistic characteristics of wind speed for the wind farm [Karki 06]. Another way of modeling wind flow in wind farms is derived based on the quasi-steady wake deficits computed in a loop involving coupling between an actuator disc model of the rotor-wake interaction and an aeroelastic model [Larsen 08]. In most of these models computational resources and the approximation of the behavior of the wind farm is not good enough [Suvire 08].

In another major study of modeling a wind farm, a detailed model of each wind turbine dynamic and the internal electrical network is developed. In this class, the model depends on the type of the wind turbines, some of the models can be found in [Slootweg 03, Fernandez 06].

Another option is to apply computational fluid dynamics (CFD) schemes, but these methods are computationally expensive. Moreover, because of the gap between engineering analytical methods and CFD models, a connection with detailed information should be developed for better wind farm and turbine design and for more efficient control strategies [Barthelmie 07]. One of the engineering analytical methods is carried out by [Frandsen 06], and is applied to calculate production losses based on conservation of the momentum deficit in the wake.

However, far too little attention has been paid to developing dynamic wind flow model for wind farms, to be implemented in the classic control algorithms. In this thesis a spatial dynamic model for wind flow in wind farms is developed, and presented in the form of ordinary differential equations (ODE).

In this method, like many other studies on wakes, we have made a division between near and far wake regions. The near wake is taken as the region just behind the rotor, where the effect of the rotor is dominant [Vermeer 03]. In the near wake region there is an intense turbulence generated by the blades, shear, and the degradation of tip vortices. The far wake is the region beyond the near wake. The objective of most models in the far wake region is to evaluate the influence of wind turbines on each other in farms [Kasmi 08]. Our approach is considered to be in this region.

In the far wake region, in the hypothetical absence of ambient shear flow, it may be assumed that the perturbation profile of velocity deficit is axis-symmetric. The only overall property of the turbines that appear as parameters in this profile is the thrust on the turbine [Crespo 99, Ainslie 88]. Hence, the flow equation for the whole wind farm is explained with Navier-Stokes equations and is solved for laminar flow. The methodology of the derivation of the model and verifications is explained in Section 2.1. The model computes the mean wind speed all over the farm, as well as in the vicinity of each wind turbine.

A quasi-steady model developed in [Brand 10] also computes the mean wind speed at the place of each wind turbine. A thorough comparison between the quasi-steady model
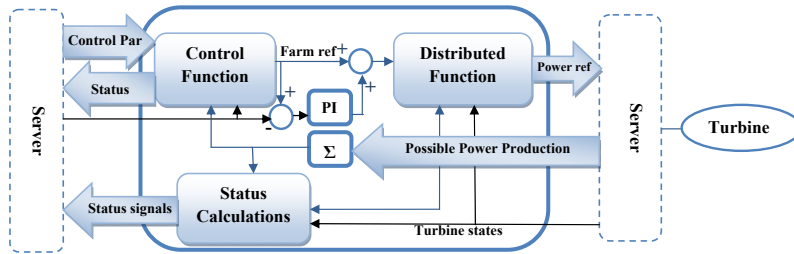
Figure 1.5: The control block digram of the Horns Rev wind farm [Kristoffersen 03]

and the wind farm model developed in this thesis has been presented in [Brand 11] which we summarize in the following.

The quasi-steady model is based on the classic momentum theory, and the dynamic model is based on linearized Navier-Stokes equations combined with a vortex cylinder model. Moreover, The quasi-steady model relates the external conditions (the wind speed, the wind direction and the turbulence intensity) of a wind farm to the state (the rotor speed and the blade pitch angle) and the output (the aerodynamic power and the mechanical loading) of all wind turbines in the wind farm, provided the yaw misalignment of the wind turbines is small. Whereas, the dynamic model relates the external conditions (the wind speed and the wind direction) of a wind farm to the state (the rotor speed and the blade pitch angle) of all wind turbines in the wind farm, while it considers the yaw angle of the wind turbines. Furthermore, the quasi-steady model can be operated either to calculate the state of all turbines needed to track a given output for given external conditions, or to predict the output of a wind farm for given external conditions. While, the dynamic model provides a structured model suitable for control algorithms, but can only predict the output of a wind farm if the turbulence intensity is low [Brand 11].

Wind farm control

Wind farms are developed to reduce the cost of wind energy produced by stand alone wind turbines [Johnson 09]. Since extracting maximum power from each wind turbine does not always result in maximal power for the entire farm, wind farm controllers need to be developed [Pao 09]. The main goal of many wind farm controllers is to make the wind farm act as a single unit instead of several individual production systems, alike Horns Rev wind farm controller. The Horns Rev wind farm is established in 2002 off the Danish coast with 80 wind turbines and total installed capacity of 160 MW [Kristoffersen 03]. A block diagram of the control approach of the Horns Rev wind farm is illustrated in Figure 1.5. The Control Functions block provides the power reference for the wind farm. The wind farm power reference is converted to power set points for the individual turbines considering their power capability and state, in the Distribution Function block [Kristoffersen 03].

Two control strategies for wind farms have been introduced by [Spruce 93] as hierarchical control and multivariable control. The so-called multivariable control, is a centralized control strategy that controls all the wind turbines dynamically. This controller gets the inputs from all the wind turbines and also the ambient flow model or measurements and sends the outputs to all the wind turbines. The hierarchical control has a plant control

and supervisory control level, and the supervisory control provides the reference signals for the plant in steady state. An archetype of this class is [Spudic 10], which provides a two level control approach. At one level, a receding horizon controller that works offline, obtains the optimal operating points for wind turbines in a relatively slow sampling rate. The next level of control reacts to disturbances, and adjusts the operating points to meet the power demand at a relatively fast sampling rate.

Another classification of wind farm control strategies is based on the control objective, which is either control of the power produced by the wind turbines, or the coordinated control of power of the farm to minimize the aerodynamic interaction between wind turbines [Pao 09]. There are numerous research in developing controllers that mostly deal with the individual wind turbine controller to maximize power. An overall wind farm control that maximizes energy capture has been proposed in [Steinbuch 88]. In his work, the wind farm controller modifies the tip speed ratios of the individual wind turbines to increase the power production. Moreover, [Spruce 93] aimed to maximize the output power while minimizing fatigue damage of the mechanical components such as drive trains.

In addition, there are many research in wind farm control that mostly consider the electrical interconnections rather than aerodynamic interaction [Pao 09]. For instance, [Zhao 06] proposed an optimization method to maximize the capacity of farms based on the limitations of the physical system such as voltage, voltage stability, generator power. Moreover, advanced controllers for wind farm electrical systems have been developed in [Fernandez 08b, Rodriguez-Amenedo 08]. The focus of [Rodriguez-Amenedo 08] is the coordinated control of wind farms in three control levels: central control, wind farm control, and individual turbine control. A comparison of three control strategies for control of active and reactive power is provided in [Fernandez 08a]. Additionally, [Sørensen 04, Hansen 06] have presented a concept with both centralized control and control for each individual wind turbine. In their approach, the controllers at turbine level ensure that relevant reference commands provided by the centralized controller are followed.

Notwithstanding all these control methods and many research efforts on fatigue load reduction on single turbines [van der Hooft 03, Lescher 07, Sutherland 00, Hammerum 07], results on the combined optimization of power and fatigue load are still lacking.

Some of the most recent efforts in developing wind farm controllers are [Madjidian 11, Soleimanzadeh 11c, Soleimanzadeh 11b, Spudic 11, Soleimanzadeh 12c], with the main purpose of reducing fatigue loads in the wind farms. The main focus have been on the power reference determination that indirectly has effect on the pitch control systems of the single turbines and will lead to a partial load reduction.

Summary

Contemplating the growing body of literature on wind farm modeling and control, there is still much work ahead developing methods which are more efficient and economic. In this regard, this thesis tries to fulfill a few gaps in the field of modeling and control of wind farms to bring us one step closer to the most apt automated control methodologies for this green application.

1.3   Outline of the Thesis

The remainder of the thesis explains the wind farm modeling and control methods. In the next chapter, the basic methodologies and prerequisite concepts are described. In Chapter 4, the outcome of the work is discussed and the ideas for future works are explained in details.

The addendum of the thesis is a collection of the most important publications, published in or submitted to ISI journals, and are listed in the following respectively.

- **Paper A** [Soleimanzadeh 12a]

  Presents a dynamical model for the wind flow in a wind farm. The model provides an approximation of the behavior of the flow in the wind farm, and obtains the wind speed in the vicinity of each wind turbine. The model is based on the spatial discretization of the linearized Navier-Stokes equations combined with the vortex cylinder theory. The spatial discretization of the model is performed using the finite difference method, which provides the state space form of the dynamic wind farm model. The model has been validated using measurement data of EWTW test wind farm in the Netherlands, and employing the outcomes of two other wind flow models. The end goal of this method has been to present the wind farm flow model by ordinary differential equations, to be applied in wind farm control algorithms along with the load and power optimizations.

- **Paper B** [Soleimanzadeh 11c]

  Presents a wind farm controller that dispatches the power references among wind turbines while it reduces the structural loads. The control algorithm determines the reference signals for each individual wind turbine controller in two scenarios based on low and high wind speed. In low wind speed, the reference signals for rotor speed are adjusted, taking the trade-off between power maximization and load minimization into account. In high wind speed, the power and pitch reference signals are determined while the structural loads are minimized.

- **Paper C** [Soleimanzadeh 12c]

  Describes a controller for wind farms to optimize load and power distribution. In this regard, the farm controller calculates the power reference signals for individual wind turbine controllers such that, the sum of the power references tracks the demanded power from the wind farm. Moreover, the reference signal is determined to reduce the load acting on wind turbines in low frequencies. Therefore, a trade-off is made for load and power control which is formulated in an optimization problem. Afterwards, the optimization problem for the wind farm modeled as a bilinear control system, has been solved using an approximation method.

- **Paper D** [Soleimanzadeh 12b]

  The wind farm has an intrinsic distributed structure, where wind turbines are counted as subsystems of the distributed system. The coupling between the subsystems is the wind flow and the power reference set-points across the turbines, which are designed to provide the total wind farm power demand. Distributed controller design commences with formulating the problem, where a structured matrix approach has

been put into practice. Finally, an H_2 control design formulation is used to find the control signals for the wind farm to minimize structural loads on the turbine while providing the desired total wind farm power.

2 | Methodology

This thesis uses variety of approaches to model and control of wind farm. In the modeling part, prior to developing the dynamic differential equations, two numerical methods are utilized that will be introduced subsequently. Furthermore, the controllers are developed engaging the information provided by the dynamic models. The controller design methodologies are two different centralized control algorithms and a distributed control approach. A classification of the methods in the modeling and control is provided in Figure 2.1, and a summary of each method is presented in the following.

2.1 Modeling Method

The final goal in the modeling part is to develop a dynamic model in the form of ordinary differential equations (ODEs) to be applied in control algorithms. The starting point is with the governing equation of the wind flow in wind farms which is a partial differential equation (PDE). A PDE expresses a relationship between a function of two or more independent variables and the partial derivatives of the function with respect to the independent variables. Then, the aim is to include the wind turbine dynamics into the PDE to get the farm model, then discretizing it, and finally transferring the equations into the form of ODEs.

Concerning this, the modeling method carries on with discretizing the PDE in space using either finite volume method (FVM) [Soleimanzadeh 10a], or finite difference method (FDM) alike Paper A, Section 2. FVM has been used in the preliminary version of the model in [Soleimanzadeh 10a, Soleimanzadeh 10b], as well as in Paper B. In the preliminary wind flow model, the governing equation of the wind flow has been simplified as much as possible. Therefore, the accuracy of the model in the above mentioned works was imperfect, and in order to improve it the flow equation has been replaced with the nonlinear version, which is the NavierStokes equation for viscose flow. Thereafter, the discretization method is changed to the finite difference method (FDM), which is much faster and converges easier. This method has been used in Paper A, to discretize the nonlinear flow equation. In both versions of the models, the dynamic of wind turbines are included in the equation after the discretization process. Though, the effect of the yaw angle on wakes is only considered in the equations of the final version, and this model ends up to be a much more accurate model than the previous version. In the sequel we continue with a brief introduction of FVM and FDM.
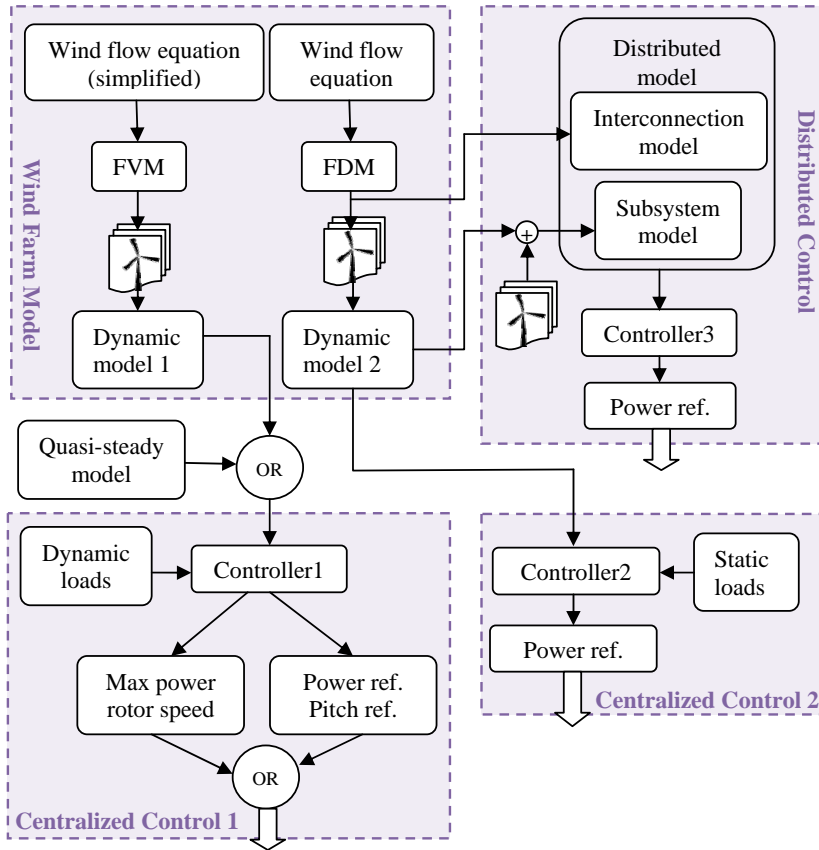
Figure 2.1: Classification of the modeling and control methodologies

Finite volume method

The core of the finite volume method is addressed in this section. The key step of the finite volume method is to divide the domain into discrete control volumes, and then integrating over the control volumes in order to discretize the equations.

In this application, the wind farm is divided into non-overlapping square control volumes, and Fig. 2.2 shows typical meshes for this problem and some indexes for each control volume (CV). The finite volume method is used to transform the flow equation to a system of discrete equations for the nodal values of U. First, the wind flow is integrated over the typical control volume depicted in Fig. 2.2a. Then, each equation is reduced to one involving only first derivatives in space. Afterwards, the first derivatives are replaced with central difference approximations [Versteeg 07].

In finite volume method, equations are integrated twice, once over the control volume and then, over a time interval. However, in this application the integration is just over the control volume, because we want to preserve the time derivative term. Therefore, the discretized equation over space is obtained in the following form.

(a) A control volume   (b) Computational grid
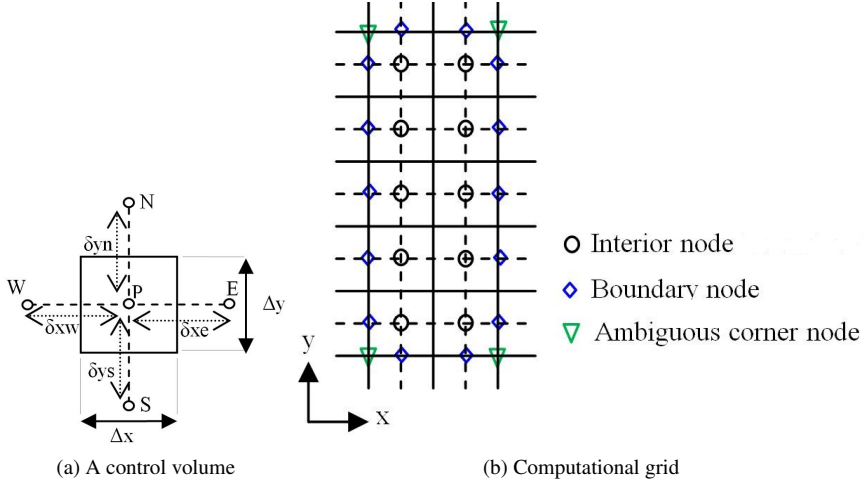
Figure 2.2: Finite volume mesh

$$\rho\frac{\partial U_{P_i}}{\partial t} + a_P U_{P_i} - a_E U_{E_i} - a_W U_{W_i} - a_N U_{N_i} - a_S U_{S_i} = b_i, \qquad (2.1)$$

in which the coefficients a_j, $j = P, E, W, N, S$ are defined in table 2.1.

Coefficients	Description
a_E	$\frac{-\Gamma}{\Delta x \delta xe}$
a_W	$\frac{-\Gamma}{\Delta x \delta xw}$
a_N	$\frac{-\Gamma}{\Delta y \delta yn}$
a_S	$\frac{-\Gamma}{\Delta y \delta ys}$
a_P	$-(a_E + a_W + a_N + a_S)$
b	S_P

Table 2.1: coefficient of the equations

A detail explanation of calculating (2.1) can be found in Paper B and [Soleimanzadeh 10b].

Finite difference method

The finite difference method (FDM) is another numerical procedure that is used in this thesis. This method also solves a partial differential equation (PDE) by discretizing the continuous domain into a discrete finite difference grid. The method approximates the individual partial derivatives in the PDE by algebraic Finite Difference Approximations (FDAs). Then, substituting the FDAs into the PDE, an algebraic finite difference equation (FDE) is obtained [Hoffmann 89].

Three different possibilities for the individual exact partial derivatives are basic. One can choose a forward, or a backward, or a centered difference; however, centered is generally more accurate than one-sided [Strang 07]. Suppose that we wish to approximate the first derivative of a function y at some point a, and assume that h is a small positive number. Where, the centered difference, forward difference, and backward difference formulas are respectively given as follows:

$$f'(a) \approx \frac{f(a+h) - f(a-h)}{2h},$$
$$f'(a) \approx \frac{f(a+h) - f(a)}{h},$$
$$f'(a) \approx \frac{f(a) - f(a-h)}{h}. \tag{2.2}$$

For second derivatives, second-order approximation is used.

$$f''(a) \approx \frac{f(a-h) - 2f(a) + f(a+h)}{h^2}. \tag{2.3}$$

The application of this method on wind farm is explained extensively in Paper A, Section 2.

To sum up, a comparison between the two methods is provided in here. The FVM is based upon an integral formulation of the governing equations, while FDM is on the basis of a differential formulation of the governing equations. The values of the conserved variables in FVM are located within the volume, which we term as cell. A value U is assigned to the cell centroid, which represents average of the variable u over the whole volume. In FDM, the concentration is on one point in space and the changes in the values of this point due to neighboring points in space. FVM works better for unstructured meshes, which is not applicable to this thesis; while in staggered grids FDM works as good as a FVM. Moreover, FDM is very easy to implement.

It should be noticed that the above mentioned methods are applied to discretize the wind flow equation which obtains a free space wind speed model, and does not include the wind turbines effect yet. Adding the wind turbine wake interactions, ends up with the total wind farm model which is explained in the following section.

Wind Farm Model

This section explains how to obtain the wind farm model from the discretized flow equations derived in the previous devision. The final goal is to model the effect of the wind turbines wake in the farm, and the basic idea originates from the momentum theory and its combination with the discretized NavierStokes equation from FVM or FDM.

In the preliminary version of the model in [Soleimanzadeh 10a, Soleimanzadeh 10b] and also in Paper B, the actuator disc approach has been used to model the effect of wind turbine on wind flow. It has been assumed that the wind direction is perpendicular to the wind turbine rotor plain which is equivalent to having zero yaw angle. Therefore, the actuator disc approach has been used based on Figure 2.3 as in [Bianchi 06].
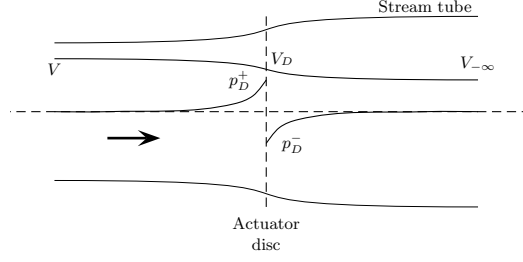
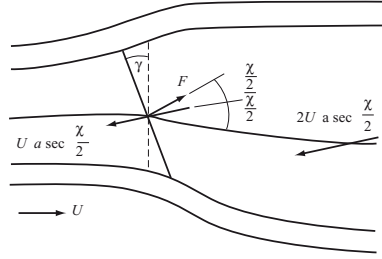Figure 2.3: The actuator disc approach, $p_D^+ - p_D^- = \frac{1}{2}(V^2 - V_{-\infty}^2)$ [Bianchi 06]

Figure 2.4: The actuator disc approach, $p_D^+ - p_D^- = \frac{1}{2}\rho V_{-\infty}^2 [4a(cos\gamma + sin\gamma tan\frac{\chi}{2} - asec^2\frac{\chi}{2})]$ [Burton 01]

The most advanced model in Paper A, uses the momentum theory for a turbine rotor in steady yaw based on Figure 2.4 as in [Burton 01]. In this approach the effect of the turbine rotor yaw angle on the wake behind the wind turbine has been taken into account.

Considering the drop pressure on all the wind turbines in the farm, and including it in the pressure term of the NavierStokes equations the wind farm model is obtained. As mentioned previously, the whole idea was to derive the model in the form of state space equations to be used in developing control algorithms, and the consequent model is in the following form (see Paper A, Section 2).

$$\dot{x}(t) = Ax(t) + Bu(t) + \sum_{j=1}^{n}(x(t)N_j)u(t), \qquad (2.4)$$

with $A \in \mathbb{R}^{n \times n}$, $B, N \in \mathbb{R}^{n \times m}$. Moreover, n is the number of states equal to the number of cells, and m is the number of wind turbines equal to the number of control inputs.

Solving the dynamic equation of the wind farm model (2.4) for appropriate initial conditions, yields to the map of pressure and velocity of the wind farm. In a simulation using Fluent software, the map of velocity vector field is obtained for a small wind farm containing 5 wind turbines. Furthermore, the wind direction is considered to be parallel to the row of wind turbines to produce the maximum wake interaction. Figure2.5 illustrates the wind velocity vector field in the wind farm obtained from solving the dynamic model of the farm.
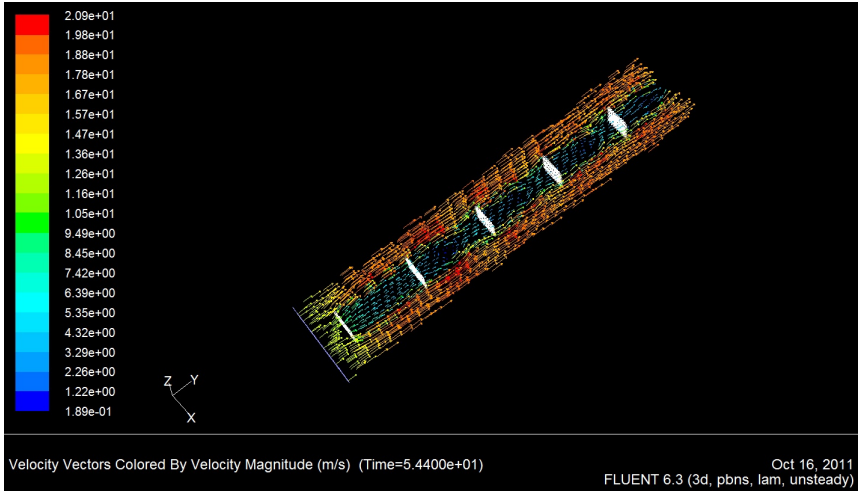
Figure 2.5: velocity vector map

| (a) Wind speed 20 m/s | (b) Wind speed 9 m/s |
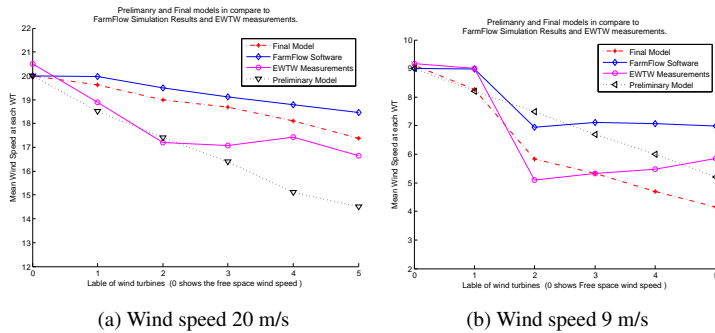
Figure 2.6: Comparing the preliminary and final model with EWTW measurements and FarmFlow software results for a small wind farm with 5 Wind turbines

Furthermore, the accuracy of the preliminary model (obtained from diffusion equation and the FVM) in compare to the final model (developed from the convection-diffusion equation and the FDM) are illustrated in 2.6a and 2.6b. In this Figure the results are also compared to measurement data from ECNs Wind turbine Test site Wieringermeer (EWTW) as well as FARMFLOW software calculations [Eecen 10]. As it can be seen in the figure, the results of the final model are more accurate and closer to measurement data.

2.2 Control Method

In this section a brief overview of the wind farm control approaches is presented. The main purpose of developing wind farm controllers in this effort is to produce required

power while reducing structural loads on individual wind turbines to increase the life time of the farm. The focus is to determine reference signals for wind turbine controllers that indirectly has effect on the partial load reduction of downstream turbines.

As noted, there are two different wind farm control strategies lined up in [Spruce 93]. First one is a hierarchical control explained in Section 1.2, and the other one is a centralized control strategy that controls all the wind turbines dynamically. This controller gets the inputs from all the wind turbines and also the ambient flow model or measurements and sends the outputs to all the wind turbines. Considering this classification, centralized control methods in this thesis will be addressed subsequently. The methods are introduced comprehensively in the addendum, in Paper B [Soleimanzadeh 11c] and Paper C [Soleimanzadeh 12c].

Afterwards, a distributed controller is designed for wind farms using a structured matrix approach. This approach reduces the computation time of the optimal controller for wind farms. A meticulous explanation of this method is presented in Paper D.

Dynamic control of wind farm

The control strategy is to consider the wind farm control problem separately for low and high wind speed. In the above rated wind speed, the farm controller provides power reference and pitch angle reference signals for each individual wind turbine controller. In below rated wind speed, the farm control has two alternatives. First one is tracking the demanded power when it is less than the available power of all the farm; and second one is to extract maximum possible power from each wind turbine. If the demanded power from the farm is less than the available power, the strategy is similar to the one in high wind speed that wind turbine controllers should track the power reference and pitch reference signals provided by the wind farm controller. Providing the reference signals is such that the total required power from the farm is tracked and structural loads on each wind turbine is minimized [Soleimanzadeh 11b].

A challenge in the controller design for wind farms is to find a model to prognosticate the effect of the wake formed behind a wind turbine on the other wind turbines. Two wind farm model are used for the basis of this control method. One is the dynamic model developed in this thesis (see section 2.1), and the other one is a quasi-steady model developed in [Brand 10]. A description of the two models including the methodologies, validation results and a comparison between them has been presented in [Brand 11]. A brief comparison between the two models has been pointed out in Section 1.2.

Control design based on the dynamic farm model

The dynamic wind flow model in the wind farm does not directly provide information on load distribution. In order to reduce the structural loads on the wind turbines, when the controller is designed on the basis of this model, the fluctuations of the wind turbines towers are minimized. Reducing the fore-aft and side-to-side fluctuations of tower, will significantly reduce fatigue loads. The reason for this selection is that the tower fore-aft motion is strongly coupled with the blade flap motion. Moreover, the tower side-to-side motion is strongly coupled with the blade edge and drive train torsion [Suryanarayanan 07]. The tower motion dynamics is approximated by a second order system of differential equations, assuming that there is no coupling between tower fore-aft and tower side-to-

side dynamics [van der Hooft 03].

$$M \times \begin{bmatrix} 1 & 0 \\ 0 & 1 \end{bmatrix} \begin{bmatrix} \ddot{x}_{FA} \\ \ddot{x}_{SS} \end{bmatrix} + D_p \times \begin{bmatrix} 1 & 0 \\ 0 & 1 \end{bmatrix} \begin{bmatrix} \dot{x}_{FA} \\ \dot{x}_{SS} \end{bmatrix} + K \times \begin{bmatrix} 1 & 0 \\ 0 & 1 \end{bmatrix} \begin{bmatrix} x_{FA} \\ x_{SS} \end{bmatrix} = \begin{bmatrix} F_T \\ f_t \end{bmatrix}, \quad (2.5)$$

where x_{FA} is the tower fore-aft displacement and x_{SS} is the tower side-to-side displacement. M, D_p and K are the mass, damping and stiffness. $F_T(.,.)$ and $f_t(.,.)$ are respectively the thrust force and the tangential force. Afterwards, the optimal controller is designed to maximize the damping factor in the differential equations [Soleimanzadeh 11b, Soleimanzadeh 11c].

Therefore, in this strategy the optimal control problem is to minimize two cost function, each for below and above rated wind speed, subject to the constraints from the wind farm model. The cost functions can be expressed as flows:

> Cost function in above rated wind speed:
>
> (Power set-point determination terms) + (Dynamic loads on each WT)
>
> Subject to:
>
> Summation of power set-points = Demanded power from the farm,
>
> Satisfying wind speed and power set-point constraints,

and

> Cost function in below rated wind speed:
>
> (Power set-point determination terms) + (Dynamic loads on each WT)
>
> Subject to:
>
> Summation of power set-points should be maximized,
>
> Satisfying wind speed and power set-point constraints.

The equations corresponding to the above mentioned simplifications are 6.36 and 6.37 in Paper B.

Control design based on the quasi-steady farm model

Designing the wind farm based on the information from the quasi-steady model, has the advantage that the load calculations are involved in the model derivation [Brand 11]. The quasi-steady farm model delivers the maps of wind, loads and energy in the wind farm. Moreover, the model uses the wind direction, mean wind speed and wind speed standard deviation, to calculate the wind speed at the turbines, turbine bending moments, aerodynamic power and torque.

The wind farm controller specifically uses the wind speed calculated near each wind turbine. Wind turbine loading considers tower bending moment and blade bending moment. Blade bending moment originates from the axial force on the rotor blade and tangential force due to gravity. Tower bending moment is the sum of the moments due to aerodynamic force on the rotor, aerodynamic force on the tower, and eccentricity of the nacelle. However, the applied wind turbine model NREL5MW, does not consider the

tower drag and the nacelle eccentricity [Spudic 10]. Therefore, only the bending moment due to the thrust force on the tower, $F_T(C_T, V)$, is considered.

$$M_{tb}(C_T, V) = h\, F_T(C_T, V), \tag{2.6}$$

where h is the tower height and $F_T(C_T, V)$ is the thrust force. Furthermore, effective blade bending moment is modeled as follows [Soleimanzadeh 11a]:

$$M_{bb}^2 = (\frac{1}{9}F_b^2 + \frac{25}{1152}m_{bd}g^2)D^2, \tag{2.7}$$

where m_{bd} is the mass of the blade, g is the acceleration of gravity, and F_b for a 3 blade wind turbine is

$$F_b = \frac{\rho\pi D^4}{12}\frac{\Omega^2 a(1-a)}{\lambda^2}, \tag{2.8}$$

with D being the rotor diameter. Combining (7.9), (2.8) and substituting $\lambda = \Omega R/V$, the effective blade bending moment is

$$M_{bb}(C_T, V) = k_1(V^2 C_T(\beta, \lambda))^2 + k_2, \tag{2.9}$$

where $k_1 = k_{11}/4 = (\pi\rho D^5/108R^2)^2$, $k_2 = 25m_{bd}g^2 D^2/1152$.

The controller design is based on the dynamic farm control strategy, which considers the problem separately for low and high wind speed, and minimizes the loads corresponding to change in wind speed. In other words, the wind farm controller computes required reference signals for each wind turbine controller, minimizing the blade and tower bending moments in a relatively fast sampling rate [Soleimanzadeh 11a].

Summary

The dynamic control strategy for wind farm has been briefly described in this section, independently on the basis of two different model. This approach, deals with the dynamic loads of wind turbines while performing all the calculations in the scale of the wind farm. Moreover, since the loads fluctuates with changing the wind speed, the reference signal calculations should be as fast as changes in dynamic load. Therefore, practical implementation of this strategy on a wind farm requires an extremely fast computer.

The outcome of implementing the controller on two wind farms with 5 and 15 wind turbines, on the basis of two different model for the wind flow and loads, is similar to each other. In both cases presented in [Soleimanzadeh 11c, Soleimanzadeh 11a], the load reduction on single turbines is considerable, specially in high wind speeds. In addition, simulations for both cases shows that by extracting less than maximum available power from the upstream wind turbines, produced power by downstream wind turbines will increase. The results in high wind speed region is more effectual.

This control strategy is presented thoroughly in Paper B, Section 3.

Static control of wind farm

The control strategy is to provide power reference signals for the individual turbines in the farm while minimizing the static loads. The power reference determination is such
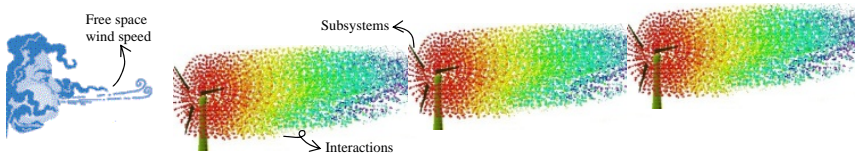
Figure 2.7: Subsystems and the interconnections between them in the distributed structure

that the summation of the power references follow the demanded power by the wind farm operator. At the same time, the optimal control approach tries to minimize the structural loads at low frequency.

The structural loads considered in this approach are the tower and blade bending moments presented in (2.6) and (2.7). They are considered as a static part plus a dynamic part, where the dynamic part is small and changes with a higher frequency (proportional to the wind speed variation). This approach aims to minimize the static parts, which are obtained by sending the equations through either low- pass or band-pass filters. The tower bending moment passes through a simple recursive low-pass filter with the corner frequency of $0.3\ Hz$. Moreover, the blade bending moment passes through a band-pass filter with a center frequency of $0.6\ Hz$ (based on NREL 5MW wind turbine data [Jonkman 09]).

Finally, the optimal control problem has been solved using Model Predictive Control toolbox, and the results comply with the previous method. In which, if we extract less power from the first wind turbine of the row, we will be able to extract more power from downstream turbines such that the total produced power is equal to the demanded power and the structural loads on the turbines will be reduced.

This approach considers the load control problem in the scale of the farm, where computing loads in a slower rate is much more practical (in compare to the previous approach). However, since the loads are considered in low frequencies, and the effect of static loads on fatigue is very small, the results on load reduction are not very significant. This work is explained in more details in Paper C [Soleimanzadeh 12c].

Distributed control of wind farm

In this approach, we have taken advantage of the intrinsic distributed property of the wind farm. The distributed structure has been depicted in Figure 2.7, and the subsystems and the interaction between them are pointed out.

The free space wind speed is an input to the dynamical model of the wind farm, explained in Section 2.1. Then, the dynamic model attains the average wind speed at the place of each wind turbine. Therefrom, the operating point of each wind turbine on the farm is obtained. Afterwards, the dynamic model of wind turbine is linearized around the operating points, and introduced as dynamic models of subsystems in the distributed structure.

The interaction between the subsystems is the demanded power from the farm and the wind flow. In this approach the interactions are modeled using the convection-diffusion equation for wind flow [Strang 07], and we carry on with the spatial discretization of the equation on a staggered grid over the wind farm. The result is a matrix algebraic equation

that can be find in [Hoffmann 89].

Then, the subsystem model, together with the interaction model are transferred to a particular matrix structured named "Sequentially Semi-Separable matrices" [Rice 10]. This structure simplifies the arithmetics and reduces the computational time significantly [Rice 09]. Therefore, for the large scale system of wind farm this structure is of great importance. Conserving the matrices structure, an H_2 control problem is designed for the wind farm such that the required power from the wind farm is satisfied and the structural loads on wind turbines are minimized. This approach and the results are presented in details in the Appendix, Paper D [Soleimanzadeh 12b].

3 | Summary of Contributions

This chapter aims to underscore the contributions of this thesis. The main contributions are either submitted to, or published in six conference papers and four ISI journal papers which the four journal papers are appended after this introductory part.

3.1 Contributions in the Modeling Method

The major contributions in developing the wind farm model can be categorized as follows:

- Representing the state-state model of the wind flow equation in wind farms.

- Computes the mean wind speed all over the wind farm

State-space model of Wind flow in the farm

The wind farm dynamic model is represented in the form of Ordinary Differential Equations (ODE). This derivation provides the possibility of implementing the classic control algorithms on this application. Furthermore, the system matrix of the model is sparse, and because of the specific structure, it simplifies some of the computations.

Mean wind speed all over the wind farm

Having the wind speed and direction outside the wind farm, the model computes the mean wind speed all over the farm which the wind farm controller utilizes the wind speed at each wind turbine location. Furthermore, the accuracy of the computations is quite comparable to measurement data and the professional software developed by [Eecen 10].

3.2 Contributions in the Control Method

The major contributions in controller design for wind farms are categorized as follows:

- Providing wind farm demanding power by specifying power references to individual wind turbines, while minimizing loads.

- Proposing a solution to reduce the fatigue load problem in wind farms.

- Implementing an structured distributed controller on wind farm for the first time

Providing wind farm demanded power

This thesis is one of the pioneer works of developing controllers for wind farms, with the strategy of minimizing the structural loads effectively by sending power references to individual turbines.

The structural load considered to be minimized are either tower fore-aft and tower side-to-side motion, or tower and blade bending moments. Moreover, the loads are either dynamic or static. Dynamic loads in here are the fluctuations of tower or blade, where they change persistently with the wind speed variation. This class of structural loads are minimized in the optimal control problem, Paper B. The results of load reduction in the farm considering dynamic loads are very satisfactory, however, this controller may not be very easy to be implemented practically. Since, the controller has to perform all the computations in wind farm scale in a relatively fast sampling rate.

In addition, Paper C solves an optimal control problem to minimize structural loads in low frequency. This class of loads are classified as static loads, and their variation rate is relatively slow. Therefore, the computations of the controller do not need to be very fast, and thus, it is easier to implement practically.

A solution to the problem of reduced wind farm lifetime

As pointed out in Section 1.1, turbulent wake causes fatigue load on downstream wind turbines. Moreover, the lifetime of the wind turbines that are most frequently in down-wind locations will be reduced due to fatigue. An objective of this work has been to assign reference signals (e.g. power reference) to individual wind turbines, such that the total produced power tracks the demanded power set-point of the wind farm, while the structural loads on wind turbines are reduced.

A solution to this problem is suggested by the two centralized controllers collectively. The general solution is explained very briefly as follows:

If we extract less than available power from the up-wind turbines, downstream wind turbines will be able to produce more power than before such that the total produced power is equal to the demanded power and the structural loads on the turbines are reduced.

The details of this solution and derivations on different wind speed conditions and power demand from the wind farm, are explained in Paper B (Section 3), and Paper C (Section 5).

Distributed controller on wind farm

A distributed controller has been developed with the aim of load reduction and power reference distribution among wind turbines. In this regard, a structured matrix approach developed by [Rice 09] has been put in to practice for the first time. This structure makes the computations fast, and therefore, it is very convenient for a huge and computational demanding problem like wind farm control. In this controller, we use the intrinsic distributed structure of wind farms which the wind turbines are counted as subsystems of the distributed system, and the wind flow and the power demand of the wind farm are the couplings between the subsystems.

4 | Conclusion

In this work, a dynamic model has been developed for wind flow in wind farms. Afterwards, three control algorithms are designed on the basis of the information that the dynamic model provides.

The wind farm model is a spatial discrete one obtained from the linearized Navier-Stokes equation combined with the momentum theory, and discretized using finite difference method.

The wind farm control algorithms provide reference signals for the controller of each wind turbine of the farm as commands. The reference signals are provided such that the demanded power from the whole farm is satisfied and also the structural load on wind turbines is minimized. Three different control strategies have been addressed in this work, two centralized and one distributed controller. The focus of all the control methods have been on designing the most efficient controllers to increase power production and reduce loads.

In the first centralized control strategy the wind farm controller obtains power setpoints and controls the static loads on the wind turbine. However, since the controller focuses on minimizing the static loads, the results on fatigue load reduction in this approach are not very significant. However, since the controller has compute the reference signals in a relatively slow rate, the controller is easy to implement on a real wind farm.

In the second centralized control strategy, the wind farm control problem has been divided into below rated and above rated wind speed conditions. The reference signals to be computed by the controller are either power and pitch angle set-points or the rotor speed set-points. The controller aims to minimize the dynamic structural loads (tower fluctuations); thus, it has to work in a relatively fast framework (almost as fast as a wind turbine controller). Therefore, implementing this method on a real wind farm may not be very easy. The simulation results of this method on power distribution and also on load reduction are very significant.

The third approach is a distributed control of wind farm using a structured matrix approach. The outcome of the controller in here are the power reference signals and load reduction results are relatively gratifying.

The major contributions of this work are embedded in the addendum.

4.1 Future Work

Several directions for further research are presented in this section. Some of the suggested works are general topics, while some others arise from the papers which have not been
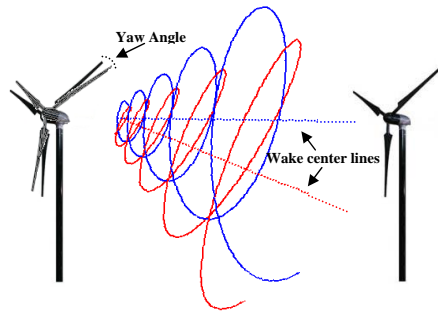
Figure 4.1: Deviating the wind turbine wake, producing extra yaw angle on the rotor plain

covered in this work.

- Wind flow model stability analysis:
  The dynamic model developed for the wind flow in wind farms is a bilinear system. One could investigate the stability analysis of this model using the classic methods by [Benallou 88].

- Solving the ARE with constraints:
  A suggested future effort is considering the constraints on the control input and state variables while solving the Algebraic Riccati Equations (ARE) to obtain the H_2 controller dynamic, in the distributed control method.

- New approaches to increase power production:
  The new approaches to control the wind farm are suggested as follows

  1. Deviating the wake of the upstream turbines by yawing the rotor plane, illustrated in Figure 4.1.
  2. Changing the downstream turbine's rotor rotational direction to comply with rotational direction of the turbulent wake, illustrated in Figure 4.2.

  Subsequently each approach is explained closely.

Wake deviation

When the wind direction is parallel to the rows of wind turbines, maximum wake interaction is produced between turbines (see Figure 1.4). The idea is to reduce the wake interaction with yawing the wind turbines in a row with small yaw angles, using either blade pitch actuators or yaw actuators, as it has suggested in Paper A.

To scrutinize this idea, the wind flow model for wind farms explained in [Soleimanzadeh 11c, Soleimanzadeh 10a] is used. Some of the simulation results of Paper A, for a small wind farm with 5 wind turbines in a row, with a wind direction parallel to the row are used in this section. The wind speed calculated by the model at the place of each wind turbine has been compared with the measurement data from ECNs Wind turbine Test site Wieringermeer (EWTW). At the time of collecting measurement data, some of the wind turbines were yawed.
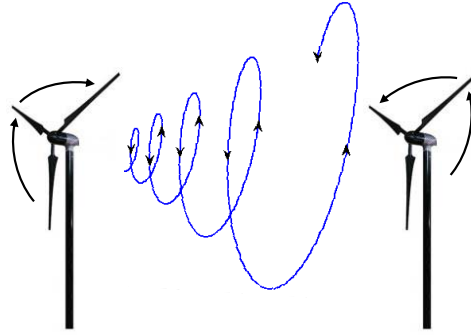
Figure 4.2: Reducing the effect of rotational turbulent wake on downstream wind turbines, by changing the rotor rotational direction

(a) wind speeds 5, 7 m/s at Meteo-Mast
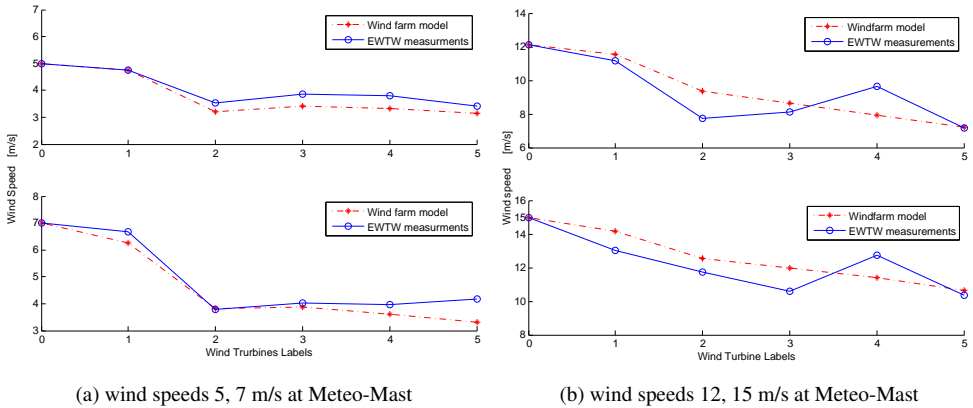
(b) wind speeds 12, 15 m/s at Meteo-Mast

Figure 4.3: Comparing the model results with EWTW measurements (a), (b)

The simulation results in Figures 4.3a and 4.3b are obtained for a wind direction exactly parallel to the wind turbine row and zero yaw angle, $\gamma = 0$. The simulations have been repeated considering the yaw angles, and the results are illustrated in Figure 4.4a and Figure 4.4b. It is seen that, the wind farm model results in compare with the measurement data has been improved, with respect to the results for zero yaw angle.

It is interesting to note that including yaw information has improved the wake deficit effect (i.e. the velocity deficit is became less). Based on these effects, it seems that if the wind direction is parallel to a row of wind turbines (maximum wake interaction), if the wind turbines are yawed with different yaw angles, the velocity deficit will be less than a case in which all the turbines have zero yaw angle. This is equivalent to more power production. However, it may also cause to increase the structural loads.

In order to study this hypothesis, the yawed wind turbines in 5 and 7 m/s are considered, as they have the largest yaw angles. The results depicted in Figure 4.4a shows that the farm model can follow the measurements very closely. Therefrom, if the yaw angle

(a) wind speeds 5, 7 m/s at Meteo-Mast   (b) wind speeds 12, 15 m/s at Meteo-Mast
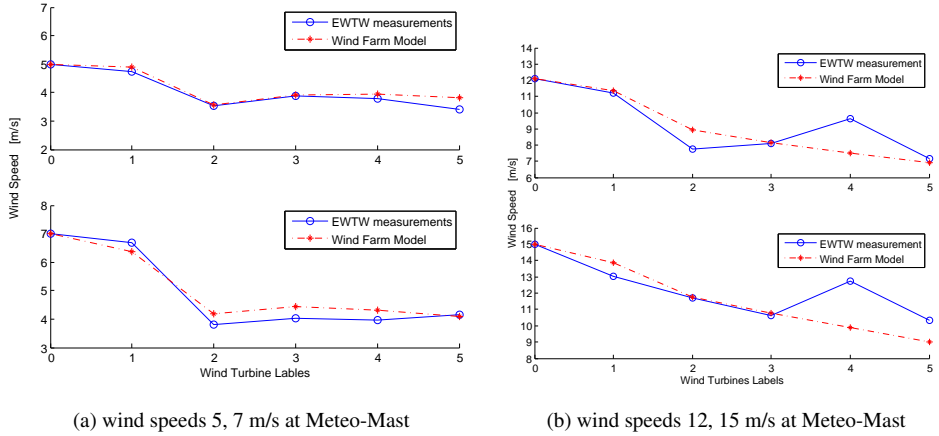
Figure 4.4: Comparing the results with measurements, considering the yaw angle (a), (b)

was zero for all the wind turbines, the measurement data would have been very close to the outcome of the wind farm model in Figure 4.3a. This means that the velocity deficit due to the wake would have been greater than in the case with yawed wind turbines. Therefore, the above mentioned hypothesis seems to be true. However, further research is required to confirm the hypothesis.

The research path can be toward calculating the structural load on yawed turbines to determine the maximum allowed yaw angle for each wind turbine. Furthermore, an optimization problem should be designed to evaluate the power production of the farm and the structural and fatigue loads. In fact, the increase in power production and the probable increase in load should be compromised.

Afterwards, to track the yaw angles determined by the controller, the command will be sent to actuators. The actuators that can be implemented to this end, are either the yaw actuator or the blade pitch actuator. The blade pitch actuator can be used to make small yaw angles for the rotor. Thus, depending on the size of yaw angles the actuator type will be determined.

Changing the rotational direction:

On the basis of the third Law of motion (law of reaction), the rotational direction of the wake behind a wind turbine is in opposite direction of the rotor rotational direction. Therefore if the downstream wind turbine rotates in the opposite direction of the upstream wind turbine (in the rotational direction of the wake), the rotational energy of the wake will decrease. Therefore, the load on the downstream turbine will also decrease. This phenomenon has been shown in Figure 4.2.

In this approach the wind farm model should be further developed, to provide the details of the wake rotational direction and turbulence intensity. The wind farm controller is supposed to determine the load and power circumstances and also the rotational direction of each wind turbine as well as the power set-points.

References

[Adams 96]   B. M. Adams. *Dynam Loads In Wind Farms II*. Rapport technique 286/R/1, Garrad Hassan and Partners Ltd, 1996.

[Ainslie 88]   J.F. Ainslie. *Calculating the flowfield in the wake of wind turbines*. Journal of Wind Engineering and Industrial Aerodynamics, vol. 27, no. 1-3, pages 213 – 224, 1988.

[Akhmatov 03]   Vladislav Akhmatov, Hans Knudsen, Arne Hejde Nielsen, Jrgen Kaas Pedersen & Niels Kjlstad Poulsen. *Modelling and transient stability of large wind farms*. International Journal of Electrical Power & Energy Systems, vol. 25, no. 2, pages 123 – 144, 2003.

[Barthelmie 07]   R.J. Barthelmie, O. Rathmann, S.T. Frandsen, K. Hansen & E. Politis. *Modelling and measurements of wakes in large wind farms*. Journal of Physics: Conference Series, vol. 75, no. 1, page 012049, 2007.

[Benallou 88]   A. Benallou, D. A. Mellichamp & D. E. Seborg. *Optimal stabilizing controllers for bilinear systems*. International Journal of Control, vol. 48, pages 1487–1501, 1988.

[Bianchi 06]   F.D. Bianchi, H. De Battista & R.J. Mantz. Wind turbine control systems: principles, modelling and gain scheduling design. Springer Verlag, 2006.

[Billinton 96]   R. Billinton, Hua Chen & R. Ghajar. *Time-series models for reliability evaluation of power systems including wind energy*. Microelectronics and Reliability, vol. 36, no. 9, pages 1253 – 1261, 1996.

[Brand 10]   A. J. Brand & J. W. Wagenaar. *A quasi-steady wind farm flow model in the context of distributed control of the wind farm*. In European Wind Energy Conference (EWEC 2010), 2010.

[Brand 11]   A. Brand & M. Soleimanzadeh. *Two Control Solutions for Wind Farm Management and Operation on the Grid*. In EWEA Offshore, Amsterdam, November, 2011.

[Burton 01]   T. Burton, D. Sharpe, N. Jenkins & E. Bossanyi. Wind energy handbook. John Wiley and Sons, 2001.

REFERENCES

[Crespo 99]   A. Crespo, J. Hernández & S. Frandsen. *Survey of modelling methods for wind turbine wakes and wind farms*. Wind Energy, vol. 2, pages 1–24, January 1999.

[Eecen 10]   P.J. Eecen & E.T.G. Bot. *Improvements to the ECN wind farm optimisation software "FarmFlow"*. In Presented at the European Wind Energy Conference & Exhibition, Warsaw, Poland, 20 - 23 April 2010.

[Elkinton 08]   C. Elkinton, J. F. Manwell & J. G. McGowan. *Algorithms for Offshore Wind Farm Layout Optimization*. Wind Engineering, vol. 32, pages 67–84, 2008.

[Fernandez 06]   Luis M. Fernandez, Jos Ramn Saenz & Francisco Jurado. *Dynamic models of wind farms with fixed speed wind turbines*. Renewable Energy, vol. 31, no. 8, pages 1203 – 1230, 2006.

[Fernandez 08a]   LM Fernandez, CA Garcia & F. Jurado. *Comparative study on the performance of control systems for doubly fed induction generator (DFIG) wind turbines operating with power regulation*. Energy, vol. 33, no. 9, pages 1438–1452, 2008.

[Fernandez 08b]   R.D. Fernandez, P.E. Battaiotto & R.J. Mantz. *Wind farm nonlinear control for damping electromechanical oscillations of power systems*. Renewable Energy, vol. 33, no. 10, pages 2258 – 2265, 2008.

[Fernandez 09]   L.M. Fernandez, C.A. Garcia, J.R. Saenz & F. Jurado. *Equivalent models of wind farms by using aggregated wind turbines and equivalent winds*. Energy Conversion and Management, vol. 50, no. 3, pages 691 – 704, 2009.

[Frandsen 06]   S. Frandsen, R. Barthelmie, S. Pryor, O. Rathmann, S. Larsen, J. Hojstrup & M. Thogersen. *Analytical modelling of wind speed deficit in large offshore wind farms*. Wind Energy, vol. 9, page 15, 2006.

[Hammerum 07]   K. Hammerum, P. Brath & N.K. Poulsen. *A fatigue approach to wind turbine control*. Journal of Physics: Conference Series, vol. 75, pages 1–11, 2007.

[Hansen 02]   A.D. Hansen, Sørensen, F. Blaabjerg & J. Becho. *Dynamic modelling of wind farm grid interaction*. Wind Engineering, vol. 26, pages 191–208, 2002.

[Hansen 06]   A.D. Hansen, P. Sørensen, F. Iov & F. Blaabjerg. *Centralised power control of wind farm with doubly fed induction generators*. Renewable Energy, vol. 31, no. 7, pages 935–951, 2006.

[Hoffmann 89]   Klaus A. Hoffmann & S.T. Chiang. Computational fluid dynamics. Austin, TX: Engineering Education System, 1989.

[Johnson 09]   K.E. Johnson & N. Thomas. *Wind farm control: Addressing the aerodynamic interaction among wind turbines*. In Proc. American Control Conf, 2009.

[Jonkman 09]   J. Jonkman, S. Butterfield, W. Musial & G. Scott. *Definition of a 5-MW reference wind turbine for offshore system development*. Rapport technique NREL/TP-500-38060, Golden, CO: National Renewable Energy Laboratory, 2009.

[Karki 06]   R. Karki, P. Hu & R. Billinton. *A simplified wind power generation model for reliability evaluation*. IEEE Transaction on Energy Conversion, vol. 21, no. 2, pages 533–540, 2006.

[Kasmi 08]   Amina El Kasmi & Christian Masson. *An extended k-epsilon model for turbulent flow through horizontal-axis wind turbines*. Journal of Wind Engineering and Industrial Aerodynamics, vol. 96, no. 1, pages 103 – 122, 2008.

[Kazachkov 03]   Y.A. Kazachkov, J.W. Feltes & R. Zavadil. *Modeling wind farms for power system stability studies*. In Power Engineering Society General Meeting, volume 3, page 1533, July 2003.

[Kristoffersen 03] JR Kristoffersen & P. Christiansen. *Horns Rev offshore windfarm: its main controller and remote control system*. Wind Engineering, vol. 27, no. 5, pages 351–359, 2003.

[Lackner 07]   M. A. Lackner & C. Elkinton. *An Analytical Framework for Offshore Wind Farm Layout Optimization*. Wind Engineering, vol. 31, pages 17–31, 2007.

[Larsen 08]   G.C. Larsen, H.A. Madsen, T.J. Larsen & N. Troldborg. *Wake modeling and simulation*. Rapport technique, Forskningscenter Risø Roskilde, 2008.

[Lescher 07]   F. Lescher, H. Camblong, O. Curea & R. Briand. *LPV Control of Wind Turbines for Fatigue Loads Reduction using Intelligent Micro Sensors*. In American Control Conference, 2007. ACC '07, pages 6061–6066, July 2007.

[Madjidian 11]   D. Madjidian, K. Mårtensson & A. Rantzer. *A Distributed Power Coordination Scheme for Fatigue Load Reduction in Wind Farms*. In American control conference, 2011.

[Nichita 02]   C. Nichita, D. Luca, B. Dakyo & E. Ceanga. *Large Band Simulation of the Wind Speed for Real-Time Wind Turbine Simulators*. Power Engineering Review, IEEE, vol. 22, no. 8, pages 63–63, Aug. 2002.

[Ozturk 04]   U. Aytun Ozturk. *Heuristic methods for wind energy conversion system positioning*. Electric Power Systems Research, vol. 70, pages 179–185, 2004.

[Pao 09]   L. Pao & K.E. Johnson. *A tutorial on the dynamics and control of wind turbines and wind farms*. In Proceedings of American Control Conf (ACC), 2009.

[Rethore 07]   P-E Rethore, A Bechmann, N. Sørensen, S. T. Frandsen & J Mann. *A CFD model of the wake of an offshore wind farm: using a prescribed wake inflow*. Journal of Physics: Conference Series, vol. 75, no. 1, page 012047, 2007.

[Rice 09]   J. Rice & M. Verhaegen. *Distributed Control: A Sequentially Semi-Separable Approach for Spatially Heterogeneous Linear Systems*. IEEE Transaction on Automatic Control, vol. 54, pages 1270–1283, 2009.

[Rice 10]   J. Rice. *Efficient Algorithms for distributed control: A Structured Matrix Approach*. PhD thesis, Technical University of Delft, 2010.

[Rodriguez-Amenedo 08] J.L. Rodriguez-Amenedo, S. Arnaltes & M.A. Rodriguez. *Operation and coordinated control of fixed and variable speed wind farms*. Renewable Energy, vol. 33, no. 3, pages 406 – 414, 2008.

[Slootweg 03]   JG Slootweg & WL Kling. *Aggregated modelling of wind parks in power system dynamics simulations*. In Power Tech Conference Proceedings, 2003 IEEE Bologna, volume 3, pages 6–pp. IEEE, 2003.

[Soleimanzadeh 10a]   M. Soleimanzadeh & R. Wisniewski. *Wind Deficit Model in a Wind Farm Using Finite Volume Method*. In Proceedings of American Control Conference (ACC), 2010.

[Soleimanzadeh 10b]   M. Soleimanzadeh & R. Wisniewski. *Wind speed dynamical model in a wind farm*. In 8th IEEE International Conference on Control & Automation (ICCA), 2010.

[Soleimanzadeh 11a]   M. Soleimanzadeh, A.J. Brand & R. Wisniewski. *A Wind Farm Controller for Load and Power Optimization in a Farm*. In IEEE Multi-conference on Systems and Control, 2011.

[Soleimanzadeh 11b]   M. Soleimanzadeh & R. Wisniewski. *An Optimization Framework for Load and Power Distribution in Wind Farms-Low wind speed*. In 18th IFAC World Congress, 2011.

[Soleimanzadeh 11c]   Maryam Soleimanzadeh & Rafael Wisniewski. *Controller design for a wind farm, considering both power and load aspects*. Mechatronics, vol. 21, no. 4, pages 720 – 727, 2011.

[Soleimanzadeh 12a]   M. Soleimanzadeh, R. Wisniewski & A. J. Brand. *State-space representation of the flow model for a wind farm*. Wind Energy, vol. (2nd revision submitted), pages –, 2012.

[Soleimanzadeh 12b]   M. Soleimanzadeh, R. Wisniewski & K. Johnson. *A distributed optimization framework for wind farms*. IEEE Transactions on Control Systems Technology, vol. (Submitted), pages –, 2012.

[Soleimanzadeh 12c]   M. Soleimanzadeh, R. Wisniewski & S. Kanev. *An Optimization Framework for Load and Power Distribution in Wind Farms*. Wind Engineering & Industrial Aerodynamics, vol. 107108, page 256262, 2012.

[Sørensen 04]   P. Sørensen, A.D. Hansen, K. Thomsen, H. Madsen, H.A. Nielsen, N.K. Poulsen & F. Iov. *Simulation and optimization of wind farm controller*. In European Wind Energy Conference and Exhibition, 2004.

[Spera 94]   D.A. Spera. Wind turbine technology. Fairfield, NJ (United States); American Society of Mechanical Engineers, 1994.

[Spruce 93]   C. Spruce. *Simulation and Control of Windfarms*. PhD thesis, Oxford, 1993.

[Spudic 10]   V. Spudic, M. Jelavic, M. Baotic & M. Peric. *Hierarchical wind farm control for power/load optimization*. In The Science of making Torque from Wind (Torque2010), 2010.

[Spudic 11]   V. Spudic, M. Jelavic, M. Baotic & M. Peric. *Wind Farm Load Reduction Via Parametric Programming Based Controller Design*. In 18th Ifac World Congress, volume 18, Universita Cattolica del Sacro Cuore, Milano, Italy, 2011.

[Steinbuch 88]   M. Steinbuch, W.W. de Boer, O.H. Bosgra, S.A.W.M. Peters & J. Ploeg. *Optimal control of wind power plants*. Journal of Wind Engineering and Industrial Aerodynamics, vol. 27, no. 1-3, pages 237 – 246, 1988.

[Strang 07]   Gilbert Strang. Computational science and engineering. Wellesley, MA: Wellesley-Cambridge Press, 2007.

[Suryanarayanan 07]   Shashikanth Suryanarayanan & Amit Dixit. *A Procedure for the Development of Control-Oriented Linear Models for Horizontal-Axis Large Wind Turbines*. Journal of Dynamic Systems, Measurement, and Control, vol. 129, no. 4, pages 469–479, 2007.

[Sutherland 00]   H.J. Sutherland. *A summary of the fatigue properties of wind turbine materials*. Wind Energy, vol. 3, no. 1, pages 1–34, 2000.

[Suvire 08]   G.O. Suvire & P.E. Mercado. *Wind farm: Dynamic model and impact on a weak power system*. In Transmission and Distribution Conference and Exposition: Latin America, 2008 IEEE/PES, pages 1–8, Aug. 2008.

[Trujillo 07]   JJ Trujillo, A. Wessel, I. Waldl & B. Lange. *Online Modeling of Wind Farm Power for Performance Surveillance and Optimization*. Wind Energy, vol. Proceedings of the Euromech Colloquium, pages 163–166, 2007.

[van der Hooft 03]   E. van der Hooft, P. Schaak & T. Van Engelen. *Wind turbine control algorithms*. Rapport technique, ECN Technical Report,ECN-C–03-111, 2003.

[Vermeer 03]   L. J. Vermeer, J. N. Sørensen & A. Crespo. *Wind turbine wake aerodynamics*. Progress in Aerospace Sciences, vol. 39, no. 6-7, pages 467 – 510, 2003.

[Versteeg 07]   H.K. Versteeg & W. Malalasekera. An introduction to computational fluid dynamics: the finite volume method. Prentice Hall, 2007.

[Zhao 06]   M. Zhao, Z. Chen & F. Blaabjerg. *Probabilistic capacity of a grid connected wind farm based on optimization method*. Renewable Energy, vol. 31, no. 13, pages 2171 – 2187, 2006.

Contributions

Journal papers:

Paper A: State-space representation of the wind flow model in wind farms

Paper B: Controller Design for a Wind Farm, Considering both Power and Load Aspects

Paper C: An Optimization Framework for Load and Power Distribution in Wind Farms

Paper D: A distributed optimization framework for wind farms

Conference papers:

- An Optimal Control Scheme to Minimize Loads in Wind Farms, *IEEE Multi-conference on Systems and Control, 2012*

- An Optimization Framework for Load and Power Distribution in Wind Farms-Low wind speed, *18th IFAC World Congress, 2011*

- A Wind Farm Controller for Load and Power Optimization in a Farm, *IEEE Multi-conference on Systems and Control, 2011*

- Two Control Solutions for Wind Farm Management and Operation on the Grid, *EWEA Offshore, 2011*

- Wind Deficit Model in a Wind Farm Using Finite Volume Method, *Proceedings of American Control Conference (ACC), 2010*

- Wind speed dynamical model in a wind farm, *8th IEEE International Conference on Control & Automation (ICCA), 2010*

Paper A

State-space representation of the wind flow model in wind farms

Maryam Soleimanzadeh, Rafael Wisniewski, and Arno Brand

Abstract

A dynamical model for the wind flow in a wind farm is developed in this paper. The model is based on the spatial discretization of the linearized Navier-Stokes equation combined with the vortex cylinder theory. The spatial discretization of the model is performed using the finite difference method, which provides the state space form of the dynamical wind farm model. The model provides an approximation of the behavior of the flow in the wind farm, and obtains the wind speed in the vicinity of each wind turbine. The model is validated using measurement data of EWTW test wind farm in the Netherlands, and employing the outcomes of two other wind flow models. The end goal of this work is to present the wind farm flow model by ordinary differential equations, to be applied in wind farm control algorithms along with load and power optimizations.

1 Introduction

Recently, the considerable growth of large wind farms intensified the need for advanced automatic wind farm controllers. The objective of the wind farm controllers is to improve the distribution of power set-points among wind turbines and to control the structural loads to optimize the energy production. To reach these goals, a wind farm flow model that can be used in control methods is imperative [1, 2].

A large and still growing body of literature has dealt with models of wind farms with either the purpose of farm layout optimization [3, 4, 5], or power quality improvement [6, 7, 8, 9]. Furthermore, several attempts have been made in modeling of the flow in the wind farms. An example of these, is the study carried out by [10]. A well known modeling approach, addressed in [10], assumes that when a field contains a large number of wind turbines, the turbines are considered as distributed roughness elements. Therefore, the ambient atmospheric flow will be modified. Therefrom, one of the main issues in wind farm modeling is introduced, which is the wake interaction and the effect of velocity deficit and turbulence increment in the place of interaction [10]. In another major study, a wind flow model for a farm is derived based on quasi-steady wake deficits computed in a loop involving coupling between an actuator disc model of the rotor-wake interaction and an aeroelastic model [11, 12]. Another way of modeling a wind farm is to provide a detailed model which considers each wind turbine dynamic and the internal electrical network [13].

Still another option is to apply computational fluid dynamics (CFD) schemes, but these methods are computationally expensive. Moreover, because of the gap between engineering analytical methods and CFD models, a connection with detailed information should be developed for better wind farm and turbine design and for more efficient control strategies [14]. One of the engineering analytical methods is carried out by [15], and is applied to calculate production losses based on conservation of the momentum deficit in the wake.

So far, however, there has been little effort on developing a structured dynamic model to be applied in control algorithms, to optimize the structural load and power in wind farms.

The basic purpose of this paper is to develop a spatial dynamic model for the wind flow in a wind farm, and to present the model in the state space form. The state space representation is a mathematical model as a set of inputs, outputs and states related by first-order differential equations. The model provides wind speed approximations all over the farm, particularly in the vicinities of the wind turbines. Spatial discretization is performed on a computational domain, using the finite difference method (FDM). The key element is to solve the flow equation for the whole wind farm, where the wind turbines are modeled by means of their thrust coefficient using the vortex cylinder model [16]. Since the purpose of developing this model has been its implementation in control algorithms, two approximations have been considered to make the model simple enough to have short execution time. One is using the 2-D approximation for the flow equation at hub height, and the second one is using coarse grids. In this case a part of the accuracy has been traded for simplicity and short computation process. This work provides an approximation of what happens downstream wind turbines in the form of ordinary differential equations. Therefore, it has been found extremely useful for wind farm control applications and to estimate fatigue loads.

The paper is organized as follows. First, we start with the flow equation for the whole wind farm. Then, considering the momentum theory and the yaw angle of each wind turbine, we continue with developing the wind flow model in the wind farm. In this section, the equations are represented in matrix form and the state space model is presented. Finally, the simulation and validation results are illustrated and the model is assessed based on the results.

2 Modeling

Flow equation

The wind flow in a wind farm can be expressed by the Navier-Stokes equation for viscous incompressible flow. The wind velocity is a divergence free vector $\mathbf{u}$, and the pressure is the scalar p [17]:

$$\frac{\partial \mathbf{u}}{\partial t} + (\mathbf{u}.\nabla)\mathbf{u} = -\nabla p + \frac{1}{Re}\Delta \mathbf{u} + \mathbf{F}, \qquad (5.1)$$

where Re is the Reynolds number, and $\mathbf{F}$, at the place of wind turbines, is the thrust force which is explained in subsequent sections. The continuity equation is as follows:

$$\nabla.\mathbf{u} = \mathbf{0}. \qquad (5.2)$$

The model is being developed for controller design, and it delivers the mean wind speed at the vicinity of each turbine to the wind farm controller. Approximating the flow equation to a 2-D instead of a 3-D equation, will loose information on wind shear and turbulence intensity (that are likely to be neglected in far wake region), but the mean wind speed information do not change considerably.

In xy plane (2-D), the components of the velocity $\mathbf{u}$ are $\nu(x, y, t)$ and $v(x, y, t)$. Moreover, $(\mathbf{u}.\nabla)\mathbf{u}$ has two components expressed as follows [17]:

$$\left(\nu\frac{\partial}{\partial x} + v\frac{\partial}{\partial y}\right)\begin{bmatrix}\nu \\ v\end{bmatrix} = \begin{bmatrix}\nu\nu_x + v\nu_y \\ \nu v_x + vv_y\end{bmatrix}, \tag{5.3}$$

where $(\cdot)_x = \partial(\cdot)/\partial x$ and $(\cdot)_y = \partial(\cdot)/\partial y$. Therefore, the momentum equation (5.1) in 2D is written in the following form:

$$\nu_t + p_x = (\nu_{xx} + \nu_{yy})/Re - (\nu^2)_x - (\nu v)_y + F_1$$
$$v_t + p_y = (v_{xx} + v_{yy})/Re - (\nu v)_x - (v^2)_y + F_2, \tag{5.4}$$

where F_1 and F_2 are the x and y components of the thrust force, and the continuity equation (5.2):

$$\nu_x + v_y = 0. \tag{5.5}$$

In order to derive the matrix representation, the nonlinear terms are replaced with linear approximations. The turbulent intensity and wind shear are not considered in the current version; our concern is a big picture of the farm, and phenomena relevant for the farm control not an individual turbine control.

Assuming velocity components ν and v are $\nu = \bar{\nu} + \hat{\nu}$ and $v = \bar{v} + \hat{v}$, where $\hat{\nu}$ and $\hat{v}$ are small variable velocity components in x and y directions and the steady state velocities $\bar{\nu}$ and $\bar{v}$ are real constants in $\mathbb{R}$. Neglecting the small terms, it can be shown that the linearized incompressible Navier-Stokes equations in the horizontal plane (two velocity components) are as follows [18]:

$$\hat{\nu}_t + p_x = (\hat{\nu}_{xx} + \hat{\nu}_{yy})/Re - \bar{\nu}\hat{\nu}_x - \bar{v}\hat{\nu}_y + F_1,$$
$$\hat{v}_t + p_y = (\hat{v}_{xx} + \hat{v}_{yy})/Re - \bar{\nu}\hat{v}_x - \bar{v}\hat{v}_y + F_2,$$
$$\hat{\nu}_x + \hat{v}_y = 0. \tag{5.6}$$

Spatial discretization of the flow equation

The wind farm is divided into non-overlapping square cells as Figure 5.1, called a staggered grid. The spatial discretization is achieved using the finite difference method where the P, U, and V locations are depicted in Figure 5.2. Capital letters are applied for numerical approximations of velocity components and pressure.
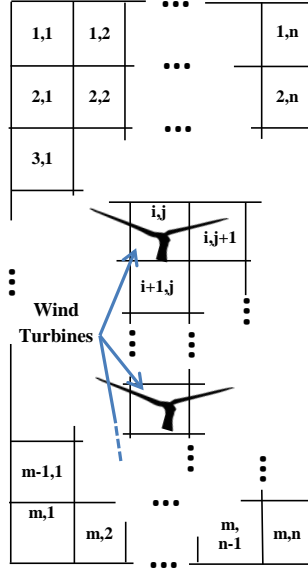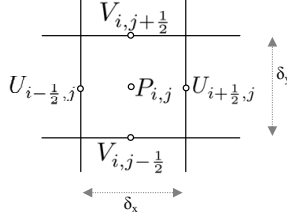
Figure 5.1: Wind Farm Grid

Figure 5.2: P, U, V in a cell

As it can be seen in Figure 5.2, the pressures P are placed in the cell midpoints (centers), the velocities U are located on the vertical cell interfaces (edges), and the velocities V are located on the horizontal cell interfaces (above and below the center).

The computational domain is chosen to be the whole farm and each partition has area of one square meter. The finite difference method provides the solution of the partial differential equation in average within a partition. This is indeed, what is needed by the feedback control algorithm, which acts in a closed loop and thus is robust against discrepancies between true and idealized model derived in the paper.

The first derivative of the velocity components can be approximated as follows

[17]:

$$(U_x)_{i+\frac{1}{2},j} \approx \frac{U_{i+1,j} - U_{i,j}}{\delta_x}, \tag{5.7}$$

which is a centered approximation of U_x in the middle between the two points. In the staggered grid, this position is the position of $P_{i,j}$. The approximation of the Laplace operator at an interior point i, j is as follows:

$$U_{xx} + U_{yy} \approx \frac{U_{i-1,j} - 2U_{i,j} + U_{i+1,j}}{\delta_x^2} + \frac{U_{i,j-1} - 2U_{i,j} + U_{i,j+1}}{\delta_y^2}, \tag{5.8}$$

The same formula holds for the component V , and for the gradient of the pressure P [17].

$$(P_x)_{i+\frac{1}{2},j} \approx \frac{P_{i+1,j} - P_{i,j}}{\delta_x}, \tag{5.9}$$

However, we will not discretize the terms with time derivation $\partial U/\partial t$, to make the equations discretized in space and continuous in time. In other words, we are going to use *semi-discretized* equations in the wind farm model.

Wind farm model

The equations (5.6) are semi-discretized using (5.7)-(5.9), and re-arranged in the following form:

$$U_t + \begin{bmatrix} G & 0 \end{bmatrix} \begin{bmatrix} U \\ V \end{bmatrix} + DP = F_1,$$

$$V_t + \begin{bmatrix} 0 & \tilde{G} \end{bmatrix} \begin{bmatrix} U \\ V \end{bmatrix} + \tilde{D}P = F_2,$$

$$\begin{bmatrix} C & \tilde{C} \end{bmatrix} \begin{bmatrix} U \\ V \end{bmatrix} = 0, \tag{5.10}$$

where G and $\tilde{G}$ are respectively coefficient matrices of U and V, and D , $\tilde{D}$ are coefficient matrices of P in the continuity equation. Moreover, C and $\tilde{C}$ are respectively coefficients of U and V in the continuity equation.

Therefore, the momentum equation can be written as follows:

$$\frac{d}{dt} \begin{bmatrix} U \\ V \end{bmatrix} + \begin{bmatrix} G & 0 \\ 0 & \tilde{G} \end{bmatrix} \begin{bmatrix} U \\ V \end{bmatrix} + \begin{bmatrix} D \\ \tilde{D} \end{bmatrix} P = \begin{bmatrix} F_1 \\ F_2 \end{bmatrix} \tag{5.11}$$

The effect of wind turbines in the equations is presented in the pressure P and the forces F_1 and F_2. Note that the wind turbine effect is considered to be in the

far wake region (in 5 to 7 rotor diameter distance), where most of the turbulence effects and wind shears are neglected.

Most studies on wakes have made a distinction between the near wake and the far wake regions. The near wake is taken as the region just behind the rotor, where the effect of the rotor is considerable [19]. In the near wake region, there is an intense turbulence generated by the blades, shear, and the decrease of tip vortices. The far wake is the region beyond the near wake. One of the basic objectives of modeling in the far wake region is the evaluation of the wind turbines effect on each other [20]. Our approach focuses on this region.

Moreover, the flow model is assumed to be at hub height, where the effect of wind shear is not included in the wake studies. This assumption also helps to reduce the computation time.

Considering the wind direction exactly perpendicular to the rotor plane, the effect of wind turbines on the wind flow can be explained by means of momentum theory [21]. However, most of the times, the wind direction is not exactly perpendicular to the rotor plane and makes an angle γ with the normal to the rotor plane (yaw angle). In this case, the pressure drop at the wind turbine place will be modeled by the *vortex cylinder model* [16]. The pressure drop across the wind turbine disc is expressed as follows [16]:

$$P_{i,j+1} - P_{i,j} = \frac{1}{2}\rho \mathbf{U}_\infty^2 C_T,$$
(5.12)

where $\mathbf{U}_\infty$ is the the upstream wind speed and

$$C_T = 4a(cos\gamma + tan\frac{\chi}{2}sin\gamma - asec^2\frac{\chi}{2}),$$
(5.13)

whence C_T and a are respectively the thrust coefficient and the axial induction factor of a turbine, ρ is the air density, γ is the yaw angle depicted in Figure 5.3, and χ is defined as follows:

$$\chi = (0.6a + 1)\gamma.$$
(5.14)

Therefore, the pressure drop in (5.11) at the location of each wind turbine is a function of C_T and wind speed, $P = f(C_T, \mathbf{U})$. Whereas, in grid cells without a wind turbine, the pressure is obtained from the approximated mean wind speed computed for each cell of the staggered grid. The first derivatives of velocity, U_x and V_y in the cell centers are obtained by the divergence of the velocity field, $\Delta\mathbf{U}$. Subsequently, based on the Poisson equation for the pressure $-\Delta P = -\frac{1}{\Delta t}\Delta\mathbf{U}$ [22].

Furthermore, F_1 and F_2 in (5.11) are the thrust forces on the wind turbines, produced respectively by the U and V wind speeds. In cells with no turbine, these forces are considered to be zero, but in the location of each wind turbine the forces are as follows:
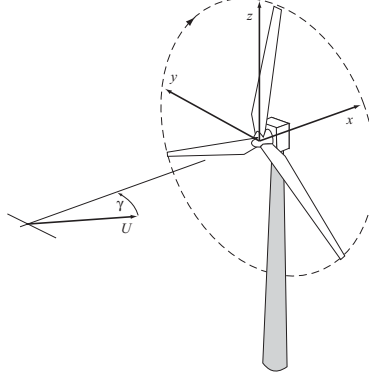
Figure 5.3: Yaw angle definition [16]

$$\mathbf{F} = \frac{1}{2}\rho\pi R^2 \mathbf{U}^2 C_T, \tag{5.15}$$

where, R is the rotor radius.

In order to express the above mentioned equation in the state space form, as explained in the following, the new state and input variables are defined and substituted in the above equations. In general, the wind speed all over the farm can be defined as state variables x, and the thrust coefficient of the wind turbines can be defined as a system input u [23].

$$x = \begin{bmatrix} U \\ V \end{bmatrix}, \quad u = C_T, \tag{5.16}$$

where x is the state variable and u is the system input. After substituting the variables in (5.11), the equations are re-written as follows:

$$\dot{x} = Ax + f(x, u), \tag{5.17}$$

where

$$f(x, u) = -\begin{bmatrix} D \\ \tilde{D} \end{bmatrix} P + \mathbf{F}(x, u). \tag{5.18}$$

However, since P and $\mathbf{F}$ are linear in $u = C_T$, the equation (5.17) can be rewritten in the following form.

$$\dot{x} = Ax + (B + < N, x >)u, \tag{5.19}$$

where the A matrix represent the linear part of the flow equation and $(B + < N, x >)u$ represents the nonlinear terms and the wind turbine effects. $< N, x >$ is the inner product of x and the known matrix N. The size of the A matrix that
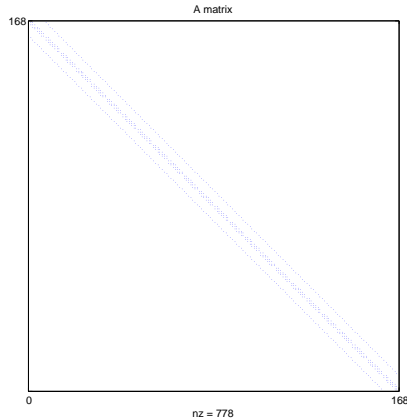
Figure 5.4: The structure of the system matrix for a 7×25 grid, where nz stands for the number of nonzero elements in the matrix.

is obtained for a 7×25 grid with 5 wind turbines is 168×168, and the structure of the matrix is shown in Figure 5.4. The clear sparse structure allows for a big reduction in computation time.

To sum up, in this section, the modeling approach commences with the linearized flow equation for the whole farm, and continues with discretizing the equations on a coarse staggered grid using FDM. The wind turbines dynamic is included using momentum theory, and more specifically a a vortex cylinder model. In this regard, some assumptions have been made which are, being in far wake region (downstream turbines are located in far wake of the upstream turbines), having the maximum wake interaction (wind direction exactly parallel to the row of turbines), and the mean wind speed in the vicinity of each turbine being of interest. The application of the modeling of wind farms with these wind condition assumptions can be find in [24, 25, 26].

3   Simulation and Validation

In order to show the capability of simulating any wind farm with the model, it has been simulated by MATLAB for two wind farms, one with 14 and the other with 5 wind turbines. In these simulations the boundary conditions, as defined at a far distance from the wind turbines, are the free stream wind speed.

The result for simulating the wind farm with 14 wind turbines is depicted in Figure 5.5. The color plot shows the pressure contour in the wind farm, and the little arrows on top of it are the normalized velocity field (with norm 1) depicting the wind direction. The wind direction and the locations of some of the turbines are illustrated in the figure. The pressure variation from high to low is depicted
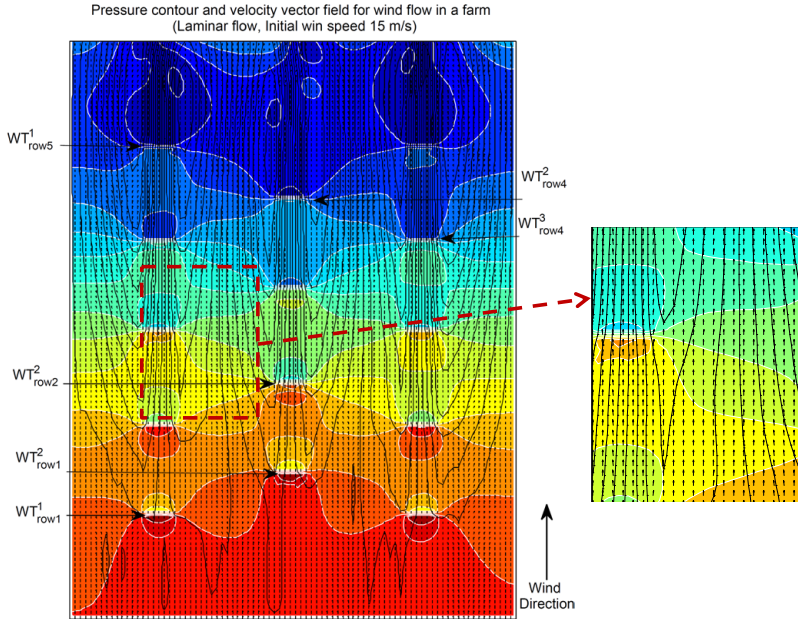
Figure 5.5: Pressure contour for wind flow in a sample farm with 14 wind turbines in Matlab

with the color variation from red to blue.

The wind farm with the 5 wind turbines is the ECNs Wind turbine Test site Wieringermeer (EWTW). The wind farm model has been validated against measurement data from the EWTW. The test wind farm has five wind turbines placed in a row and 304 meters apart, illustrated in Figure 5.6. In order to validate the flow model for a wind farm, the wind speed is calculated behind each turbine and is compared with measurements. The measurements are 10 minutes average from the nacelle anemometer of the turbines. Validation investigates whether the conceptual and computational model and the simulations agree with the real world observations. The purpose is to identify the error and uncertainties by comparing the simulation results with measurement data [27].

In addition to measurement data, simulation results are compared with FARM-FLOW software calculations [28], and the ECN's quasi-steady farm model developed in [12].

The computed mean wind speed from the farm model is compared to measurements and the other models in different wind speed conditions from 5 to 20 m/s. Moreover, the wind direction in all cases is parallel to the wind turbine row, equal to 275 ± 0.25 deg. In all the figures showing the simulation results, zero on the horizontal axis depicts the Meteo-Mast position and numbers from 1 to 5
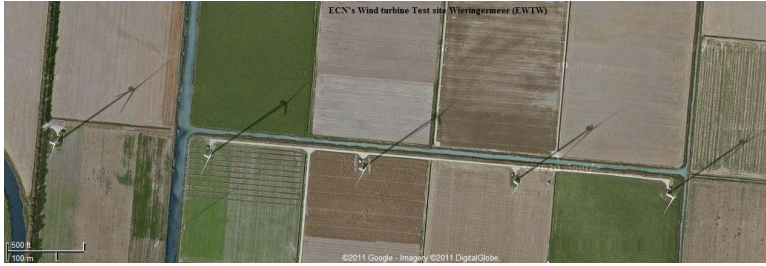
Figure 5.6: Top view of the EWTW wind farm, which consists of 5 wind turbines in a row

stand for wind turbine labels. The wind farm model in this paper does not consider the turbulence intensity, and the FarmFlow simulations have been performed in a constant turbulence intensity (for all the cases 0.08). The grid size for this simulations is 35×125, and each wind turbine occupies several cells.

The simulation results in Figures 5.7, 5.8 and 5.9 are obtained for a wind direction exactly parallel to the wind turbine row and zero yaw angle, $\gamma = 0$. As it can be seen in the Figures 5.8 and 5.9, the results of the wind farm model are in a good range, and in some points very close to measurements.

Notwithstanding, after scrutinizing the measurement data, it turned out that some of the wind turbines were yawed, at the time of collecting measures. The yaw angle has been measured and the simulations have been repeated considering the measured yaw angle. Since neither the FarmFlow software nor the ECN's quasi-steady farm model consider the yaw, only the wind farm model results are changed with respect to the results depicted in Figures 5.8 and 5.9. The yaw angles of the wind turbines in wind speeds 5, 7, 12 and 15 m/s are presented in Table 5.1. The results of the simulations considering the yaw angles, are illustrated in Figure 5.10 and Figure 5.11. It is seen that, the wind farm model results compared to measurement data has been improved, with respect to the results for zero yaw angle.

It is interesting to note that including yaw information has improved the wake deficit effect (i.e. the velocity deficit is became less). This is explained as a hypothesis in the following way.

In a condition that the wind direction is parallel to a row of wind turbines (maximum wake interaction), if the wind turbines are yawed with different yaw angles, the velocity deficit will be less than a case in which all the turbines have zero yaw angle. This is equivalent to more power production. However, it may also cause to increase the structural loads.

In order to study this hypothesis, the yawed wind turbines in 5 and 7 m/s are considered, as they have the largest yaw angles. The results depicted in Figure 5.10 shows that the farm model can follow the measurements very closely. There-
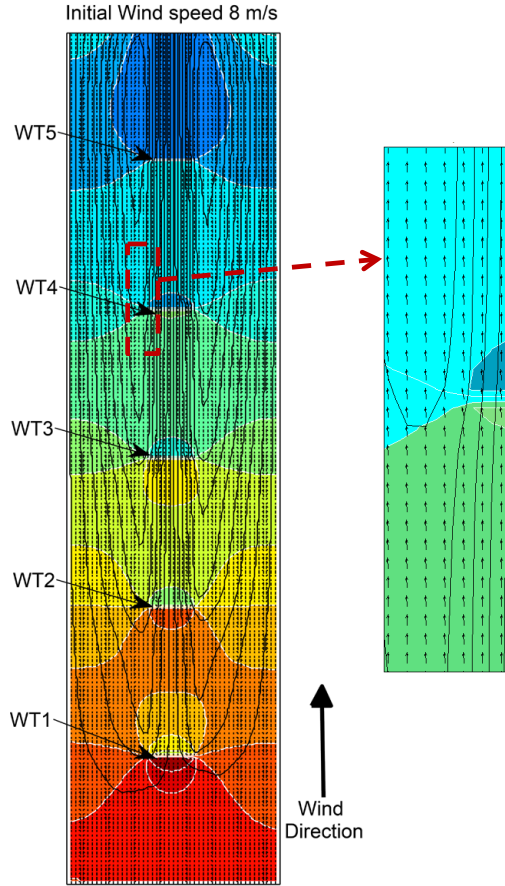
Figure 5.7: Simulation results for EWTW wind farm - Pressure field and wind direction

from, if the yaw angle was zero for all the wind turbines, the measurement data would have been very close to the outcome of the wind farm model in Figure 5.8. This means that the velocity deficit due to the wake would have been greater than in the case with yawed wind turbines. Therefore, the above mentioned hypothesis seems to be true.

Furthermore, the measurement data for different yaw angles in wind speeds 5 m/s (low) and 20 m/s (high) has been presented in Figure 5.12. In this figure, two sets of measurements have been presented for both wind speeds. The yaw angles for each set are also presented in the figures. It is seen that the wind speeds with larger yaw are higher than those with smaller yaw angles (i.e., the velocity deficit is less). This observation also agrees with the above mentioned hypothesis. However, further research is required to confirm the hypothesis.
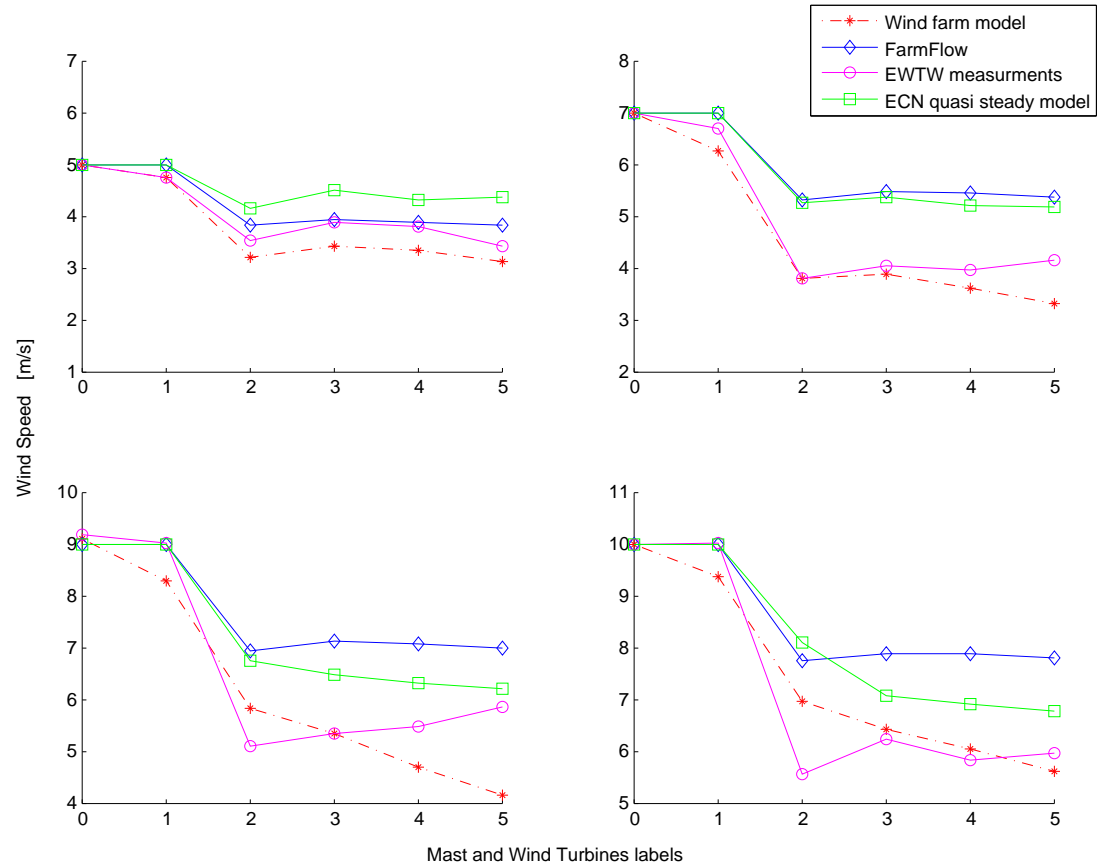
Figure 5.8: Comparing the results with results from two other models and EWTW measurements for wind speeds 5,7,9,10 m/s at Meteo-Mast

Table 5.1: Yaw Angle for each of the 5 wind turbines in different wind speeds

Yaw angle [deg]	Wind speed [m/s]			
	5	7	12	15
WT No.				
1	19.38	34.58	5.18	0.42
2	15.72	2.81	1.78	0.91
3	13.34	5.35	-16.55	-16.48
4	22.57	-25.72	11.75	4.21
5	19.49	7.96	-1.06	-6.24

4 Conclusion

This paper has presented a dynamical model for the wind flow in a wind farm which is founded on the linearized Navier-Stokes equation, and is discretized on
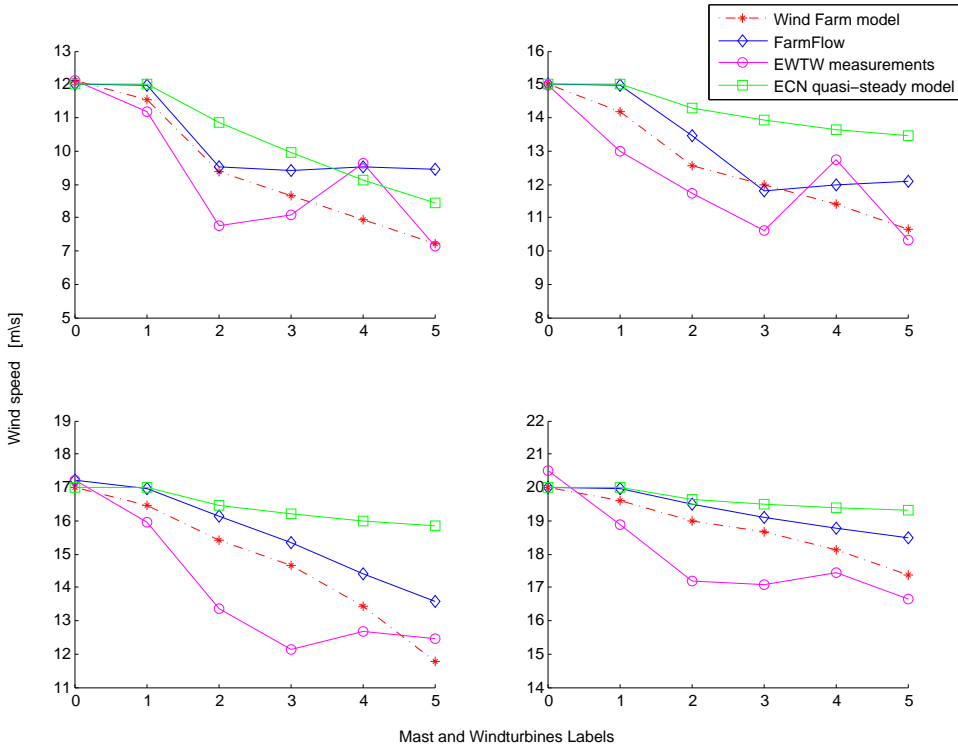
Figure 5.9: Comparing the results with results from two other models and EWTW measurements for wind speeds 12, 15, 17, 20 m/s at Meteo -Mast

a staggered grid using the finite difference method. A state space representation of the model has been provided to be used in wind farm control algorithms along with load and power optimizations. As far as the wind speed is concerned, the outcome of the model has been compared with measurement data of the EWTW wind farm, FarmFlow software, and ECN's quasi-steady wind flow model. Afterwards, the yaw angle information has been added to the model and the simulations repeated. The comparison results were seen very satisfactory, especially after incorporating the yaw angle measurements.

The most important drawback of this model is neglecting wind shear and lack of a turbulence model to make the calculations much more accurate. However, since the main goal of developing the model is to be implemented in control algorithms, a less accurate model is acceptable and it can be compensated in future works. Furthermore, the finer the staggered grid, the better the accuracy and the larger the system matrices. Therefore, considering the computational resources of the control algorithm, a trade-off has been made between the size of the grid and accuracy. The numerical accuracy of the method will be estimated in future
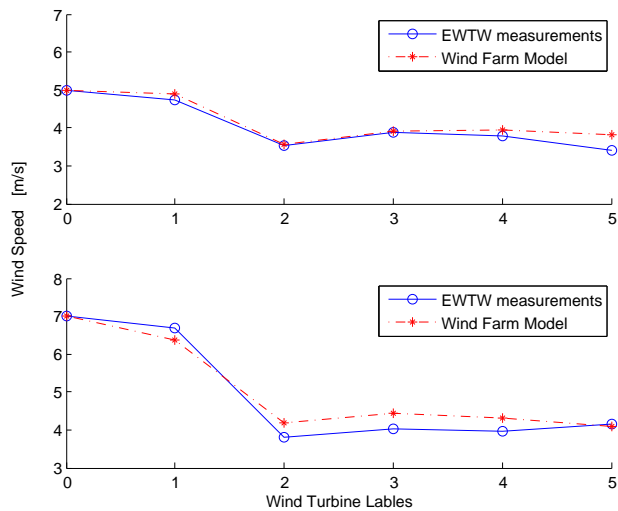
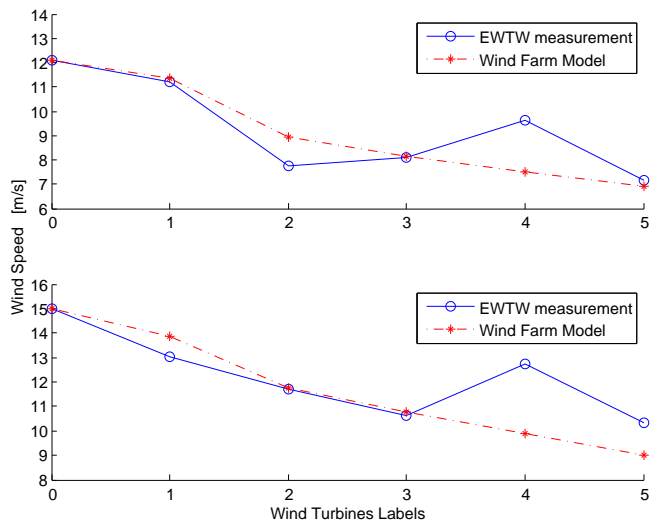Figure 5.10: Comparision of results with measurements in low wind speed, considering the yaw angle

Figure 5.11: Comparision of results with measurements in high wind speed, considering the yaw angle
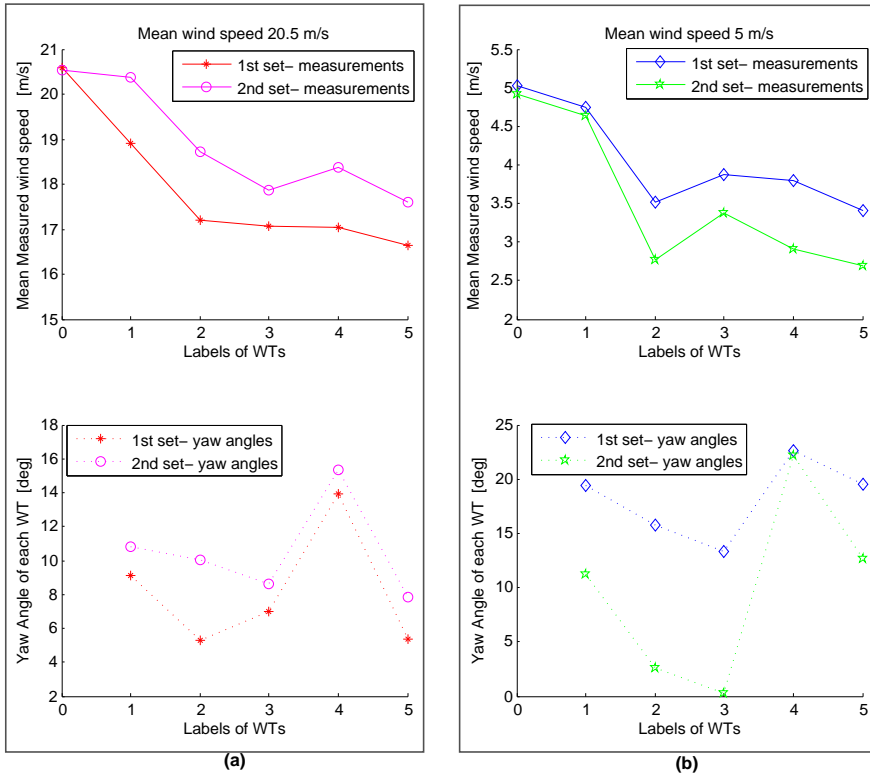
Figure 5.12: Comparing the yaw angles of the two sets of measurements; (a) initial mean wind speed for both sets= 20.5 m/s, (b) initial mean wind speed for both sets= 5 m/s

works, to be used in other applications.

References

[1] L. Fernandez, C. Garcia, J. Saenz, and F. Jurado, "Equivalent models of wind farms by using aggregated wind turbines and equivalent winds," *Energy Conversion and Management*, vol. 50, no. 3, pp. 691 – 704, 2009.

[2] P.-E. Rethore, A. Bechmann, N. Sørensen, S. T. Frandsen, and J. Mann, "A cfd model of the wake of an offshore wind farm: using a prescribed wake inflow," *Journal of Physics: Conference Series*, vol. 75, no. 1, p. 012047, 2007.

[3] U. A. Ozturk, "Heuristic methods for wind energy conversion system positioning," *Electric Power Systems Research*, vol. 70, pp. 179–185, 2004.

[4] M. A. Lackner and C. Elkinton, "An analytical framework for offshore wind farm layout optimization," *Wind Engineering*, vol. 31, pp. 17–31, 2007.

[5] C. Elkinton, J. F. Manwell, and J. G. McGowan, "Algorithms for offshore wind farm layout optimization," *Wind Engineering*, vol. 32, pp. 67–84, 2008.

[6] V. Akhmatov, H. Knudsen, A. H. Nielsen, J. K. Pedersen, and N. K. Poulsen, "Modelling and transient stability of large wind farms," *International Journal of Electrical Power & Energy Systems*, vol. 25, no. 2, pp. 123 – 144, 2003.

[7] Y. Kazachkov, J. Feltes, and R. Zavadil, "Modeling wind farms for power system stability studies," in *Power Engineering Society General Meeting*, vol. 3, July 2003, p. 1533.

[8] J. Trujillo, A. Wessel, I. Waldl, and B. Lange, "Online modeling of wind farm power for performance surveillance and optimization," *Wind Energy*, vol. Proceedings of the Euromech Colloquium, pp. 163–166, 2007.

[9] J. Rodriguez-Amenedo, S. Arnaltes, and M. Rodriguez, "Operation and coordinated control of fixed and variable speed wind farms," *Renewable Energy*, vol. 33, no. 3, pp. 406 – 414, 2008.

[10] A. Crespo, J. Hernández, and S. Frandsen, "Survey of modelling methods for wind turbine wakes and wind farms," *Wind Energy*, vol. 2, pp. 1–24, Jan. 1999.

[11] G. Larsen, H. Madsen, T. Larsen, and N. Troldborg, "Wake modeling and simulation," Forskningscenter Risø Roskilde, Tech. Rep., 2008.

[12] A. J. Brand and J. W. Wagenaar, "A quasi-steady wind farm flow model in the context of distributed control of the wind farm," in *European Wind Energy Conference (EWEC 2010)*, 2010.

[13] L. M. Fernandez, J. R. Saenz, and F. Jurado, "Dynamic models of wind farms with fixed speed wind turbines," *Renewable Energy*, vol. 31, no. 8, pp. 1203 – 1230, 2006.

[14] R. Barthelmie, O. Rathmann, S. Frandsen, K. Hansen, and E. Politis, "Modelling and measurements of wakes in large wind farms," *Journal of Physics: Conference Series*, vol. 75, no. 1, p. 012049, 2007.

[15] S. Frandsen, R. Barthelmie, S. Pryor, O. Rathmann, S. Larsen, J. Hojstrup, and M. Thogersen, "Analytical modelling of wind speed deficit in large offshore wind farms," *Wind Energy*, vol. 9, p. 15, 2006.

[16] T. Burton, D. Sharpe, N. Jenkins, and E. Bossanyi, *Wind Energy Handbook*. John Wiley and Sons, 2001.

[17] G. Strang, *Computational science and engineering*. Wellesley, MA: Wellesley-Cambridge Press, 2007.

[18] W. Kress and J. Nilsson, "Boundary conditions and estimates for the linearized navier-stokes equations on staggered grids," *Computers & Fluids*, vol. 32, no. 8, pp. 1093–1112, 2003.

[19] L. J. Vermeer, J. N. Sørensen, and A. Crespo, "Wind turbine wake aerodynamics," *Progress in Aerospace Sciences*, vol. 39, no. 6-7, pp. 467 – 510, 2003.

[20] A. E. Kasmi and C. Masson, "An extended k-epsilon model for turbulent flow through horizontal-axis wind turbines," *Journal of Wind Engineering and Industrial Aerodynamics*, vol. 96, no. 1, pp. 103 – 122, 2008.

[21] F. Bianchi, H. De Battista, and R. Mantz, *Wind turbine control systems: principles, modelling and gain scheduling design*. Springer Verlag, 2006.

[22] B. Seibold, "A compact and fast matlab code solving the incompressible navier-stokes equations on rectangular domains," applied Mathematics, Massachusetts Institute of Technology, 2008.

[23] M. Soleimanzadeh and R. Wisniewski, "Wind deficit model in a wind farm using finite volume method," in *Proceedings of American Control Conference (ACC)*, 2010.

[24] ——, "Controller design for a wind farm, considering both power and load aspects," *Mechatronics*, vol. 21, no. 4, pp. 720 – 727, 2011.

[25] D. Madjidian, K. Mårtensson, and A. Rantzer, "A distributed power coordination scheme for fatigue load reduction in wind farms," in *American control conference*, 2011.

[26] M. Soleimanzadeh, R. Wisniewski, and S. Kanev, "An optimization framework for load and power distribution in wind farms," *Wind Engineering & Industrial Aerodynamics*, vol. 107108, p. 256262, 2012.

[27] , *AIAA Guide for the Verification and Validation of Computational Fluid Dynamics Simulations*. American Institute of Aeronautics & Astronautics, 1998, no. AIAA-G-077-1998.

[28] P. Eecen and E. Bot, "Improvements to the ecn wind farm optimisation software "farmflow"," in *Presented at the European Wind Energy Conference & Exhibition, Warsaw, Poland*, 20 - 23 April 2010.

Paper B

Controller Design for a Wind Farm, Considering both Power and Load Aspects

Maryam Soleimanzadeh and Rafael Wisniewski

Abstract

In this paper, a wind farm controller is developed that distributes power references among wind turbines while it reduces their structural loads. The proposed controller is based on a spatially discrete model of the farm, which delivers an approximation of wind speed in the vicinity of each wind turbine. The control algorithm determines the reference signals for each individual wind turbine controller in two scenarios based on low and high wind speed. In low wind speed, the reference signals for rotor speed are adjusted, taking the trade-off between power maximization and load minimization into account. In high wind speed, the power and pitch reference signals are determined while structural loads are minimized. To the best of authors' knowledge, the proposed dynamical model is a suitable framework for control, since it provides a dynamic structure for behavior of the flow in wind farms. Moreover, the controller has been proven exceptionally useful in solving the problem of both power and load optimization on the basis of this model.

1   Introduction

Wind farms help reduce the average cost of wind energy compared to individual turbines located far from each other [1]. Furthermore, the strategy of extracting maximum power of each wind turbine does not result in maximal power capture for the entire farm [2]. The reason is that the upwind turbines slow down the wind that reaches downwind turbines, by extracting too much power. Therefore, a controller should be designed for the farm to adjust the power extraction. Design of controllers for wind farms presents a challenge to prognosticate the effect of the wake formed behind a wind turbine on the other wind turbines. This challenge originates in the significant decrement in mean wind speed reaching downwind turbines, and the increment in turbulence. The increase in turbulence intensity in wakes behind wind turbines can result in a substantial increase in fatigue [3].

The research area of wind farm control can chiefly be divided into two main categories. The first is the quality control of the generated electrical power, which is not the subject of interest in this paper. The second is the coordinated control of power generated by each individual turbine such that the aerodynamic interactions between turbines are minimized [2]. In spite of some results on aerodynamic interactions in a farm [1, 4], the subject is still immature.

There are numerous research in modeling and control of wind farms. An overall wind farm control that maximizes energy capture has been proposed in [4]. An optimization method to maximize the production of farms based on limitations of the physical system, e.g., voltage, voltage stability, generator power, has been proposed in [5]. Advanced controllers for wind farm electrical systems have been developed in [6, 7]. The focus of [7] is the coordinated control of wind farms in three control levels: central control, wind farm control, and individual turbine control. A comparison of three control strategies for control of active and reactive power is provided in [8]. In [9], a concept with both centralized control and

Nomenclature and Abbreviations

β	Pitch angle of a wind turbine
β_i	Pitch angle of the ith turbine
λ	Tip speed ratio
Ω	Rotor speed of a wind turbine
Ω_i	Rotor speed of the ith turbine
Γ	diffusion coefficient
ρ	Air density
cv	Abb. for Control volume
C_T	Thrust coefficient
C_P	Power coefficient
C_Q	Torque coefficient
D	Damping factor
F_T	Thrust force
f_t	Tangential force
K	Tower Stiffness
M	Tower Mass
P_{Wt_i}	Produced power by i^{th} turbine
$P_{ref}^{Wt_i}$	Reference power for i^{th} turbine
P_{ref}^{Wf}	Reference power for the wind farm
R	Rotor diameter
S	Source term, Gradient of pressure
$S_{P_{i,j}}$	Gradient of pressure in control volume (i,j)
$U_{i,j}$	Mean Wind speed in control volume (i,j)
U	Spatially distributed wind speed
V	Mean Wind speed at a wind turbine
V_i	Mean Wind speed at i^{th} turbine
WT	Abb. for Wind turbine
WS	Abb. for Wind speed
X	State space variable for U
x_{FA}	Tower fore-aft (longitudinal)displacement
x_{SS}	Tower side-to-side (lateral) displacement

control for each individual wind turbine is presented. In this approach, the controllers at turbine level ensure that relevant reference commands provided by the centralized controller are followed. Despite these control methods and many research efforts on fatigue load reduction in single turbines [10, 11, 12, 13], results on combined optimization of power and fatigue load are lacking.

In large wind farms, the upwind turbines extract most of the power from wind and increase the turbulence intensity in the wake reaching other turbines. Thus, the fluctuations and vibrations of the downwind turbines are greater than upwind turbines and results in more fatigue loads on them [14]. Therefore, the lifetimes of turbines that most frequently are in the downwind location are shortest. This fact results in reduction of the effective lifetime of the whole farm. In conclusion, wind farm controllers should employ proper strategies to reduce the extreme fatigue loads. Indeed, this can be performed by power set-point adjustment. This is possible since the wind farm controller is responsible for distribution of the power set-points between the turbines and for ensuring that the total time varying power reference commanded by the operator is satisfied.

In this regard, the aim of the present work is to develop a wind farm controller which aims at optimal distribution of power references among wind turbines, while it lessens the structural loads. An optimal control method is applied for controller design. In short, the controller computes required reference signals for each wind turbine controller. However, the specific wind turbine controller that tracks the reference is not addressed in this study as there are huge number of references that address this particular problem, e.g., [15, 16, 17]. The optimal control problem studied in this paper, is founded on a wind flow dynamic model [18], which is based on finite volume method and delivers an approximation of wind speed in the vicinity of each wind turbine.

2 Wind Farm Configuration and Modeling

Farm Configuration

The case study in this paper is a small wind farm that consists of five wind turbines arranged in a row, as shown in Fig. 6.1. It is one of the two configurations that has been modeled in [18]. The model for the chosen configuration has been validated using appropriate measurement data in [18]. The control procedure proposed here can be generalized to larger farms by substituting the model used in this work by the model of a farm with the several rows of turbines.

The distance between each wind turbine is about 300 meters. There are two meteorological masts located in the positions $\triangle 1$ and $\triangle 2$. For all cases wind is assumed to be in the direction indicated in Fig. 6.1. As a consequence, the measurements of mast 1 will be used in simulation as the initial conditions. In the paper, the wind turbines are assumed to have individual variable speed-variable
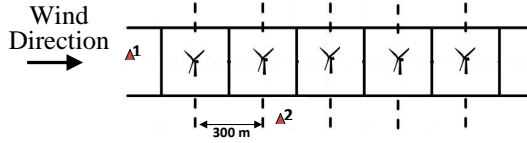
Figure 6.1: Wind farm configuration

pitch control (each turbine has its own control). Finally, wind flow model and measurements are assumed to be at the hub-height and in the far wake region.

Wind Flow Model in a Farm

The controller design is based on a dynamical model for wind speed in a wind farm, developed in [18]. The model is based on the finite volume discretization of Navier-Stokes equation in the far wake region, using thin shear layer approximation. With this approximation in the flow equation, the turbulence and viscosity terms are neglected. Since the ambient flow is to some extent affected by the wakes of the upstream turbines, our approach is to solve the flow equation for the whole wind farm instead of its part. Combining the flow equation and the continuity equation [19] forms the following differential equation system, which is solved in [18] by finite volume method to model the wake flow:

$$\frac{\partial}{\partial x}(\Gamma\frac{\partial U}{\partial x}) + \frac{\partial}{\partial y}(\Gamma\frac{\partial U}{\partial y}) + S = \rho\frac{\partial U}{\partial t}, \tag{6.1}$$

where U, Γ and ρ are the mean wind speed, diffusion coefficient and air density, respectively. S is the gradient of pressure [19].

In order to solve (6.1), the first step is to define a finite volume grid. The wind farm is divided into non-overlapping control volumes (cells) in $\mathbb{R}^2$ by the lines that define their boundaries. The pattern created by the lines is called a computational grid or a mesh.

The control volume integration forms the key step of the finite volume method, which is used to transform (6.1) to a system of discrete equations for the nodal values of U. First, (6.1) is integrated over a typical control volume depicted in Fig. 6.2. This reduces each equation to one involving only first derivatives in space. Subsequently, these derivatives are replaced with central difference approximations [19].

$$\int_{\Delta t}\int_{cv}\left[\frac{\partial}{\partial x}(\Gamma\frac{\partial U}{\partial x}) + \frac{\partial}{\partial y}(\Gamma\frac{\partial U}{\partial y})\right]dvdt + \int_{\Delta t}\int_{cv}Sdvdt = \int_{\Delta t}\frac{\partial}{\partial t}\left(\int_{cv}\rho Udv\right)dt. \tag{6.2}$$
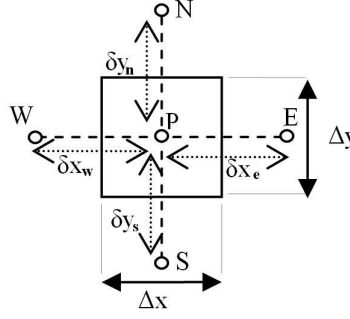
Figure 6.2: A typical control volume

The central difference approximation for each term of (6.2) is:

$$\int_{cv} \frac{\partial}{\partial x}(\Gamma \frac{\partial U}{\partial x})dv \approx \left[\Gamma \frac{U_E - U_P}{\delta x_e} - \Gamma \frac{U_P - U_W}{\delta x_w}\right] \Delta y, \qquad (6.3)$$

$$\int_{cv} \frac{\partial}{\partial y}(\Gamma \frac{\partial U}{\partial y})dv \approx \left[\Gamma \frac{U_N - U_P}{\delta y_n} - \Gamma \frac{U_P - U_S}{\delta y_s}\right] \Delta x, \qquad (6.4)$$

$$\int_{cv} S dv \approx S_P \Delta x \Delta y, \qquad (6.5)$$

$$\frac{\partial}{\partial t}\int_{cv} \rho U dv \approx \rho \frac{\partial U_P}{\partial t}\Delta x \Delta y, \qquad (6.6)$$

where $\delta(.)_{(.)}$ and P,N,E,S,W in $U_{(.)}$ are defined in Fig. 6.2. After substitution of equations (6.3)-(6.6) into (6.2) and rearranging, we derive a discrete-space equation for the nodal values of U for each control volume:

$$\rho\frac{\partial U_{P_{i,j}}}{\partial t} + a_P U_{P_{i,j}} - a_E U_{E_{i,j}} - a_W U_{W_{i,j}} - a_N U_{N_{i,j}} - a_S U_{S_{i,j}} = S_{P_{i,j}}. \quad (6.7)$$

The (i,j) subscript refers to the cell $(i,j)^{th}$ in the mesh, and the coefficients a_o, $o \in \{P, E, W, N, S\}$ are defined in Table 6.1.

The wind turbines are modeled by means of their thrust coefficient using the actuator disc approach [16]. The influence of the wind turbines on the wind flow are modeled in the source term S as drop pressure and reduction in wind velocity. The source term is proportional to wind pressure gradient that should be updated for each wind turbine in every computation loop. As a consequence, the velocity will be updated and an approximation of the wind speed will be obtained for each cell. Therefore, the mean wind speed in the middle of each control volume is defined as a state space variable, and the total number of state variables is equal

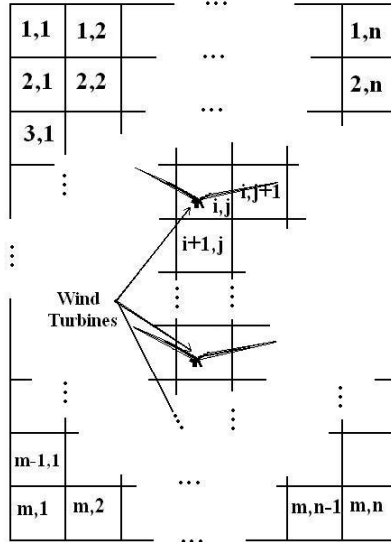| Coefficients	Value
a_E	$\frac{-\Gamma}{\Delta x \delta xe}$
a_W	$\frac{-\Gamma}{\Delta x \delta xw}$
a_N	$\frac{-\Gamma}{\Delta y \delta yn}$
a_S	$\frac{-\Gamma}{\Delta y \delta ys}$
a_P	$-(a_E + a_W + a_N + a_S)$

Table 6.1: coefficients of (6.7)

Figure 6.3: Wind farm $n \times m$ mesh

to the number of cells in the mesh. Thus, the state vector X in (8) corresponds to a $n \times m$ mesh as shown in Fig. 6.3. In the simulations, a 30×160 mesh has been used. The mesh has 160 cells in the direction of wind and 30 cells in the direction orthogonal to the wind direction.

$$X = \left[U_{P_{1,1}}, U_{P_{1,2}}, \cdots, U_{P_{1,n}}, U_{P_{2,1}}, U_{P_{2,2}}, \cdots, U_{P_{2,n}}, \cdots, U_{P_{m,1}}, U_{P_{m,2}}, \cdots, U_{P_{m,n}} \right]^T .$$
(6.8)

Then, the dynamic equations of the wind farm are as follows:

$$\dot{x}_1 = \frac{-1}{\rho}\left(a_P x_1 - a_E x_2 - a_S x_{n+1} - \left[S_{P_{1,1}} + a_W U_{W_{1,1}} + a_N U_{N_{1,1}}\right]\right)$$

$$(6.9)$$

$$\dot{x}_2 = \frac{-1}{\rho}\left(a_P x_2 - a_W x_1 - a_E x_3 - a_S x_{n+2} - \left[S_{P_{1,2}} + a_N U_{N_{1,2}}\right]\right) \quad (6.10)$$

$$\vdots \qquad\qquad (6.11)$$

$$\dot{x}_n = \frac{-1}{\rho}\left(a_P x_n - a_W x_{n-1} - a_S x_{2n} - \left[S_{P_{1,n}} + a_E U_{E_{1,n}} + a_N U_{N_{1,n}}\right]\right)$$

$$\dot{x}_{n+1} = \frac{-1}{\rho}\left(a_P x_{n+1} - a_N x_1 - a_E x_{n+2} - a_S x_{2n+1} - \left[S_{P_{2,1}} + a_W U_{W_{2,1}}\right]\right)$$

$$(6.12)$$

$$\dot{x}_{n+2} = \frac{-1}{\rho}\left(a_P x_{n+2} - a_W x_{n+1} - a_N x_2 - a_E x_{n+3} - a_S x_{2n+2} - S_{P_{2,1}}\right)$$

$$(6.13)$$

$$\vdots \qquad\qquad (6.14)$$

$$\dot{x}_l = \frac{-1}{\rho}\left(a_P F_{WT} x_l - a_W x_{l-1} - a_N x_{l-n} - a_E x_{n+3} - a_S x_{2n+2} - S_{P_{i,j}}\right)$$

$$\dot{x}_{l+1} = \frac{-1}{\rho}(a_P F_{WT} x_{l+1} - a_W x_l - a_N x_{l+1-n} - a_E x_{l+2} - a_S x_{l+n+1}$$

$$-S_{P_{i,j+1}})$$

$$\vdots \qquad\qquad (6.15)$$

$$\dot{x}_{l+n} = \frac{-1}{\rho}(a_P x_{l+n} - a_W x_{l+n-1} - a_E x_{l+n+1} - a_N F_{WT} x_l - a_S x_{l+2n}$$

$$-S_{P_{i+1,j}})$$

$$\vdots \qquad\qquad (6.16)$$

$$\dot{x}_{mn} = \frac{-1}{\rho}\left(a_P x_{mn} - a_W x_{mn-1} - a_N x_{mn-n} - \left[S_{P_{m,n}} + a_E U_{E_{m,n}} + a_S U_{S_{m,n}}\right]\right),$$

$$(6.17)$$

where $F_{WT} = (1 - 2a_{WT})$, $WT = 1, ..., 5$, and $a_{WT} = 1/2(1 + \sqrt{1 - C_{T_i}})$. F_{WT} is proportional to the control input. $S_{P_{i,j}}$ is the gradient of pressure of each cell with respect to the adjacent cell, and it is also related to the control input by $S_P \approx (\rho/2)U^2 C_T$ [16]. In conclusion, the equations (6.9)-(6.17) are the dynamic equations of the wind farm and are written in the following form:

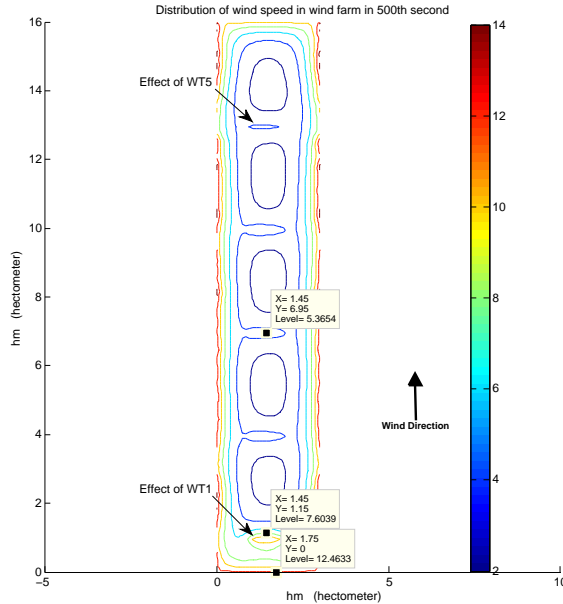$$\dot{X} = A(t, u)X + B(t, u). \qquad (6.18)$$

Figure 6.4: Simulation of the wind farm behavior in a few second

In (6.18), X is a vector of mean wind speed over the farm as in (6.8); A is a block diagonal matrix; u is the thrust coefficient and thereby a function of the pitch angle. Thus, u is the system input. Validation and accuracy of the model have been investigated in [18].

The wind distribution in the farm has been computed from (6.18), and the simulation result in second 500th (in 1 second) has been shown in Fig. 6.4. In the figure, the location of the first turbine is indicated by $WT1$ and the fifth one by $WT5$. The wind is assumed to blow in the depicted direction. The reduction of wind speed after each wind turbine can be seen in the figure by comparing the colors, the colors closer to blue represent lower wind speeds. The model will define the boundaries of the optimal control problem in Section 3.

3 The Overall Farm Control System

Conventionally, a system operator determines the production of the wind farm based on the status of the network. The operator sends a power demand to the wind farm controller, and the controller distributes the demanded power between wind turbines almost equally (this will be elaborated in Section 3) and sends them out to every wind turbine [9].

In this paper, in low wind speed, the maximum possible power from each wind turbine should be extracted while fatigue loads are minimized. In other words, a
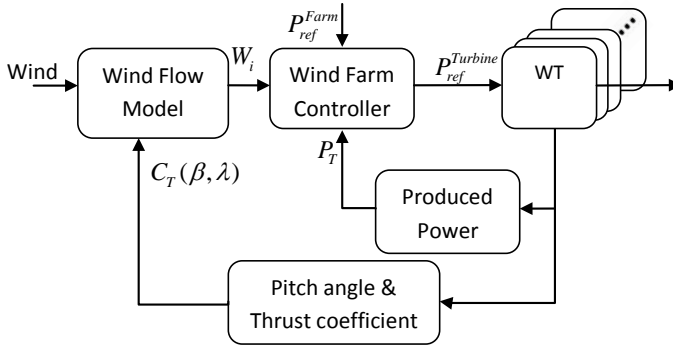
Figure 6.5: Overall control system

trade-off is considered between maximum power production and load reduction. In this operation region, the rotor speed varies to produce the optimum power. Accordingly, the goal of the farm controller in low wind speed is to determine the rotor speed set-points for each wind turbine, such that the trade-off between power production and wind turbines loads is resolved.

In high wind speed, wind farm controller will provide power reference and pitch reference for each wind turbine control system. The power references provided by the controller should track the total demanded power by the operator. Furthermore, the power and the pitch angle set-points should be determined considering fatigue load minimization.

The overall control system is shown in Fig. 6.5. The Wind Farm Controller controls the power production of the wind farm by sending out power references to each individual wind turbine. The controller of each wind turbine ensures that the reference sent from the wind farm controller is executed. Though, the controllers for individual wind turbines are not addressed in this paper, but there are huge numbers of references on this particular [15, 16, 17].

Control Strategy

Since the turbines are assumed to be variable speed, they can reduce the fluctuations of the drive train torque either by reducing the rotor speed or by pitching the blades [20]. Structural load analysis has shown that pitching the blades to reduce the power has a small influence on loads. Whereas, reducing the speed considerably decreases the structural load. Therefore, a trade-off should be made between reduction of fluctuations and power capture [21, 20].

Below rated wind speed, wind turbines are to produce as much power as possible, so the pitch angle is kept almost constant. Furthermore, the aerodynamic loads below rated wind speed are generally lower than those above it. Above

the rated wind speed, the pitch angle variations strongly influence the turbine dynamics, in particular the tower dynamics. As the blades pitch to regulate the aerodynamic torque, the aerodynamic thrust on the rotor changes substantially. These substantial changes result in tower vibration [22]. As analyzed in [23], the tower fore-aft motion is strongly coupled with the blade flap motion. Moreover, the tower side-to-side motion is strongly coupled with the blade edge and drive train torsion. Accordingly, one of our objectives is to reduce the tower fluctuations (fore-aft and side-to-side), which will significantly reduce fatigue loads.

The tower motion dynamics can be approximated by a second order system of differential equations. Assuming that there is no coupling between tower fore-aft and tower side-to-side dynamics, the following equations are devised [10, 24]:

$$M \times \begin{bmatrix} 1 & 0 \\ 0 & 1 \end{bmatrix} \begin{bmatrix} \ddot{x}_{FA} \\ \ddot{x}_{SS} \end{bmatrix} + D \times \begin{bmatrix} 1 & 0 \\ 0 & 1 \end{bmatrix} \begin{bmatrix} \dot{x}_{FA} \\ \dot{x}_{SS} \end{bmatrix} + K \times \begin{bmatrix} 1 & 0 \\ 0 & 1 \end{bmatrix} \begin{bmatrix} x_{FA} \\ x_{SS} \end{bmatrix} = \begin{bmatrix} F_T \\ f_t \end{bmatrix}, \quad (6.19)$$

where x_{FA} is the tower fore-aft displacement and x_{SS} is the tower side-to-side displacement. M, D and K are the mass, damping and stiffness. $F_T(.,.)$ is the thrust force, and is equal to:

$$F_T(C_T, V) = \frac{1}{2} \rho \pi R^2 V^2 C_T, \quad (6.20)$$

where ρ and R are respectively air density and rotor radius. V is the mean wind speed in the vicinity of a wind turbine. Whenever we specifically refer to the mean wind speed at i^{th} wind turbine, we use the notation V_i. $C_T(\beta, \lambda)$ is the thrust coefficient and β and λ are the pitch angle and the tip speed ratio, where $\lambda = \Omega R / V$. Moreover, Ω is the rotor speed of each wind turbine and Ω_i is the rotor speed at i^{th} turbine. We use similar notation for pitch angle β and the ith wind turbine pith angle β_i. $f_t(.,.)$ is the tangential force, and is equal to [22]:

$$f_t(C_Q, V) = \frac{1}{2} \rho \pi R^2 V^2 C_Q. \quad (6.21)$$

$C_Q(\beta, \lambda)$ is the torque coefficient and $C_Q = C_P/\lambda$, where $C_P(\beta, \lambda)$ is the power coefficient.

As previously mentioned, one of our goals is to reduce fatigue by means of increasing tower damping. Bearing this in mind, we increase the tower damping factor D, in dynamic equations to a desired level. In order to maximize the conversion efficiency in the low wind speed region, the rotor speed is changed in proportion to the wind speed to maintain the optimal level; whereas, the pitch angle is kept constant at an initial value. For high wind speeds, the rotor speed is kept constant, and the pitch angle is increased to limit the captured power at its rated value. Therefore, the control problem will be considered separately for low and high wind speed.

Below rated wind speed control

In the low wind speed region, since the pitch angle is kept constant, an additional thrust can be produced by rotor speed variations to increase damping, $\Delta F_T(C_T, V) \propto \Delta C_T(\lambda(V, \Omega))$. In this regard, the variation of $C_T(\lambda(V, \Omega))$ is approximated by a linear function:

$$\Delta C_T(V, \Omega) = \frac{\partial C_T(V, \Omega)}{\partial \Omega} \Delta \Omega, \tag{6.22}$$

where $\Delta \Omega$ is the small variations of rotor speed that causes torque perturbation, which increases effective damping. Hence, $\Delta \Omega$ increases the damping factor D, and is proportional to $-\dot{x}_{FA}$:

$$\Delta \Omega \approx \frac{-D_P}{\frac{1}{2} \rho \pi R^2 V^2 \partial C_T(V, \Omega) / \partial \Omega} \dot{x}_{FA}, \tag{6.23}$$

where D_P is additional damping factor. Therefore, in low wind speed:

$$\Delta F_T(C_T, V) = \frac{1}{2} \rho \pi R^2 V^2 \frac{\partial C_T(V, \Omega)}{\partial \Omega} \Delta \Omega \approx -D_P \dot{x}_{FA}. \tag{6.24}$$

In other words, tower damping D in the tower model is added to another damping factor D_P because of the rotor speed perturbations. As a result, the system model has a new set of parameters.

The tangential force variations can be approximated as follows:

$$\Delta f_t(C_P, V) \propto \Delta(C_Q) \propto \Delta(C_P / \lambda), \tag{6.25}$$

$$\Delta C_Q(V, \Omega) \approx \frac{\partial(\Omega C_P(V, \Omega))}{\partial \Omega} \Delta \Omega \approx \left[C_P(V, \Omega) + \Omega \frac{\partial C_P(V, \Omega)}{\partial \Omega} \right] \Delta \Omega. \tag{6.26}$$

In a similar way to fore-aft movement, side-to-side additional damping will be introduced as follows:

$$\Delta \Omega \approx \frac{-D_P}{\frac{1}{2} \rho \pi R^2 V^2 \left[C_P + \Omega \partial C_P(V, \Omega) / \partial \Omega \right]} \dot{x}_{SS}, \tag{6.27}$$

then:

$$\Delta f_t(C_Q, V) = \frac{1}{2} \rho \pi R^2 V^2 \frac{\partial(\Omega C_P(V, \Omega))}{\partial \Omega} \Delta \Omega \approx -D_P \dot{x}_{SS}. \tag{6.28}$$

On the other hand, the extracted power from each wind turbine is expressed as (for i^{th} turbine):

$$P_{Wt_i}(V_i, C_{P_i}) = \frac{1}{2}\rho\pi R^2 V_i^3 C_{P_i}, \tag{6.29}$$

where $C_P(\beta, \lambda)$ is the power coefficient, which is a function of pitch angle β, and tip speed ratio λ. In order to extract maximum power from wind farm, the total power should be maximized:

$$P_{total} = \sum_{i=1}^{N} P_{Wt_i}. \tag{6.30}$$

The summands P_{Wt_i} are given in (6.29), where $C_P(\beta, \lambda)$ is used as a part of the cost function for the controller. Since pitch is constant in low wind speed, $C_P(\beta, \lambda)$ only depends on V and Ω, thus we write $C_P(\lambda(V, \Omega))$. Finally, N is the number of wind turbines.

In order to solve the trade-off between load and power, the damping factors $\partial C_T(V, \Omega)/\partial \Omega$ and $C_P + \Omega \partial C_P(V, \Omega)/\partial \Omega$, based on (6.24) and (6.28), and the power coefficients $C_P(V, \Omega)$ based on (6.30), should be maximized. Hence, the cost function for the entire farm in low wind speed is (6.31), which should be maximized over Ω.

$$J_1(\Omega_1, ..., \Omega_N) = \gamma \int_{t_0}^{t_n} \sum_{i}^{N} C_{p_i}(V_i, \Omega_i) dt + (1 - \gamma) \int_{t_0}^{t_n} \Big(\sum_{i}^{N} \frac{\partial C_{T_i}(V_i, \Omega_i)}{\partial \Omega_i}$$
$$+ \sum_{i}^{N} \left[C_{P_i} + \Omega_i \frac{\partial C_{P_i}(V_i, \Omega_i)}{\partial \Omega_i} \right] \Big) dt, \tag{6.31}$$

subject to the dynamical constrain (6.18), which relates the wind speed V in the farm with the turbines aerodynamic interactions. Furthermore, $C_{P_i}(V_i, \Omega_i) \in [C_{P_i}^L, C_{P_i}^U]$, and $\Omega_i \in [\Omega_i^L, \Omega_i^U]$.

Above rated wind speed control

In the high wind speed, the pitch angle variation is used to limit the captured power, since the rotor speed is kept constant. It is analogous to (6.23)-(6.30) with the difference that in this region $\Delta F_T(C_T, V)$ and $\Delta f_t(C_Q, V)$ are estimated knowing the pitch angle variations, $\Delta \beta$.

$$\Delta F_T(C_T, V) \approx \frac{1}{2}\rho\pi R^2 V^2 \frac{\partial C_T(V, \beta)}{\partial \beta}\Delta\beta = -D_P \dot{x}_{FA}$$
$$\Delta f_t(C_P/\lambda, V) \approx \frac{1}{2}\rho\pi R^2 V^2 \frac{\partial C_P(V, \beta)}{\partial \beta}\Delta\beta = -D_P \dot{x}_{SS}, \tag{6.32}$$

where D_P is additional damping. This method significantly increases the tower damping and reduces the fatigue loads. Although, sometimes this type of analysis may not be sufficient, and it would be essential to design additional feedback to adjust some other parameters (e.g. blade passing frequency; for more information see [24]).

In the high wind speed, the captured power from wind farm which is a sum of power outputs from all wind turbines should be equal to the reference power. This means that $\sum_i^N P_{Wt_i}(V_i, C_{p_i}) - P_{ref}^{Wf}$ should be kept at 0. In other words, the power produced by all turbines $\sum_i^N P_{Wt_i}(V_i, C_{p_i})$ should follow the wind farm power reference signal; or the power produced by each turbine $P_{Wt_i}(V, C_p)$, should follow each turbine reference signal $P_{ref}^{Wt_i}$. Since in this region the rotor speed is kept constant and power coefficient depends on pitch and wind speed, $C_p(V, \beta)$, the produced power is written as a function of pitch angle $P_{Wt}(V, \beta)$. In summary, the $P_{Wt}(V, \beta) - P_{ref}^{Wt}$ value is a part of a cost function for the controller. Hence, for 1st to N^{th} wind turbine the cost function in high wind speed is (6.33), which should be maximized over β and $P_{ref}^{Wt_i}$.

$$
J_2(\beta_1, ..., \beta_N, P_{ref}^{Wt_i}) = -\gamma \int_{t_0}^{t_n} \sum_i^N (P_{Wt_i}(V_i, C_{p_i}) - P_{ref}^{Wt_i})^2 dt
$$

$$
+ (1 - \gamma) \int_{t_0}^{t_n} \left[\sum_i^N \frac{\partial C_{T_i}(V_i, \beta_i)}{\partial \beta_i} + \sum_i^N \frac{\partial C_{P_i}(V_i, \beta_i)}{\partial \beta_i} \right] dt,
$$

$$(6.33)$$

subject to the dynamical constraint (6.18), and $\sum_i^N P_{ref}^{Wt_i} = P_{ref}^{Wf}$, and $\beta_i \in [\beta_i^L, \beta_i^U]$.

Control solution

To complete the model, mathematical expressions for the functions $C_P(.,.)$ and $C_T(.,.)$ are derived in the sequel. In this paper, the mathematical relations are estimated based on numerical tables of NREL wind turbine [25]. The estimated nonlinear polynomial for $C_P(.,.)$ is expressed as follows,

$$
C_P(\beta, \lambda) = p_{00} + p_{10}\beta + p_{01}\lambda + p_{20}\beta^2 + p_{11}\beta\lambda + p_{02}\lambda^2. \qquad (6.34)
$$

The graph of the $C_P(.,.)$ function is shown in Fig. 6.6. The available data provides the possibility to estimate the $C_T(.,.)$. The estimated nonlinear polynomial for $C_T(.,.)$ is:
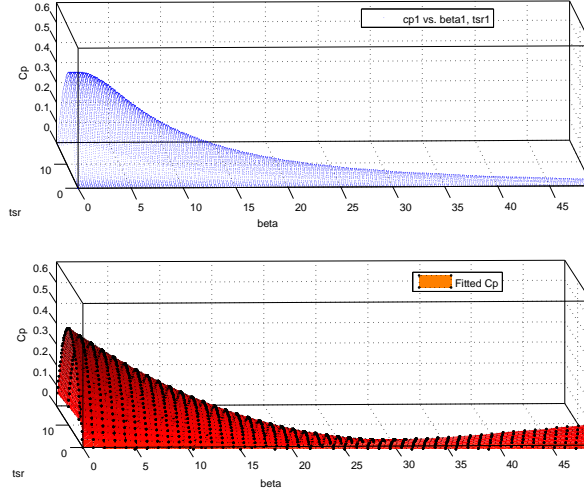
Figure 6.6: Estimated function for $C_P(\beta, \lambda)$

$$C_T(\beta, \lambda) = k_{00} + k_{10}\beta + k_{01}\lambda + k_{20}\beta^2 + k_{11}\beta\lambda + k_{02}\lambda^2$$
$$+k_{30}\beta^3 + k_{21}\beta^2\lambda + k_{12}\beta\lambda^2 + k_{03}\lambda^3. \tag{6.35}$$

The optimal control problem is formulated and solved using YALMIP, a software tool for dynamic optimization [26]. The problems to be solved are specified as follows,

$$\min J_1(\Omega_1, ..., \Omega_N) \text{ such that } \begin{cases} C_{P_i}(V_i, \Omega_i) \in [C_{P_i}^L, C_{P_i}^U], \ i = 1 \cdots N \text{ (number of turbines)} \\ \Omega_i \in [\Omega_i^L, \Omega_i^U], \ i = 1 \cdots N \text{ (number of turbines)} \\ \dot{X} = A(t, u)X + B(t, u), \text{ which is equation (6.18)} \end{cases} \tag{6.36}$$

$$\min J_2(\beta_1, ..., \beta_N, P_{ref}^{Wt_i}) \text{ such that } \begin{cases} \sum_i^N P_{ref}^{Wt_i} = P_{ref}^{Wf}, \ P_{ref}^{Wf} \text{ is the farm demanded pow} \\ \beta_i \in [\beta_i^L, \beta_i^U], \ i = 1 \cdots N \text{ (number of turbines)} \\ \dot{X} = A(t, u)X + B(t, u), \text{ which is equation (6.18)} \end{cases} \tag{6.37}$$

In low wind speed, the problem (6.36) is solved using NREL 5MW turbines data [25] in 19 iterations with a variable step size between 0.25 to 1. Results are presented in Table 6.2. The wind speed graph for both low and high wind speed is shown in Fig. 6.7.
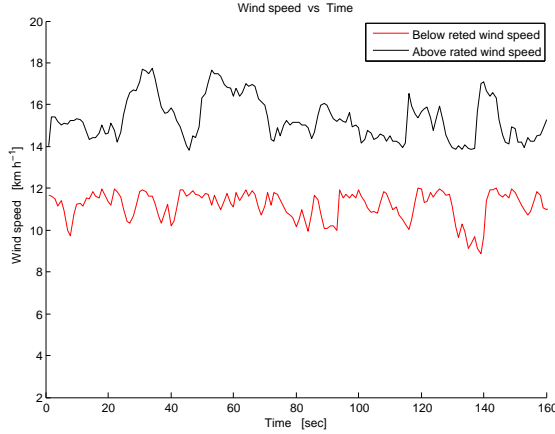
Figure 6.7: Wind speed graph

A comparison between the following two strategies in low wind speed is shown in Fig. 6.8. In red is the farm controller proposed in this paper, in blue is the conventional strategy, where each wind turbine produces as much energy as possible. The total power produced with the controller is 7.6201e+006 W, which is less than with conventional strategy, 8.2790e+006 W. The reason is that the farm controller has made a trade-off between load and power.

WS condition: Min WS= 8.88, Max Ws= 11.9 [m/s]
Maximum available power will be extracted from each turbine
Reference Ω obtained for each WT [m/s]
$\Omega_{Wt1} \approx 1.27$
$\Omega_{Wt2} \approx 0.885$
$\Omega_{Wt3} \approx 0.575$
$\Omega_{Wt4} \approx 0.670$
$\Omega_{Wt5} \approx 0.600$

Table 6.2: Optimal control solution for low wind speed

In high wind speed, problem (6.37) is solved using above mentioned data in 23 iterations with a variable step size between 0.0625 to 1. Results are presented in Table 6.3, where the power reference and reference pitch angle for each wind turbine is computed.

Power set-points for wind turbines determined by the proposed controller in high wind speed is compared with the power set-points determined by a conventional method. The comparison results are depicted in Fig. 6.9. For both strategies, the total power set-point of the farm is $P_{ref}^{Wf} = 1.5 \times 10^6 W$. The power
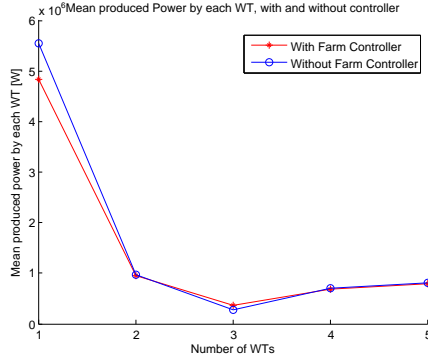
Figure 6.8: Comparison of mean produced power by each WT in low wind speed, with and without wind farm controller

set-points for individual wind turbines using a conventional strategy (shown with blue) are determined by $P_{ref}^{Wt_i} = P_{ref}^{Wf}(P_{avail}^{Wt_i}/\sum_i P_{avail}^{Wt_i})$, where $P_{avail}^{Wt_i}$ is the available power for each wind turbine. As seen in the figure, applying the farm controller the reference power set-point for the first wind turbine is considerably less than in the conventional approach. Whereas, other turbines produce a little more power, such that the total power for both cases is equal.

Furthermore, tower head displacements have been shown in Fig. 6.10. The optimal controller is proposed to increase the damping factor in the tower dynamics. In this regards, the oscillations of the tower are damped as shown by blue graph in the Fig. 6.10; and the result is the fatigue load decrement.

WS condition: Min WS= 13.84, Max Ws= 17.75 [m/s]	
β_{ref} mean value for each WT [Deg]	P_{ref}^{Wt} Mean value for each WT [W]
$\beta_{Wt1} \approx 20.5343$	$P_{ref}^{Wt1} \approx 7.3773 \times 10^5$
$\beta_{Wt2} \approx 7.9084$	$P_{ref}^{Wt2} \approx 5.1700 \times 10^5$
$\beta_{Wt3} \approx 1.0588$	$P_{ref}^{Wt3} \approx 8.1758 \times 10^4$
$\beta_{Wt4} \approx 0.3986$	$P_{ref}^{Wt4} \approx 8.1758 \times 10^4$
$\beta_{Wt5} \approx 0.8059$	$P_{ref}^{Wt5} \approx 8.1758 \times 10^4$

Table 6.3: Optimal control solution for high wind speed

4   Conclusions

A wind farm controller has been developed in this paper, which aims at optimal distribution of power reference among wind turbines and reduction of structural loads. This paper is one of a few researches in wind farm control that focuses on optimization of both power and load simultaneously, and the only one that
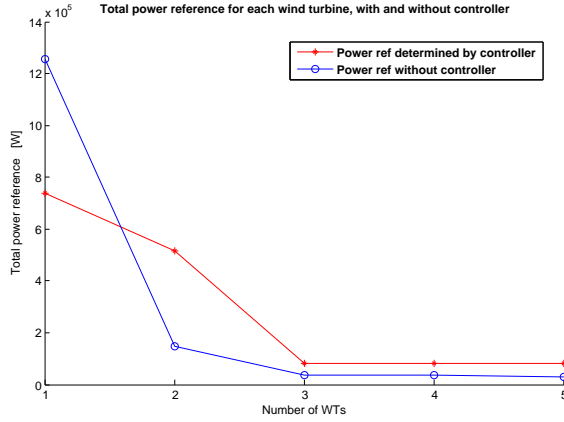
Figure 6.9: Total power reference for each wind turbine in high wind speed, with and without controller. Total demanded power from the wind farm for both cases is: $\sum_i^N P_{ref}^{Wt_i} = P_{ref}^{Wf} = 1.5 \times 10^6 W$
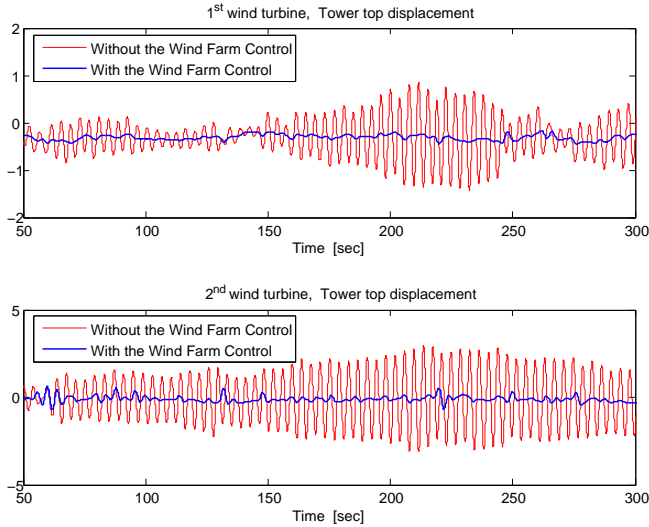

Figure 6.10: Tower top displacements of two wind turbines

founded on the dynamical model of the flow in wind farms. The wind farm model delivers wind speed in the vicinity of each wind turbine, and the proposed controller considers the turbine performance in both low and high wind speed. The control algorithm determines either the reference signals of power and pitch angle or the rotor speed for each wind turbine controller.

The controller strategy is applicable on any larger wind farm, if the farm dynamical model could provide required information. The main drawbacks of the dynamical model which is used as a basis of the controller design, are as follows:

- It considers only one wind direction for all the cases. (Wind turbines are not yawed)

- It does not consider the meandering between several rows and columns of wind turbines in a large farm.

Furthermore, the main drawback of the controller is that it does not consider the interactions between wind turbine controllers and the farm controller. Sending pitch angle reference signal to wind turbine controller may cause in instability in wind turbine control system. This important issue will be considered in future works.

References

[1] K. Johnson and N. Thomas, "Wind farm control: Addressing the aerodynamic interaction among wind turbines," in *Proc. American Control Conf*, 2009.

[2] L. Pao and K. Johnson, "A tutorial on the dynamics and control of wind turbines and wind farms," in *Proceedings of American Control Conf (ACC)*, 2009.

[3] J. Sørensen, S. Frandsen, and N. Tarp-Johansen, "Effective turbulence models and fatigue reliability in wind farms," *Probabilistic Engineering Mechanics*, vol. 23, no. 4, pp. 531 – 538, 2008.

[4] M. Steinbuch, W. de Boer, O. Bosgra, S. Peters, and J. Ploeg, "Optimal control of wind power plants," *Journal of Wind Engineering and Industrial Aerodynamics*, vol. 27, no. 1-3, pp. 237 – 246, 1988.

[5] M. Zhao, Z. Chen, and F. Blaabjerg, "Probabilistic capacity of a grid connected wind farm based on optimization method," *Renewable Energy*, vol. 31, no. 13, pp. 2171 – 2187, 2006.

[6] R. Fernandez, P. Battaiotto, and R. Mantz, "Wind farm non-linear control for damping electromechanical oscillations of power systems," *Renewable Energy*, vol. 33, no. 10, pp. 2258 – 2265, 2008.

[7] J. Rodriguez-Amenedo, S. Arnaltes, and M. Rodriguez, "Operation and co-ordinated control of fixed and variable speed wind farms," *Renewable Energy*, vol. 33, no. 3, pp. 406 – 414, 2008.

[8] L. Fernandez, C. Garcia, and F. Jurado, "Comparative study on the performance of control systems for doubly fed induction generator (dfig) wind turbines operating with power regulation," *Energy*, vol. 33, no. 9, pp. 1438–1452, 2008.

[9] A. Hansen, P. Sørensen, F. Iov, and F. Blaabjerg, "Centralised power control of wind farm with doubly fed induction generators," *Renewable Energy*, vol. 31, no. 7, pp. 935–951, 2006.

[10] E. van der Hooft, P. Schaak, and T. Van Engelen, "Wind turbine control algorithms," ECN Technical Report,ECN-C–03-111, Tech. Rep., 2003.

[11] F. Lescher, H. Camblong, O. Curea, and R. Briand, "Lpv control of wind turbines for fatigue loads reduction using intelligent micro sensors," in *American Control Conference, 2007. ACC '07*, July 2007, pp. 6061–6066.

[12] H. Sutherland, "A summary of the fatigue properties of wind turbine materials," *Wind Energy*, vol. 3, no. 1, pp. 1–34, 2000.

[13] K. Hammerum, P. Brath, and N. Poulsen, "A fatigue approach to wind turbine control," *Journal of Physics: Conference Series*, vol. 75, pp. 1–11, 2007.

[14] B. M. Adams, "Dynam loads in wind farms ii," Garrad Hassan and Partners Ltd, Tech. Rep. 286/R/1, 1996.

[15] E. Bossanyi, "Individual blade pitch control for load reduction," *Wind Energy*, vol. 6, no. 2, pp. 119 – 128, 2003.

[16] F. Bianchi, H. De Battista, and R. Mantz, *Wind turbine control systems: principles, modelling and gain scheduling design.* Springer Verlag, 2006.

[17] E. Hau, *Wind turbines: fundamentals, technologies, application, economics.* Springer Verlag, 2006.

[18] M. Soleimanzadeh and R. Wisniewski, "Wind deficit model in a wind farm using finite volume method," in *Proceedings of American Control Conference (ACC)*, 2010.

[19] H. Versteeg and W. Malalasekera, *An introduction to computational fluid dynamics: the finite volume method.* Prentice Hall, 2007.

[20] P. Sørensen, A. Hansen, K. Thomsen, H. Madsen, H. Nielsen, N. Poulsen, and F. Iov, "Simulation and optimization of wind farm controller," in *European Wind Energy Conference and Exhibition*, 2004.

[21] K. Thomsen, "Operation and control of large wind turbines and wind farms - design load basis," Risø National Laboratory," TECHREPORT, 1967.

[22] T. Burton, D. Sharpe, N. Jenkins, and E. Bossanyi, *Wind Energy Handbook*. John Wiley and Sons, 2001.

[23] S. Suryanarayanan and A. Dixit, "A procedure for the development of control-oriented linear models for horizontal-axis large wind turbines," *Journal of Dynamic Systems, Measurement, and Control*, vol. 129, no. 4, pp. 469–479, 2007.

[24] E. Bossanyi, "Wind turbine control for load reduction," *Wind Energy*, vol. 6, no. 3, pp. 229–244, 2003.

[25] J. Jonkman, S. Butterfield, W. Musial, and G. Scott, "Definition of a 5-mw reference wind turbine for offshore system development," Golden, CO: National Renewable Energy Laboratory, Tech. Rep. NREL/TP-500-38060, 2009.

[26] J. Lfberg, "Yalmip : A toolbox for modeling and optimization in MATLAB," in *Proceedings of the CACSD Conference*, Taipei, Taiwan, 2004.

Paper C

An Optimization Framework for Load and Power Distribution in Wind Farms

Maryam Soleimanzadeh, Rafael Wisniewski, and Stoyan Kanev

Abstract

The aim of this paper is to develop a controller for wind farms to optimize the load and power distribution. In this regard, the farm controller calculates the power reference signals for individual wind turbine controllers such that the sum of the power references tracks the power demanded by a system operator. Moreover, the reference signals are determined to reduce the load acting on wind turbines at low frequencies. Therefore, a trade-off is made for load and power control, which is formulated as an optimization problem. Afterwards, the optimization problem for the wind farm modeled as a bilinear control system is solved using an approximation method.

1 Introduction

The research area of wind farm control can be divided into two main categories. The first is the quality control of the generated power; the second, which is the subject of interest in this paper, is the coordinated control of the power generated by each individual turbine such that the aerodynamic interactions between the turbines are minimized [1]. As wind farms increase in size and number, there is an increased demand for optimized performance and longer life time for each wind turbine. To extend the lifetime of the wind turbine components, a load assessment should be included in the controller design [2].

There are numerous scientific studies on the modeling and control of wind farms. However, the results on the combined optimization of power and load are still lacking. An example of considering the load in the overall wind farm control has been presented in [3]. Furthermore, an optimization method to maximize the production capacity of farms based on the limitations of the physical system, such as voltage stability and generator power, has been proposed in [4]. In [5], a concept with both centralized control and control for each individual wind turbine is presented. In this approach, the controllers at the turbine level ensure that the relevant reference commands provided by the centralized controller are followed. In [6], the optimal control problem of load and power distribution is solved, providing the pitch angle and rotor speed reference signals along with power set-points to each wind turbine controller. However, in this work, only the power set-points are obtained by the wind farm controller as reference signals for the wind turbines.

Likewise, there are many studies on load reduction in single turbines [7, 8, 9, 2], but the results on load control in wind farms are still lacking.

In this regard, the aim of this study is to develop a wind farm controller for the optimal distribution of power references among wind turbines while it lessens low frequency structural loads. The controller computes the required reference signals for each individual wind turbine controller. The problem has been formulated as a linear quadratic regulator (LQR) problem with constraints on the state and input, subject to a wind farm dynamic model. The wind farm dynamic model delivers an

approximation of the wind speed in the vicinity of each wind turbine [10], which is suitable for optimization.

The optimal control problem is solved using model predictive control methods, and the results have been compared to the results of a numerical optimization method that uses a nonlinear model of the wind farm.

The output of the farm controller is the vector of power reference signals for each wind turbine controller. The farm controller does not directly consider the individual wind turbine controllers. However, to provide the optimal pitch angle for the wind farm control loop, the dynamics of the wind turbines have been partly combined with the wind farm dynamic model.

This paper first gives a brief overview of the wind farm model. Subsequently, the approach for the controller design is explained, and the optimal control problem is formulated. Finally, the optimal control problem has been solved, and the results are compared to the numerical simulation.

The research area of wind farm control can be divided into two main categories. The first is the quality control of the generated power; the second, which is the subject of interest in this paper, is the coordinated control of the power generated by each individual turbine such that the aerodynamic interactions between the turbines are minimized [1]. As wind farms increase in size and number, there is an increased demand for optimized performance and longer life time for each wind turbine. To extend the lifetime of the wind turbine components, a load assessment should be included in the controller design [2].

There are numerous scientific studies on the modeling and control of wind farms. However, the results on the combined optimization of power and load are still lacking. An example of considering the load in the overall wind farm control has been presented in [3]. Furthermore, an optimization method to maximize the production capacity of farms based on the limitations of the physical system, such as voltage stability and generator power, has been proposed in [4]. In [5], a concept with both centralized control and control for each individual wind turbine is presented. In this approach, the controllers at the turbine level ensure that the relevant reference commands provided by the centralized controller are followed. In [6], the optimal control problem of load and power distribution is solved, providing the pitch angle and rotor speed reference signals along with power set-points to each wind turbine controller. However, in this work, only the power set-points are obtained by the wind farm controller as reference signals for the wind turbines.

Likewise, there are many studies on load reduction in single turbines [7, 8, 9, 2], but the results on load control in wind farms are still lacking.

In this regard, the aim of this study is to develop a wind farm controller for the optimal distribution of power references among wind turbines while it lessens low frequency structural loads. The controller computes the required reference signals for each individual wind turbine controller. The problem has been formulated as a

linear quadratic regulator (LQR) problem with constraints on the state and input, subject to a wind farm dynamic model. The wind farm dynamic model delivers an approximation of the wind speed in the vicinity of each wind turbine [10], which is suitable for optimization.

The optimal control problem is solved using model predictive control methods, and the results have been compared to the results of a numerical optimization method that uses a nonlinear model of the wind farm.

The output of the farm controller is the vector of power reference signals for each wind turbine controller. The farm controller does not directly consider the individual wind turbine controllers. However, to provide the optimal pitch angle for the wind farm control loop, the dynamics of the wind turbines have been partly combined with the wind farm dynamic model.

This paper first gives a brief overview of the wind farm model. Subsequently, the approach for the controller design is explained, and the optimal control problem is formulated. Finally, the optimal control problem has been solved, and the results are compared to the numerical simulation.

2   Wind Farm Model

A dynamical model for the flow in wind farms has been presented in [10, 11], which calculates an approximation of the mean wind speed over the farm, especially in the vicinity of each wind turbine. This model represents the wind farm flow model approximated by ordinary differential equations, which will be applied in the wind farm control algorithms.

The modeling commences with the flow model (Navier-Stokes equations) for the whole wind farm, assuming there is no wind turbine effect. The wind turbine dynamics are added afterwards, and their influence on the wake is studied. In this regard, we start by finding a linear approximation to the Navier-Stokes equations in 2-D at the hub height. Afterwards, the dynamics of the wind turbines correspond to the pressure and force terms of the equations (the drop pressure at the location of a wind turbine is a function of thrust coefficient using the momentum theory [12], and the force term at the location of each turbine is the thrust force).

The next step has been to divide the whole wind farm into non-overlapping cells and then define the flow equation in each cell such that the equation agrees on the boundaries of the cells. The spatial discretization for these equations is performed using the finite difference method (FDM), and the partial differential equations (PDE) have been transformed into ordinary differential equations (ODE). The model is considered to be in the far wake region, and the ambient shear flow has been neglected. The profile of velocity deficit is assumed to be axis-symmetric. Finally, the dynamic equations of the wind farm have been written in the following form, expressed in [10, 11].

$$\frac{dx_1(t)}{dt} = f_1(x_1(t), ..., x_n(t), u_1(t), ..., u_m(t)), \tag{7.1}$$

$$\vdots$$

$$\frac{dx_n(t)}{dt} = f_n(x_1(t), ..., x_n(t), u_1(t), ..., u_m(t)). \tag{7.2}$$

The equations above can be summarized as follows, when the coefficients of the ODEs are re-written in the following matrix form

$$\dot{x}(t) = Ax(t) + \tilde{B}\tilde{u}(t) + \sum_{j=1}^{n}(x(t)^T \tilde{N}_j)\tilde{u}(t), \tag{7.3}$$

In this equation, x is a vector in $\mathbb{R}^n$ that represents the average wind speed over each partition in a time period of 5-10 minutes, where n is the number of partitions covering the wind farm.

The matrix $A(t)$ is a block diagonal matrix in $\mathbb{R}^{n \times n}$; $\tilde{u}$ is the thrust coefficient in $\mathbb{R}^m$, where m is the number of wind turbines. The dimension of the matrices $\tilde{B}$ and $\tilde{N}_j$ are respectively $n \times m$ and $1 \times m$.

In the following, $\tilde{u}$ (the thrust coefficient) is obtained based on $u = P_{ref}$, which is the control input of the farm controller.

$$\tilde{u}_i = \frac{u_i}{0.5\rho\pi R^2(1-a_i)x_i^3} \quad \Rightarrow \quad \tilde{u} = K(x)u, \tag{7.4}$$

where $u_i = P_{ref}^{WT_i}$, ρ is the air density, R is the rotor diameter, and a_i is the induction factor of the ith turbine. Substituting $\tilde{u}_i$ in (7.3) with its equivalent in (7.4), the wind farm model is written as follows:

$$\dot{x}(t) = Ax(t) + Bu(t) + \sum_{j=1}^{n}(x(t)^T N_j)u(t), \tag{7.5}$$

where $A \in \mathbb{R}^{n \times n}$ and $B \in \mathbb{R}^{n \times m}$; thus, $N_j \in \mathbb{R}^{1 \times m}$.

The model has been validated using real measurement data from the EWTW wind farm in the Netherlands. The measurements were the mean wind speed over a specific time interval. Therefore, the model has been simulated for this specific time interval, mean wind speed has been calculated, and the results are compared to the EWTW data. This model provides an approximation of wind speed over the entire farm and presents it as an approximate description of what is occurring downstream of a wind farm. Therefore, it is useful to estimate the loads and total power production of wind farms.

3   Control Strategy

The wind farm controller design in this paper is based on the wind turbine control strategy. At low wind speeds, the rotor speed in a wind turbine changes according to the wind speed to maintain the optimal tip speed ratio while the pitch angle is kept constant. At high wind speeds, the rotor speed is kept constant, and the pitch angle is increased to limit the power captured at its rated value. The wind turbine control system receives the optimal power set-points from the wind farm controller. Additionally, the power set-points computed by the farm controller should track the total power demanded by the operator. Furthermore, it should be determined by considering load minimization.

Above the rated wind speed, the pitch angle variations strongly influence the turbine dynamics, in particular, the tower dynamics. As the blades pitch to regulate the aerodynamic torque, the aerodynamic thrust on the rotor changes substantially, which affects the structural dynamics of the wind turbine [12].

As analyzed in [13], the blade edge motion is strongly coupled with the tower side-to-side motion and the drive train torsion. Accordingly, one of our objectives is to reduce the blade bending (bb) moment in both the edge and flap directions and to reduce the tower bending (tb) moment in the fore-aft direction. Based on the model explained in [14], both the tower and blade bending moments can be estimated as a function of the C_T coefficient.

The tower bending moment due to the thrust force, $F_T(C_T, V)$, will be assumed to be [14]

$$M_{tb}(C_T, V) = h\, F_T(C_T, V), \tag{7.6}$$

where h is the tower height and F_T is given by

$$F_T(V, \beta, \lambda) = \frac{1}{2}\rho\pi R^2 V^2 C_T(\beta, \lambda), \tag{7.7}$$

where ρ, R and V are, respectively, the air density, rotor radius and wind speed. Additionally, $C_T(\beta, \lambda)$ is the thrust coefficient. Therefore, the tower bending moment is expressed as

$$M_{tb}(\beta, \Omega R/V) = k_{tb}V^2 C_T(\beta, \Omega R/V), \tag{7.8}$$

with $k_{tb} = \frac{1}{2}h\rho\pi R^2$.

The effective blade bending moment M_{bb} due to the edge and flap motion of the blade is modeled as follows [14]

$$M_{bb}^2 = (\frac{1}{9}F_b^2 + \frac{25}{1152}m_{bd}g^2)D^2, \tag{7.9}$$

where m_{bd} is the mass of the blade, g is the acceleration of gravity, D is the rotor diameter, and F_b for a 3 blade wind turbine is

$$F_b = \frac{\rho \pi D^4}{12} \frac{\Omega^2 a(1-a)}{\lambda^2}, \tag{7.10}$$

where a is the induction factor of a turbine. Combining (7.9) and (7.10) and substituting $\lambda = \Omega R/V$, the effective blade bending moment is

$$
\begin{aligned}
M_{bb}^2 &= k_{11}(V^2 a(1-a))^2 + k_2 \\
&= k_1(V^2 C_T(\beta, \lambda))^2 + k_2,
\end{aligned} \tag{7.11}
$$

where $k_1 = k_{11}/4 = (\pi \rho D^5/108 R^2)^2$ and $k_2 = 25 m_{bd} g^2 D^2/1152$.

4   Optimization Problem

Load control

In this section, we approximate the bending moment equations (7.8) and (7.11) with two linear functions. The linearization will be around the mean wind speed, the mean pitch angle and the mean rotor speed.

$$
\begin{aligned}
M_{tb}(\Omega, \beta, V) \approx M_{tb}(\bar{\Omega}, \bar{\beta}, \bar{V}) + \left.\frac{\partial M_{tb}}{\partial \Omega}\right|_{\bar{\Omega}, \bar{\beta}, \bar{V}} (\Omega - \bar{\Omega}) + \\
\left.\frac{\partial M_{tb}}{\partial \beta}\right|_{\bar{\Omega}, \bar{\beta}, \bar{V}} (\beta - \bar{\beta}) + \left.\frac{\partial M_{tb}}{\partial V}\right|_{\bar{\Omega}, \bar{\beta}, \bar{V}} (V - \bar{V}).
\end{aligned} \tag{7.12}
$$

Therefore, M_{tb} can be approximated by the following equation.

$$M_{tb}(\Omega, \beta, V) \approx \delta_0 + \delta_1 \Omega + \delta_2 \beta + \delta_3 V, \tag{7.13}$$

where δ_i , $i = 1, 2, 3$, are the linearization factors obtained from (7.12). In a similar way, a linear approximation for the blade bending moment is

$$M_{bb}(\Omega, \beta, V) \approx \varsigma_0 + \varsigma_1 \Omega + \varsigma_2 \beta + \varsigma_3 V, \tag{7.14}$$

where ς_i , $i = 1, 2, 3$ are the linearization factors. The linear approximation above for the tower and blade bending moments are used in the wind farm cost function and should be minimized to reduce the structural loads. However, controlling the loads on the farm level will be much slower than the load control by the wind turbine controller. The wind turbine controller changes β_{ref} to control the dynamic loads, and the wind farm controller determines P_{ref} such that the static

loads are minimized. Therefore, a low-pass and a band-pass filter are used to drop the high frequency tower and blade bending moments.

The tower bending moment is limited by a simple recursive low-pass filter with a corner frequency of $0.3\ Hz$. The band-pass filter for the blade bending moment has a center frequency of $0.6\ Hz$ and a bandwidth of $0.35 - 0.85\ Hz$ (based on NREL 5MW wind turbine data [15]).

Power reference determination

On the other hand, the system operator determines the power demanded from the wind farm. Therefore, the power captured from the wind farm, which is the sum of the output powers from all wind turbines, should track the power demanded. Thus. $\sum_i^N P_{Wt_i}(V_i, C_{p_i}) - P_{ref}^{Wf}$ should be minimized. In other words, the power produced by all turbines $\sum_i^N P_{Wt_i}(V_i, C_{p_i})$ should follow the wind farm power reference signal, which is determined by the system operator. This corresponds to the fact that the power produced by each turbine, $P_{Wt_i}(V_i, C_{p_i})$, should follow each reference signal $P_{ref}^{Wt_i}$. This reference signal for each wind turbine has to be determined by the wind farm controller.

When the wind speed is above the rated power, the rotor speed is kept constant, and the power coefficient, $C_p(V_i, \beta_i)$, depends on the pitch and wind speed. Therefore, the power produced is written as a function of the pitch angle $P_{Wt_i}(V_i, \beta_i)$. In summary, the following value is a part of a cost function:

$$P_{Wt_i}(V_i, \beta_i) - P_{ref}^{Wt_i}, \tag{7.15}$$

where P_{ref}^{Wt} should be obtained during the minimization process.

Therefore, the following terms should be minimized with the first term due to the power reference determination and the second term $M_{tb} + M_{bb}$:

$$Z_i = |(P_{Wt_i}(V_i, C_{p_i}) - P_{ref}^{Wt_i})| +$$
$$c_1((\varsigma_1 + \delta_1)\Omega + (\varsigma_2 + \delta_2)\beta + (\varsigma_3 + \delta_3)V), \tag{7.16}$$

where $\sum_i^N P_{ref}^{Wt_i} = P_{ref}^{Wf}$ and c_1 is a weighting factor. At in high wind speed, the controller keeps the rotor speed constant, and thus we can neglect the term $(\varsigma_1 + \delta_1)\Omega$. Moreover, replacing P_{Wt_i} with its linear approximation, which, at high wind speeds (after neglecting the constants) is $k_{p_1}V + k_{p_3}\beta$, the function to be minimized is

$$Z_i = |k_{p_1}V + k_{p_3}\beta - P_{ref}^{Wt_i}| +$$
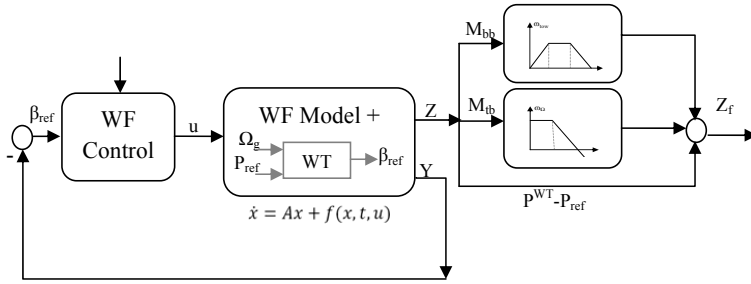$$c_1((\varsigma_3 + \delta_3)V + (\varsigma_2 + \delta_2)\beta), \tag{7.17}$$

Figure 7.1: The wind farm control block diagram

Furthermore, defining $u = P_{ref}^{wt}$ and x to be the wind speed (the same as (7.5)), we may re-write (7.17) in the following form

$$Z = Gx + Hu + f(\beta), \tag{7.18}$$

where the affine term $f(\beta)$ is the function of β expressed in (7.17), where β is calculated by the wind turbine controllers.

In this paper, reducing the load and power production are equally important. Therefore, in the simulations, c_1 is set equal to one.

Optimal control

The block diagram of the optimal control problem is shown in Figure 7.1. The load control focuses on minimizing the loads at low frequencies; in other words, the static loading of the turbines is controlled by the wind farm controller. The individual wind turbine controller is responsible for dynamic load control. The dynamic of the system is (7.5). In Figure 7.1, the WT block represents the relation between P_{ref}, the input to the wind turbine controller, and β_{ref}. The details are shown in Figure 7.2 [15], which is a PI controller and is a part of the control system of the wind turbine. The PI controller is responsible for pitch control and for producing the pitch reference signal. The pitch reference signal is the feedback to the wind farm controller.

In Figure 7.1, $Y = \beta$. To find an expression for the output Y based on the state x and input u, we may approximate this relation in the following way. The C_T coefficient of each wind turbine has been approximated by a polynomial using the lookup table of the NREL 5MW [15] wind turbine, and the polynomial is approximated by a linear function:

$$C_T(\beta, \lambda) = \sum_{i=0}^{3} \sum_{j=0}^{3} k_{i,j} \beta^i \lambda^j \approx \iota_0 + \iota_1 \lambda + \iota_2 \beta, \tag{7.19}$$
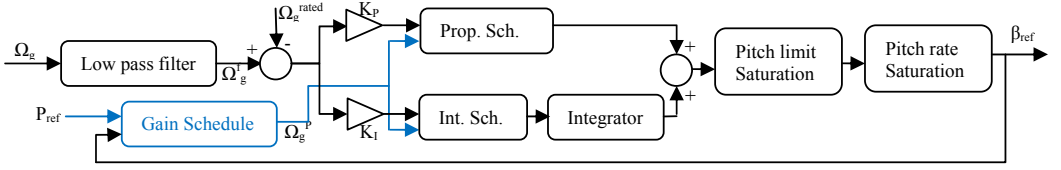
Figure 7.2: WT block; the pitch control system of a wind turbine [15]

where ι_i are the linearization factors. Here,

$$C_T(\beta, \lambda) = \iota_0 + \iota_1\lambda + \iota_2\beta,$$
$$C_T(P_{ref}^{WT}, x) = \frac{P_{ref}^{WT}}{K_p x^3 (1 - a)}, \tag{7.20}$$

where Ω is assumed to be constant, $K_p = \frac{1}{2}\rho\pi R^2$, and a is the induction factor that is entered into the equations using (7.20). Setting the equations above equal to each other and re-arranging, we will have

$$\beta_{ref}^{WT}(P_{ref}^{WT}, x) = \frac{P_{ref}^{WT}}{\iota_2 K_p x^3 (1 - a)} - \frac{1}{\iota_2}(\iota_0 + \iota_1\lambda) \tag{7.21}$$
$$\approx k_{\beta_0} + k_{\beta_1} x + k_{\beta_2} u,$$

where, neglecting the constant term, $Y = \beta = Cx + Du$, with $C = k_{\beta_1}$ and $D = k_{\beta_2}$.

When the wind speed is below the rated speed, we define $Y = \Omega$ and in a similar way, it can be approximated as $Y = \Omega = \grave{C}x + \grave{D}u$, where $\grave{C}$ and $\grave{D}$ are linearization factors.

The cost function is defined as

$$J(\beta, P_{ref}^{Wt_i}) = \int_{t_0}^{t_f} \sum_i^N [Z_i^T Z_i] dt$$
$$= \int_{t_0}^{t_f} [x^T F u + u^T R u + x^T Q x] dt, \tag{7.22}$$

where $Q = G^T G$, $R = H^T H$ and $F = G^T H$. Moreover,

$$\sum P_{ref}^{Wt} = P_{ref}^{Wf}, \tag{7.23}$$
$$x(t_0) = x_0, \quad x(t_f) \text{ is free}, \quad t = [t_0, t_f]$$
$$u \in [u_{min}, u_{max}]$$
$$x \in [x_{min}, x_{max}],$$

subject to the differential equation (7.5).

After linearizing the bilinear differential equation around the operating point, as $\dot{x} = Ax + Bu$, the optimal control problem is a constraint quadratic problem subject to a linear system, where the constraints are imposed on both the state and input. This problem can be solved using a standard model predictive control (MPC) approach.

However, linearizing the load, power and dynamic model of the system to obtain the quadratic structure will reduce the accuracy of the results and the load control. Therefore, the problem has also been formulated in another way, with less linearization and a better approximation of the load and power set points.

In the alternate formulation of the control problem, the cost function contains the tower and blade bending moments for low frequencies, and equation (7.15), without linearization, to determine the power set point. Moreover, the wind speed all over the wind farm is obtained off-line from the dynamic model of the flow in the farm, which is a bilinear system, and then it is implemented in the optimal control problem. This process will lead to a nonlinear optimization that is solved numerically using the Yalmip [16] toolbox in MATLAB.

5   Results and Discussion

The optimal control problem (7.22)-(7.23) has been solved using the Model Predictive Control toolbox in MATLAB for a small wind farm with 5 wind turbines in a row, where the distance between two wind turbines is almost four rotor diameters. The reason is explained in Figures 7.3a and 7.3b, which show a wind farm with 25 wind turbines, where the direction of the wake propagations are depicted with green lines. As it has been shown, the maximum wake interaction for a row of wind turbines occurs when the wind direction is parallel to the row. Therefore, the optimal control problem is solved for a sample farm with 5 wind turbines in a row, and the wind direction is assumed to be parallel to the row of turbines.

The control input u, which is the vector of the power references, has been obtained as a time series. Then, the average value of the power reference in 10 minutes for each wind turbine is calculated.

The results have been illustrated in Figure 7.4 for a wind speed below the rated wind speed in the blue graph. In this case, the wind speed at the vicinity of each

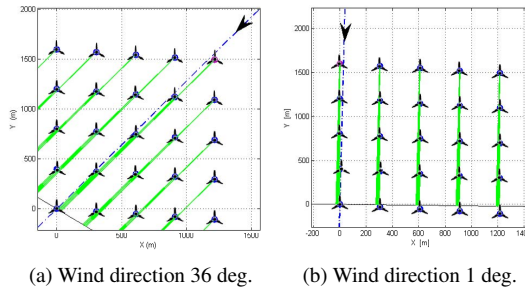(a) Wind direction 36 deg.   (b) Wind direction 1 deg.

Figure 7.3: Two wind directions that produce the maximum wake interaction; the reason for choosing one row of turbines for simulation

wind turbine is below the rated speed (the free stream wind speed is approximately 8 m/s), and the total power demanded from the wind farm is 4.9 MW. In addition, the optimal control problem excluding the linear approximations has been solved numerically using the Yalmip toolbox [16] in MATLAB. The results, the average power set-point for each wind turbine, are depicted in Figure 7.4 in the red graph. The outcome of the controls mentioned above for the wind farm has been compared to that of a conventional wind farm control, where the power set-points are divided between the turbines proportional to the power coefficients. In the conventional method, the controller either extracts the maximum available power or dispatches the set-points equally between the turbines based on the amount of power demanded and the operating regime of the wind turbines. The numerical results are expected to be closer to reality, because linear approximations are used less often in this approach.

Based on these results, if we extract less power from the first wind turbine of the row, we will be able to extract more power from downstream turbines, such that the total produced power is equal to the power demanded and the structural loads on the turbines will be reduced. A comparison between the tower bending moments in all 3 cases is illustrated in Figure 7.5. Due to the scale of the graphs, the plots seem to be the same, but there are differences between them. The differences between the case without a controller with the other two cases are also depicted in the figure.

The calculations have been repeated for a case when the free space wind speed is above the rated speed, and the results are depicted in Figure 7.6.

It should be noted that, whenever the free space wind speed is a slightly higher than wind turbine rated speed, with very low turbulence intensity, it may cause the velocity deficit to the below rated speed in the vicinity of some of the down wind turbines.
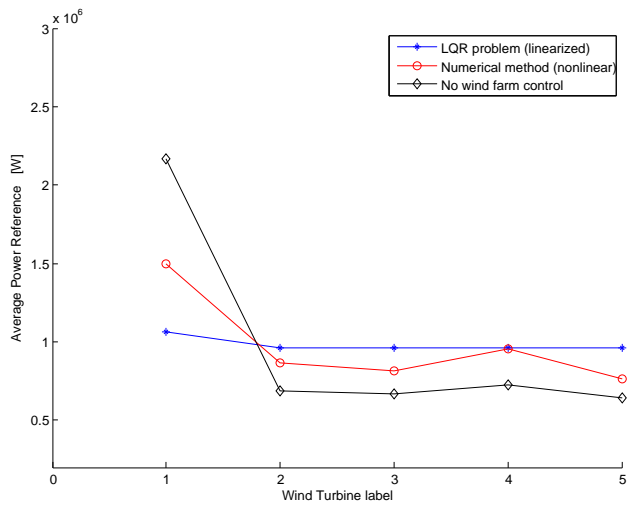
Figure 7.4: Power references for each wind turbine in a row (5 turbines) below the rated wind speed
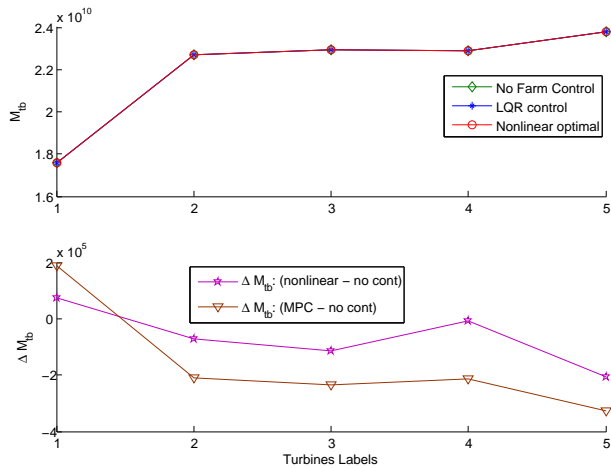

Figure 7.5: Changes in mean tower bending moments after using the controller for the 5 turbines in a row
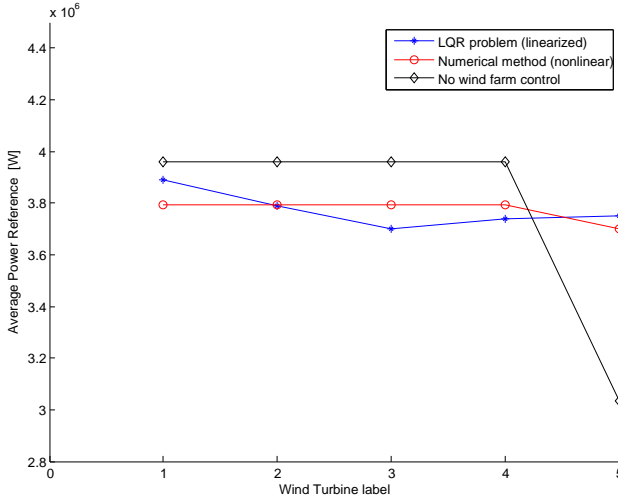
Figure 7.6: Power references for each wind turbine in a row (5 turbines) above the rated wind speed

Here, the free space wind speed is appriximately 14 m/s, and based on the wind farm dynamical model for five wind turbines in a row with maximum wake interactions, the wind speed that reaches the last turbine of the row is below the rated speed. Figure 7.6 shows the optimal way to distribute the power references between the wind turbines with regard to load reduction.

The first 4 wind turbines are able to produce nominal power, and the total power demanded from the farm is 18.9 MW. The results show that, if less power is extracted from the upstream wind turbines, it will influence the wake effect on the last turbine of the row, such that the turbine will be able to produce more power. Thus, the total power demanded will be satisfied, and the low frequency loads on the first 4 wind turbine have decreased. The last wind turbine will experience an increased static load; however, the structural loads due to the turbulent wake of the upwind turbines are reduced on this turbine.

In the case where all the turbines are operating above the rated wind speed and are able to produce nominal power, the power references will be divided between the turbines proportionally.

The load reduction in the farm is found by comparing the blade and tower bending moments with and without the controller. Although the power references are the same for the first four wind turbines, the turbines experience different bending moments due to the different wind speeds and turbulence intensity conditions. Because, the loads are considered for low and medium frequencies, the static loads are minimized. Therefore, we do not expect a great improvement in
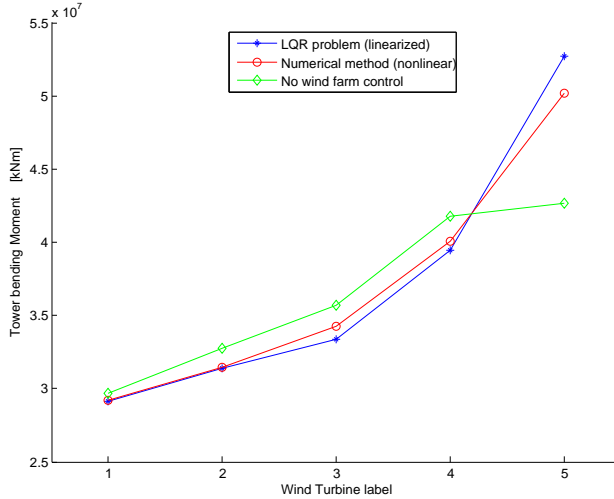
Figure 7.7: Reduction of the mean tower bending moments after using the controller for the 5 turbines in a row; the free stream wind speed is 14 m/s

the overall loads. Specifically, the average tower bending moments for each wind turbine with a free stream wind speed of 14 m/s are depicted in Figure 7.7. As expected, the static load on the first four turbines has been decreased; for example, using the numerical method, the loads on the first wind turbine decreased by 1.5% and, on the next three turbines, by 4%. However, in this approach, the static load on the last turbine has increased by 15% because the power production level is higher. Nevertheless, because this turbine is able to produce more power than before (compared to the case with no farm controller, a higher wind speed is available at this turbine), the effect of the upwind turbine wakes has been reduced on this turbine. In other words, we conclude that the dynamic loads, which are the origin of fatigue, are decreased on this turbine, which is a hypothesis that needs to be proven in future works.

6   Conclusion

In this work, a centralized optimal controller has been developed for wind farms. The main advantage of this controller is that it considers power optimization and load minimization simultaneously. The controller calculates and sends the power reference signals to each wind turbine of the farm, such that the structural loads on the turbines are reduced. The loads that are considered for minimization are the tower and blade bending moments at low frequency. The wind farm control strategy developed in this work can easily be implemented on large wind farms with variable wind speeds and arbitrary wind directions. The only requirement is

that the wind farm model should be extended using meandering effects and turbulence models. To provide the optimal pitch angle for the wind farm controller, the dynamics of wind turbines have been partly combined with the wind farm dynamic. We remark that the farm controller does not deal with the wind turbines individual controllers.

Since mostly dynamic loads are responsible for fatigue and the reduced life time of wind turbines in wind farms, the main limitation of this work is considering the static loads of the turbines. The reason is that the individual wind turbine controllers control the dynamic load; moreover, considering dynamic loads at the farm scale requires very fast computation facilities.

References

[1] L. Pao and K. Johnson, "A tutorial on the dynamics and control of wind turbines and wind farms," in *Proceedings of American Control Conf (ACC)*, 2009.

[2] K. Hammerum, P. Brath, and N. Poulsen, "A fatigue approach to wind turbine control," *Journal of Physics: Conference Series*, vol. 75, pp. 1–11, 2007.

[3] M. Steinbuch, W. de Boer, O. Bosgra, S. Peters, and J. Ploeg, "Optimal control of wind power plants," *Journal of Wind Engineering and Industrial Aerodynamics*, vol. 27, no. 1-3, pp. 237 – 246, 1988.

[4] M. Zhao, Z. Chen, and F. Blaabjerg, "Probabilistic capacity of a grid connected wind farm based on optimization method," *Renewable Energy*, vol. 31, no. 13, pp. 2171 – 2187, 2006.

[5] A. Hansen, P. Sørensen, F. Iov, and F. Blaabjerg, "Centralised power control of wind farm with doubly fed induction generators," *Renewable Energy*, vol. 31, no. 7, pp. 935–951, 2006.

[6] M. Soleimanzadeh and R. Wisniewski, "Controller design for a wind farm, considering both power and load aspects," *Mechatronics*, vol. 21, no. 4, pp. 720 – 727, 2011.

[7] E. van der Hooft, P. Schaak, and T. Van Engelen, "Wind turbine control algorithms," ECN Technical Report,ECN-C–03-111, Tech. Rep., 2003.

[8] F. Lescher, H. Camblong, O. Curea, and R. Briand, "Lpv control of wind turbines for fatigue loads reduction using intelligent micro sensors," in *American Control Conference, 2007. ACC '07*, July 2007, pp. 6061–6066.

[9] H. Sutherland, "A summary of the fatigue properties of wind turbine materials," *Wind Energy*, vol. 3, no. 1, pp. 1–34, 2000.

[10] M. Soleimanzadeh and R. Wisniewski, "Wind speed dynamical model in a wind farm," in *8th IEEE International Conference on Control & Automation (ICCA)*, 2010.

[11] M. Soleimanzadeh, R. Wisniewski, and A. J. Brand, "State-space representation of the flow model for a wind farm," *Wind Energy*, vol. (2nd revision submitted), pp. –, 2012.

[12] T. Burton, D. Sharpe, N. Jenkins, and E. Bossanyi, *Wind Energy Handbook*. John Wiley and Sons, 2001.

[13] S. Suryanarayanan and A. Dixit, "A procedure for the development of control-oriented linear models for horizontal-axis large wind turbines," *Journal of Dynamic Systems, Measurement, and Control*, vol. 129, no. 4, pp. 469–479, 2007.

[14] A. J. Brand and J. W. Wagenaar, "A quasi-steady wind farm flow model in the context of distributed control of the wind farm," in *European Wind Energy Conference (EWEC 2010)*, 2010.

[15] J. Jonkman, S. Butterfield, W. Musial, and G. Scott, "Definition of a 5-mw reference wind turbine for offshore system development," Golden, CO: National Renewable Energy Laboratory, Tech. Rep. NREL/TP-500-38060, 2009.

[16] J. Lfberg, "Yalmip : A toolbox for modeling and optimization in MATLAB," in *Proceedings of the CACSD Conference*, Taipei, Taiwan, 2004.

Paper D

A distributed optimization framework for wind farms

Maryam Soleimanzadeh, Rafael Wisniewski, Kathryn Johnson

Abstract

The wind farm has an intrinsic distributed structure, where wind turbines are counted as subsystems of the distributed system. The coupling between the subsystems is the wind flow and the power reference set-points across the turbines, which are designed to provide the total wind farm power demand. Distributed controller design commences with formulating the problem, where a structured matrix approach has been put in practice. Afterwards, an H_2 control design formulation is used to find the control signal set points for the wind farm to minimize structural loads on the turbine while providing the desired total wind farm power.

1   Introduction

Development of large scale wind farms helps the economic efficiency of the wind energy industry. As wind farms grow in size and number, a demand for optimized performance in terms of power production and fatigue loading for each wind turbine arises. The upwind turbines in the wind farms extract most of the power from the wind and increase the turbulence intensity in the wake reaching other turbines. Thus, the fluctuations and vibrations of the downwind turbines are greater than upwind turbines, resulting in greater fatigue loads [1]. As a result, the lifetime of the turbines that most frequently are in the downwind location are shortest, which reduces the effective lifetime of the whole farm. Therefore, the wind farm controllers should employ proper strategies to reduce the structural loads, which can be performed by power set-point adjustment. The wind farm controller is therefore responsible for distribution of the power set-points among the turbines and for ensuring that the total time varying power reference commanded by the operator is satisfied.

There are numerous research papers in modeling and control of wind farms. An overall wind farm control that maximizes energy capture has been proposed in [2]. An optimization method to increase the power production of wind farms based on the limitations of the physical system, e.g., voltage stability and generator power, has been proposed in [3]. Advanced controllers for wind farm electrical systems have been developed in [4, 5]. The focus of [5] is the coordinated control of wind farms in three control levels: central control, wind farm control, and individual turbine control. In [6], a concept with both centralized control and control for each individual wind turbine is presented. In this approach, the controllers at turbine level ensure that relevant reference commands provided by the centralized controller are followed.

In addition to these control methods, there are some new results on combined optimization of power and fatigue loads in the wind farms developed in [7]. The approach in [7] presents the optimization on a global scale in a centralized framework.

Furthermore, there are some new efforts on distributed control of wind farms [8, 9]; however, the problem of optimizing the distribution of power references among wind turbines while also considering the load minimization in distributed frameworks is still lacking.

The wind farm has an intrinsic distributed structure, where each wind turbine can be seen as a sub-system of a distributed system. The coupling between these sub-systems is the wind flow and the distribution of the power reference signal to each turbine to meet the overall power demand to the wind farm. The wind flow model in this paper is based on the spatial discretization of the linearized Navier-Stokes equation. The spatial discretization of the model is performed using the finite difference method, which provides the state space form of the dynamic wind field model. Therefore, the total system model is presented as a spatially distributed system combined with interactions between subsystems. The wind farm system model will be represented in a structured matrix format based on [10], which makes it easy to find rational approximations to solutions of the parametric Lyapunov and Riccati equations, resulting in spatially invariant distributed controllers.

The paper is organized in the following way. In Section 2 definitions and notations are introduced; then, in Section 3 the wind turbine model is presented and a model for interaction between wind turbines is devised. Section 4 presents the wind farm model utilized for controller design, and afterwards, in Sections 5 and 6 the distributed controller is developed and the simulation results (power reference signals for wind turbines and resulting loads) are presented, respectively.

2 Preliminaries

Nomenclature

Nomenclature and abbreviations for the remainder of the paper:

Definition

"Sequentially Semi-Separable" ($\mathcal{SSS}$) matrices are defined as the input-output matrices of mixed causal [11] linear time varying (LTV) systems over a finite time interval. These matrices are also called quasi-separable and matrices of low Hankel rank [10].

3 Control Model of the Subsystems and Interactions

In this section, we present a model of the wind turbine subsystems and interactions between them for use in control design.

β	Blade pitch angle	p	Output power
λ	Tip speed ratio	P_{op}	Operating point power
μ	Generator efficiency	$P_{ref}^{wt_i}$	power reference of the ith turbine
$\delta.$	cell length	P_l	Algebraic Riccati equation variable
ρ	Air density	P_f	Algebraic Riccati equation variable
ω_r	Rotor speed	Re	Reynold number
ω_g	Generator speed	R	Rotor radius
a	Induction factor	T_g	Generator torque
A_w	Wind flow system matrix	T_r	Rotor torque
A_{wt}	Wind turbine system matrix	$\mathbf{u}_d$	Wind velocity, continuous components: u,v
B_{wt}	Wind turbine model matrix	U	Component of $\mathbf{u}_d$ (discrete)
C_T	Thrust coefficient	V	Component of $\mathbf{u}_d$ (discrete)
C_Q	Torque coefficient	w_d	Disturbance (noise)
F_T	Thrust force, components:F_1, F_2	W_{op}	Operating point wind speed
M_{shaft}	Shaft moment	$x_{(.)}$	state space variable
N	Number of subsystems	u_c	Control input vector
P	Pressure	$\bar{K}$	Controller for the entire system
P_{ref}	power reference	K	Controller for each subsystem

The wind farm in this paper includes a finite number of wind turbines in a row as in Figure 8.1. It can be modeled as a distributed system with interconnections. The systems that are spatially distributed are wind turbines and the interconnections are the wind flow model in the wind farm.
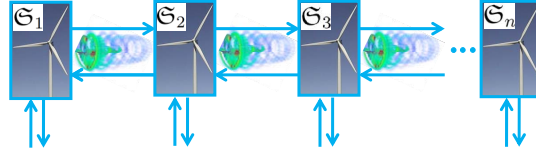

Figure 8.1: Wind farm configuration, where $\mathfrak{S}$ represents the model of each wind turbine

Wind turbine model

The wind turbine model is the linearized model of the 5MW NREL wind turbine [12] presented in the state-space form defined as [13]:

$$
\begin{aligned}
\dot{x}_{wt}(t) &= A_{wt}x_{wt}(t) + B_{wt}\mathbf{u}_d(t) + B_u u_c(t), \\
z(t) &= C^1 x_{wt}(t) + D^1\mathbf{u}_d(t) + D_u^1 u_c(t), \\
y(t) &= C^2 x_{wt}(t) + D^2\mathbf{u}_d(t) + D_u^2 u_c(t),
\end{aligned}
\tag{8.1}
$$

with

$$x_{wt} = \begin{bmatrix} \beta & \omega_r & \omega_g \end{bmatrix}^T, \tag{8.2}$$

$$u_c = \begin{bmatrix} P_{ref} \end{bmatrix}, \tag{8.3}$$

$$\mathbf{u}_d = \begin{bmatrix} v & u \end{bmatrix}^T, \tag{8.4}$$

$$z = \begin{bmatrix} F_t & M_{shaft} \end{bmatrix}^T, \tag{8.5}$$

$$y = [p], \tag{8.6}$$

where, β, ω_r and ω_g are respectively the pitch angle, rotor and generator angular velocities. P_{ref} is the power reference to a given turbine, and the components of wind velocity in 2-dimensions are v and u. Moreover, p, F_t and M_{shaft} are generated power, thrust force and shaft moment. The system matrices are obtained based on the wind turbine operating point and they change with the wind speed variations. Thus they can be denoted as $A_{wt}(\mathbf{u}_d), B_{wt}(\mathbf{u}_d), C(\mathbf{u}_d), D(\mathbf{u}_d), B_u(\mathbf{u}_d), D_u(\mathbf{u}_d)$. The wind speed and power operating points for each wind turbine $W_{op} and P_{op}$ are obtained using the wind flow dynamic model [14, 15]. Given the free space wind speed (can be obtained from a farm-representative meteorological tower), the dynamic wind flow model computes the wind speed in the vicinity of each wind turbine (W_{op}). Then, a lookup table for the NREL 5MW [12], is used to obtain P_{op}. The system matrices for an example operating point are given in Appendix A.

In the following section, a concise description of the dynamic wind flow model that is used to find the operating points of the turbines, is presented.

Determination of operating points using dynamic wind flow model

To find the operating point of each wind turbine, a dynamic wind flow model for wind farms is utilized [14]. The input to this model is the free space wind speed, and the output is the mean wind speed in the vicinity of each wind turbine.

The dynamic wind flow model is based on the spatial discretization of the linearized Navier-Stokes equation combined with the vortex cylinder theory. The spatial discretization of the model is performed using the finite difference method, which provides the state space form of the dynamic wind farm model as well as the wind speed in the vicinity of each wind turbine [14, 15].

The wind flow in a wind farm is expressed with the Navier-Stokes equation for viscous flow. The wind velocity is a divergence free vector $\mathbf{u}_d$, and the pressure is the scalar P: [16]

$$\frac{\partial \mathbf{u}_d}{\partial t} + (\mathbf{u}_d.\nabla)\mathbf{u}_d = -\nabla P + \frac{1}{Re}\Delta \mathbf{u}_d + \mathbf{F}, \tag{8.7}$$

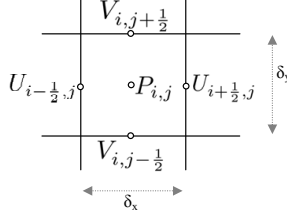Figure 8.2: P, U, V in a cell, , where the length of a cell is given by δ_y and the width of the cell is given by δ_x.

where Re is the Reynolds number, and $\mathbf{F}$ is the thrust force on each turbine, which is explained in equations (8.15). The continuity equation is:

$$\nabla.\mathbf{u}_d = 0. \tag{8.8}$$

In the xy plane (2-D), the components of the velocity $\mathbf{u}_d$ are $u(x,y,t)$ and $v(x,y,t)$. Moreover, $(\mathbf{u}_d.\nabla)\mathbf{u}_d$ has two components expressed as follows [16]:

$$\left(u\frac{\partial}{\partial x} + v\frac{\partial}{\partial y}\right)\begin{bmatrix}u\\v\end{bmatrix} = \begin{bmatrix}uu_x + vu_y\\uv_x + vv_y\end{bmatrix}, \tag{8.9}$$

where $(\cdot)_x = \partial(\cdot)/\partial x$ and $(\cdot)_y = \partial(\cdot)/\partial y$.

Considering (8.9) in 2-D, it can be shown that a linear approximation of the incompressible Navier-Stokes equations in the horizontal plane (two velocity components) is given by [17]:

$$\hat{u}_t + P_x = (\hat{u}_{xx} + \hat{u}_{yy})/Re - \bar{u}\hat{u}_x - \bar{v}\hat{u}_y + F_1,$$
$$\hat{v}_t + P_y = (\hat{v}_{xx} + \hat{v}_{yy})/Re - \bar{u}\hat{v}_x - \bar{v}\hat{v}_y + F_2,$$
$$\hat{u}_x + \hat{v}_y = 0. \tag{8.10}$$

where F_1 and F_2 are the x and y components of the thrust force.

Afterwards, the wind farm is divided into non-overlapping square cells called a staggered grid. The spatial discretization is achieved using the finite difference method where the P, U, and V locations are depicted in Figure 8.2. Capital letters are applied for numerical approximations of velocity components and pressure. As it can be seen in Figure 8.2, the pressure P locations are placed in the cell midpoints (center), the velocities U are located on the vertical cell interfaces (edges), and the velocities V are located on the horizontal cell interfaces (above and below the center).

The first derivative of velocity can be approximated by [16]:

$$(U_x)_{i+\frac{1}{2},j} \approx \frac{U_{i+1,j} - U_{i,j}}{\delta_x}, \tag{8.11}$$

which is a centered approximation of U_x in the middle of the cell between the two points. In the staggered grid, this position is the position of $P_{i,j}$. The approximation of the Laplace operator at an interior point i, j is as follows:

$$U_{xx} + U_{yy} \approx \frac{U_{i-1,j} - 2U_{i,j} + U_{i+1,j}}{\delta_x^2} + \frac{U_{i,j-1} - 2U_{i,j} + U_{i,j+1}}{\delta_y^2}, \qquad (8.12)$$

The same formula holds for the component V, and for the gradient of the pressure P [16].

$$(P_x)_{i+\frac{1}{2},j} \approx \frac{P_{i+1,j} - P_{i,j}}{\delta_x}, \qquad (8.13)$$

Substituting (8.11)-(8.13), the momentum equation (8.10) can be written as follows:

$$\frac{d}{dt}\begin{bmatrix} U \\ V \end{bmatrix} + \begin{bmatrix} G & 0 \\ 0 & \tilde{G} \end{bmatrix}\begin{bmatrix} U \\ V \end{bmatrix} + \begin{bmatrix} D \\ \tilde{D} \end{bmatrix} P = \begin{bmatrix} F_1 \\ F_2 \end{bmatrix}, \qquad (8.14)$$

where G and $\tilde{G}$ are the coefficient matrices of U and V, respectively. The influence of wind turbines in (8.14) is observed in the pressure drop P and the forces F_1 and F_2. Moreover, the wind turbine effect is considered to be in the far wake region, which means the next turbine is in the far wake of the previous one. The horizontal and vertical thrust force components F_1 and F_2 are given by:

$$F_1 = \frac{1}{2}\rho\pi R^2 U^2 C_T(\beta, \lambda),$$
$$F_2 = \frac{1}{2}\rho\pi R^2 V^2 C_T(\beta, \lambda), \qquad (8.15)$$

where C_T is the thrust coefficient. The thrust coefficient can be written based on P_{ref}, which is the control input of the farm controller, as given by:

$$C_{T_i} = \frac{P_{ref}^{WT_i}}{0.5\rho\pi R^2(1-a_i)\mathbf{u}_{d_i}^3} \approx K_u\mathbf{u}_d + K_u u_c, \qquad (8.16)$$

where K_u and K_u are linearization factors, $u_c = P_{ref}$, $\mathbf{u}_d$ is the wind velocity vector, ρ is the air density, R is the rotor diameter, and a_i is the axial induction factor of the ith turbine.

The solution of the dynamic wind flow model equations (8.14)-(8.16) provides the wind speed at each wind turbine (W_{op}) [14, 15]. Therefore, P_{op} and the matrices of the wind turbine model in (8.1) are obtained for each operating point. Thus, with wind speed variations the matrices of the wind turbine control model (8.1) change.
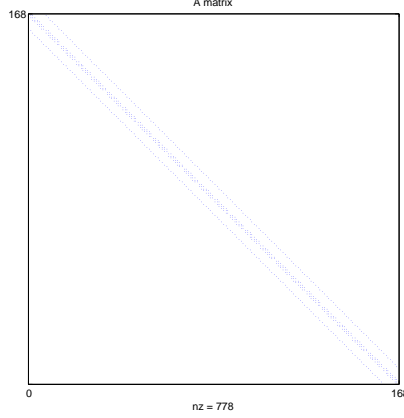
Figure 8.3: The structure of the system matrix for a 7×25 grid, where nz stands for the number of nonzero elements in the matrix.

Subsystems interaction

The wind flow interaction between turbines (subsystems) is computed using a linear mapping via a sparse matrix. We start with convection-diffusion equation for wind flow [16], and we carry on with the spatial discretization of the equation on a staggered grid over the wind farm. If we define the wind velocity $\mathbf{u}_d = (u_{d1}, ..., u_{dn})^T$, with n being the number of grid cells, where the velocity components in the xy plane are (U, V). It can be shown that the wind inflows to the individual turbines $u_d(n + 1)$ can be computed as [18]:

$$\mathbf{u}_d^{(n+1)} = A_w \mathbf{u}_d^n, \tag{8.17}$$

where $(\mathbf{u}_d)^n$ addresses the velocity in n^{th} cell, and A_w is a sparse matrix illustrated in Figure 8.3, for a 7×25 grid.

4 The Wind Farm Control Model

As noted, the wind farm is modeled as a spatially distributed system, with subsystems defined as wind turbines and the interconnections defined as wind flow and power reference distribution between them. It is assumed that the interconnections are governed by the same relationships, and has been considered as equation (8.17). Therefore, the whole wind farm consists of subsystems $\mathfrak{S}_s$, governed by the dynamic equations (8.1) and wind flow interactions governed by (8.17).

Inserting (8.1) in a single matrix structure together with (8.17) results in

$$\mathfrak{S}_s : \begin{bmatrix} \dot{x}_s \\ U^p_{s-1} \\ V^m_{s+1} \\ z_s \\ y_s \end{bmatrix} = \begin{bmatrix} A_s & B^p_s & B^m_s & B^1_s & B_2 \\ C^p_s & W^p_s & 0 & L^p_s & V^p_s \\ C^m_s & 0 & W^m_s & L^m_s & V^m_s \\ C^1_s & J^p_s & J^m_s & D^{11}_s & D^{12}_s \\ C^2_s & H^p_s & H^m_s & D^{21}_s & D^{22}_s \end{bmatrix} \begin{bmatrix} x_s \\ U^p_s \\ V^m_s \\ w_{d_s} \\ u_{c_s} \end{bmatrix}, \qquad (8.18)$$

where $x_s = [x_{wt_s}]^T$, w_{d_s} is disturbance (a small noise), and u_{c_s} is the power reference for each wind turbine.

The wind turbines are considered to be similar, but since at different operating points the matrices of the dynamic model change, the dynamic equations for each subsystem is different from the other one. The resulting system is a heterogeneous system.

To study the case with the maximum wake interaction between turbines, we assume the wind direction is parallel to the wind turbine row. Therefore, the right and left boundary conditions are varying. The left boundary condition is the free space wind speed, but the right is behind the wind farm, and we can neglect that (as the wind blows in one direction). Thus, the small left boundary and the interior are heterogeneous.

Resolving the interconnection variables in (8.18), using the method in [10], the interconnected system

$$\bar{\mathfrak{S}} : \begin{bmatrix} \dot{\bar{x}} \\ \bar{z} \\ \bar{y} \end{bmatrix} = \begin{bmatrix} \bar{A} & \bar{B}_1 & \bar{B}_2 \\ \bar{C}_1 & \bar{D}_{11} & \bar{D}_{12} \\ \bar{C}_2 & \bar{D}_{12} & \bar{D}_{22} \end{bmatrix} \begin{bmatrix} \bar{x} \\ \bar{w} \\ \bar{u}_c \end{bmatrix}, \qquad (8.19)$$

is obtained, where the $(\bar{\cdot})$ indicates "lifted" variable for vectors [19]; for example $\bar{x} = [x_1^T \, x_2^T \, \cdots \, x_N^T]^T$, and $x_s = [x_{wt_s}]^T$, $s = 1, ..., N$ with N the number of wind turbines. The interconnected system matrices $(\bar{A}, \bar{B}_1, \bar{B}_2, \bar{C}_1, \bar{D}_{11}, \bar{D}_{12}, \bar{C}_2, \bar{D}_{12}, \bar{D}_{22})$ have the sequentially semi-separable structure defined in Section 2. For instance, for a wind farm with 5 wind turbines ($N = 5$) equation (8.20) is obtained [10].

$$\begin{bmatrix} \dot{x}_1 \\ \dot{x}_2 \\ \dot{x}_3 \\ \dot{x}_4 \\ \dot{x}_5 \end{bmatrix} = \overbrace{\begin{bmatrix} A_1 & B^p_1 C^p_2 & B^p_1 W^p_2 c^p_3 & B^p_1 W^p_2 W^p_3 C^p_4 & B^p_1 W^p_2 W^p_3 W^p_4 C^p_5 \\ B^m_2 C^m_1 & A_2 & B^p_2 C^p_3 & B^p_2 W^p_3 C^p_4 & B^p_2 W^p_3 W^p_4 C^p_5 \\ B^m_3 W^m_2 C^m_1 & B^m_3 C^m_2 & A_3 & B^p_3 C^p_4 & B^p_3 W^p_4 C^p_5 \\ B^m_4 W^m_3 W^m_2 C^m_1 & B^m_4 W^m_3 C^m_2 & B^m_4 C^m_3 & A_4 & B^p_4 C^p_5 \\ B^m_5 W^m_4 W^m_3 W^m_2 C^m_1 & B^m_5 W^m_4 W^m_3 C^m_2 & B^m_5 W^m_4 C^m_3 & B^m_5 C^m_4 & A_5 \end{bmatrix}}^{\bar{A}} \overbrace{\begin{bmatrix} x_1 \\ x_2 \\ x_3 \\ x_4 \\ x_5 \end{bmatrix}}^{\bar{x}}$$
$$+ \bar{B}_1 \bar{w} + \bar{B}_2 \bar{u}_c. \qquad (8.20)$$

In (8.20), $\bar{A}$ is denoted as

$$\bar{A} = \mathcal{SSS}(B^m_s, W^m_s, C^m_s, A_s, B^p_s, W^p_S, C^p_s), \qquad (8.21)$$

in which the arguments of the function $\mathcal{SSS}(\cdot)$ are called "generator matrices" of $\bar{A}$. All the other matrices in (8.20) are also in $\mathcal{SSS}$ structure, and structure preserving iterations will be used to compute a H_2 controller [10]. That will therefore have the same $\mathcal{SSS}$ structure. The configuration of the system and the controller, which consists of N sub-controllers, can be seen in Figure 8.4.
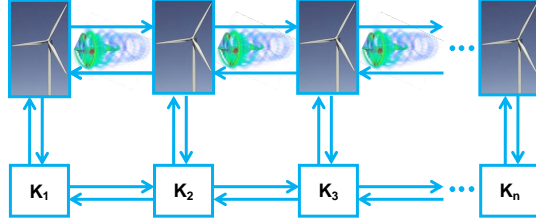

Figure 8.4: Distributed controllers K_s

The block diagram of the distributed wind farm system has been illustrated in Figure 8.5, which shows not only the closed loop connections of subsystems and the individual controllers but also the interactions between them. Whereas Figure 8.4 represents the physical implementation of turbines in a wind farm and their respective distributed controllers K, Figure 8.5 places the mathematical equations (8.26) and the distributed controllers to be designed in Section 5 in context. Note that Figure 8.5 is rotated 90 deg clockwise from 8.4.

The control problem is to minimize the norm of Z_s with $s = 1, ..., N$, and provide the demanded power by the operator, $\sum_{i=1}^{n} \bar{u}_{c_i} = P_{dem}$. This control problem statement is equivalent to:

$$\bar{u}_{c_n} = P_{dem} - \sum_{i=1}^{n-1} \bar{u}_{c_i}. \tag{8.22}$$
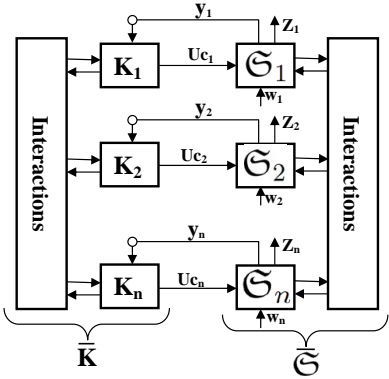
Substituting (8.22) in (8.19), we obtain:

$$\bar{B}_2 \bar{u}_c = \bar{B}_2 \begin{bmatrix} 1 & 0 & \cdots & 0 \\ 0 & 1 & \cdots & 0 \\ \vdots & \vdots & \vdots & \vdots \\ -1 & -1 & \cdots & -1 \end{bmatrix} \begin{bmatrix} \bar{u}_{c_1} \\ \bar{u}_{c_2} \\ \vdots \\ \bar{u}_{c_{n-1}} \end{bmatrix} + \bar{B}_2 \begin{bmatrix} 0 \\ 0 \\ \vdots \\ P_{dem} \end{bmatrix} \tag{8.23}$$

$$= \tilde{B}_2 \, \tilde{u}_c + \tilde{B}_{P_{dem}}, \tag{8.24}$$

where $\tilde{u}_c = [\bar{u}_{c_1}, \cdots, \bar{u}_{c_{n-1}}]^T$. In a similar way $\bar{D}_{12}\bar{u}_c$ and $\bar{D}_{22}\bar{u}_c$ are restructured to produce constant terms $\tilde{D}_{P_{dem}}^{12}$ and $\tilde{D}_{P_{dem}}^{22}$. Next step is to perform a change of coordinates, to remove the constants as in

$$x = \tilde{x} - \bar{A}^{-1}\tilde{B}_{P_{dem}} \tag{8.25}$$

Therefore, (8.19) is rewritten as

Figure 8.5: The block diagram of the subsystems, the individual controllers, and the interactions between them.

$$\bar{\mathfrak{S}} : \quad \begin{bmatrix} \dot{\tilde{x}} \\ \tilde{z} \\ \tilde{y} \end{bmatrix} = \begin{bmatrix} \bar{A} & \bar{B}_1 & \tilde{B}_2 \\ \bar{C}_1 & \bar{D}_{11} & \tilde{D}_{12} \\ \bar{C}_2 & \bar{D}_{12} & \tilde{D}_{22} \end{bmatrix} \begin{bmatrix} \bar{x} \\ \bar{w} \\ \tilde{u}_c \end{bmatrix}, \tag{8.26}$$

where $\tilde{z} = \bar{z} - (\tilde{D}^{12}_{P_{dem}} - \bar{C}_1 \bar{A}^{-1} \tilde{B}_{P_{dem}})$ and $\tilde{y} = \bar{y} - (\tilde{D}^{22}_{P_{dem}} - \bar{C}_2 \bar{A}^{-1} \tilde{B}_{P_{dem}})$, with $\bar{y}$ and $\bar{z}$ defined in (8.19).

The measured output of the wind farm system is the vector of power outputs $y = p = [p_1, p_2, ..., p_N]^T$, with N being the number of wind turbines. The linear approximation of the power is given by

$$p_i \approx K_{P_1} \beta_i + K_{P_2} \omega_{r_i} + K_{P_3} V_i \tag{8.27}$$
$$= [K_{P_1}, K_{P_2}, 0]^T x_i + K_{P_3} V_i, \tag{8.28}$$

where K_{P_i} are linearization factors of p_i around mean values of wind speed, rotor speed and pitch angle. Therefore, all measurements y are related to mean wind speeds V (since the wind blows in one direction the velocity component V is dominant) and the wind disturbance w; in other words, $\bar{D}_{12}$ in (8.26) has the full row rank.

The force and moment output vector $z = [F_T, \ M_{sh}]^T = [[F_{t_1}, ..., F_{t_N}]^T, [M_{sh_1}, ..., M_{sh_N}]^T]^T$. F_{t_i} is obtained from combination of (8.15) and (8.16). So,

$$F_{t_i} \approx \frac{1}{2} \rho \pi R^2 \mathbf{u}_d^2 (K_f P_{ref} + K_\mathbf{u} \mathbf{u}_d), \tag{8.29}$$

where K_f and $K_\mathbf{u}$ are linearization factors of C_{T_i} around mean values of wind speed and power reference. M_{sh_i} is obtained as follows [13]:

$$M_{sh_i} = K^1_{J_r, J_g} T_g + K^2_{J_r, J_g} T_r, \tag{8.30}$$

with

$$T_g = \frac{P_{ref}}{\omega_g \mu}, \tag{8.31}$$

$$T_r = \frac{1}{2} \rho \pi R^3 \mathbf{u}_d^2 C_Q, \tag{8.32}$$

where T_g and T_r are generator and rotor torque, ω_g is the generator velocity, μ is the generator efficiency and C_Q is the torque coefficient. Therefore, each element of z is related to each element of input vector P_{ref}; in other words $\bar{D}_{21}$ has the full column rank.

Equations (8.26)-(8.32) provide the foundation upon distributed optimization wind farm controller is to be developed.

5 Distributed Control Using H_2 Synthesis

The controller is obtained via H_2 synthesis. The objective is to minimize a norm of the map from w_i to z_i in Figure 8.5. The following Riccati equations should be solved to pursue the optimal H_2 synthesis. The solution to the Riccati equation is obtained using the matrix sign iteration method, as in [10].

$$A^T P_l + P_l^1 A - (P_l B_2 + S) R_l^{-1} (B_2^T P_l + S_l^T) + Q_l = 0 \tag{8.33}$$
$$A P_f + P_f A^T - (P_f C_2 + S) R_f^{-1} (C_2 P_f + S_f^T) + Q_f = 0, \tag{8.34}$$

where,

$$Q_l = C_1^T C_1, \quad R_l = D_{12}^T D_{12}, \quad S_l = C_1^T D_{12} \tag{8.35}$$
$$Q_f = B_1 B_1^T, \quad R_f = D_{21} D_{21}^T, \quad S_f = B_1 D_{21}^T, \tag{8.36}$$

and the gain matrix for the two equations (8.33) and (8.34) is respectively as follows:

$$L = R_l^{-1} (B_2^T P_l + S_l^T) \tag{8.37}$$
$$F = R_f^{-1} (C_2 P_f + S_f^T). \tag{8.38}$$

The Hamiltonian matrices associated with the Riccati equations are

$$H_1 = \begin{bmatrix} A & R_l \\ -Q_l & -A^T \end{bmatrix}, \ H_2 = \begin{bmatrix} A^T & R_f \\ -Q_f & -A \end{bmatrix} \tag{8.39}$$

The relationship between H_1 and H_2 can be seen in the following similarity transformation of H, which uses $\hat{P}_l$, the solution to the Riccati equation [20].

$$H_x = \begin{bmatrix} I & 0 \\ -\hat{P}_l & I \end{bmatrix} \begin{bmatrix} A & R_l \\ -Q_l & -A^T \end{bmatrix} \begin{bmatrix} I & 0 \\ -\hat{P}_l & I \end{bmatrix} = \begin{bmatrix} A + R_l \hat{P}_l & R_l \\ 0 & -A^T - \hat{P}_l R_l \end{bmatrix}, \tag{8.40}$$

and similarly

$$H_y = \begin{bmatrix} A^T + R_f \hat{P}_f & R_f \\ 0 & -A - \hat{P}_f R_f \end{bmatrix}. \tag{8.41}$$

Then, the optimal stabilizing controller $\bar{K}$ of the H_2 synthesis problem is given by (Theorem 6.9 of [20]):

$$K = \begin{bmatrix} A_k & B_k \\ C_k & D_k \end{bmatrix}, \tag{8.42}$$

with $A_k = A - FC_2 - B_2L + FD_{22}L$, $B_k = F$, $C_k = -L$, and $D_k = 0$.

Finally, the controller input u_c to each wind turbine subsystem is given by

$$
\begin{aligned}
\dot{x}_k(t) &= A_k x_k(t) + B_k \tilde{y}, \\
u_c(t) &= C_k x_k(t) + D_k \tilde{y},
\end{aligned} \tag{8.43}
$$

with $\tilde{y}$, the system output, typically calculated from (8.26).

The distributed controller is designed, such that the closed-loop system is internally stable and the performance criterion $\|z\|_2^2$ is minimized. To this aim, the state variables (pitch angle, rotor speed and generator speed of the wind turbines) and the control input (power reference vector) should satisfy their constraints. To satisfy both state and input constraints, the control gain (8.37) is tuned by a scalar γ, which is introduced by $D_{12} = \gamma D_{12}$. The smaller the value for γ is chosen, the smaller the control gain L will be. More details about control design trade-offs and gain selection are given in Appendix B.

As noted, (8.26) is a linear approximation of the actual system, thus, the control input calculation has been repeated using actual y. Since it is defined to be the measured power, we have used the power equation

$$y = \frac{1}{2}\rho\pi R^2 \mathbf{u}_d^3 C_p, \tag{8.44}$$

in the simulation tests to compare the linearized with this simple nonlinear turbine model. The control input vector u_c using linear approximated $\tilde{y}$ and the the actual y is compared in Figure 8.6 for two sample wind speeds (The mean wind speed at each turbine obtained for 5 minute wind speed inputs, using the wind flow model [14]).

Furthermore, the uncertainty in calculating power reference vectors using the linearized output $\tilde{y}$ compared to the nonlinear output y can be seen in the standard deviations, which for each set are respectively:

$$
\begin{aligned}
\sigma_1(u_c, u_{c_{nl}}) &= [0.0467, 0.2196, 0.3059, 0.1756, 0.1452], \\
\sigma_2(u_c, u_{c_{nl}}) &= [0.4859, 0.0921, 0.1415, 0.1354, 0.1179].
\end{aligned} \tag{8.45}
$$

where u_c is the control input vector by the linear model, $u_{c_{nl}}$ the control input from the nonlinear model y. The smaller the standard deviation, the smaller the uncertainty.
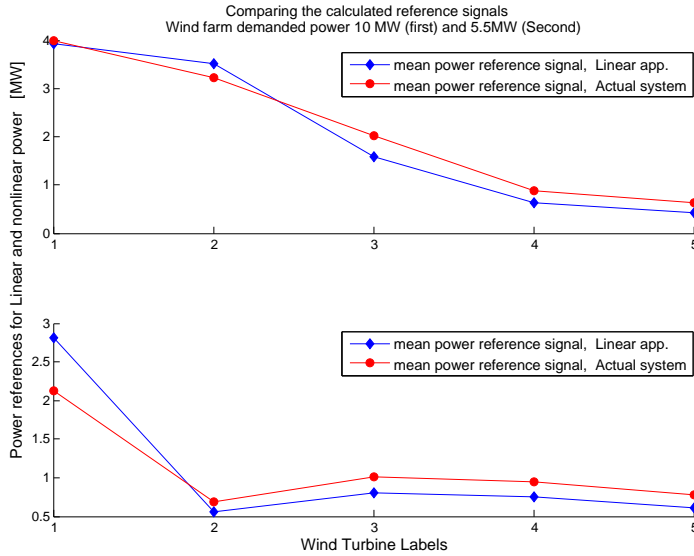
Figure 8.6: Comparison of 5 minute average power references calculated from linear and nonlinear model. The wind farm power demand for each case has been 10 and 5.5 MW.
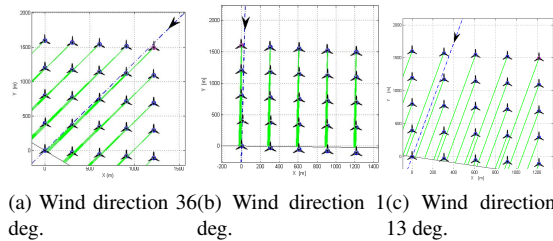

(a) Wind direction 36 deg.

(b) Wind direction 1 deg.

(c) Wind direction 13 deg.

Figure 8.7: Three wind directions, which two of them produce the maximum wake interaction

6   Results and Discussion

The distributed control problem is formulated for a small wind farm with 5 wind turbines in a row; and as mentioned before, with a wind direction parallel to the row of wind turbines. The reason that this fully aligned case is considered the most important is illustrated in Figure 7.3, which shows a wind farm with 25 wind turbines, where the directions of the propagating wakes are depicted with green lines. As it can be seen in Figure 7.3, the maximum wake interaction for a row of wind turbines happens when the wind direction is parallel to a row of wind turbines.

For the simulation results given in this section, we have used the $\mathcal{SSS}$ Matrix Toolbox for Matlab [21], and the control input u, which is the vector of the power references has

been determined using equations (8.43). Then, the power reference signal for each turbine is computed over the 10-minute time-varying wind speed input simulation. The control input vector has been obtained for four different scenarios. In each scenario, the available power at each wind turbine is computed, given the wind farm dynamic model.

In these scenarios, the wind farm power demand is chosen to be much less than the available power. In the absence of a distributed wind farm controller, if the demanded power is much less than the produced power and in the absence of storage, many of the turbines would likely be shut down. The solution described in this paper improves on the shut-down default by finding a proper distribution of power references between wind turbines such that the demanded power is provided and the structural loads on the individual turbines are minimized.

In the first scenario, the total available power of the wind farm is about 20.5 MW, but the demanded power is 15 MW. The power reference distribution among wind turbines is illustrated in Figure 8.9. In this case the free space wind speed is about 14 m/s, and the nominal wind speed for all the turbines is about 11.3 m/s. The mean wind speed at each wind turbine, which is calculated from the wind farm dynamical model presented briefly in Section 3, is also shown in Figure 8.9 . The validation of the wind farm dynamical model against measurement data and also a commercial software in low and high wind speed is illustrated in Figure 8.8. More validation results for this model are presented in [14].

The structural loads (8.5) to be minimized are the shaft moment M_{shaft} and the thrust force F_t that results in the fore-aft fluctuations of the turbine. The mean values of these loads in this scenario are presented in Figure 8.10.

The second scenario has the same wind conditions as the previous one (available power: 20.5 MW), but the demanded power is only 9.5 MW. The calculated mean wind speed and the power reference distribution solution are presented in Figure 8.11. Moreover, the effect of the power reference determination on the structural loads is illustrated in Figure 8.12.

In the third scenario, the mean wind speed all over the farm is below rated wind speed. Moreover, the wind farm demanded power is 5.5 MW while the total available power in the farm is about 8.5 MW. The power reference distribution among wind turbines along with the calculated speeds at each individual turbine are illustrated in Figure 8.13. In addition, the structural loads on the individual wind turbines given the distributed farm controller is compared in Figure 8.14 to a case without a wind farm controller. Again, structural loads are reduced compared to the no distributed control case.

In the last scenario the demanded power from the wind farm is fixed around 10MW, while the wind speed is changing from 8 m/s to around 18 m/s. When the free space wind speed is around 8 m/s the available power of the farm is less than demanded power. Therefore, in this case the wind farm produces the maximum possible power, though the demanded power can not be satisfied. The mean wind speed at the place of each wind turbine and also the power reference signals corresponding to this wind speed, are depicted with the green graphs in Figure 8.15. However, in all the other wind speeds, the demanded power is satisfied. In very high wind speed, for instance the pink graph in Figure 8.15 which the wind farm has 25 MW power available, the wind farm control solution helps to provide the demanded power (10 MW) without turning off any wind turbine in the farm.
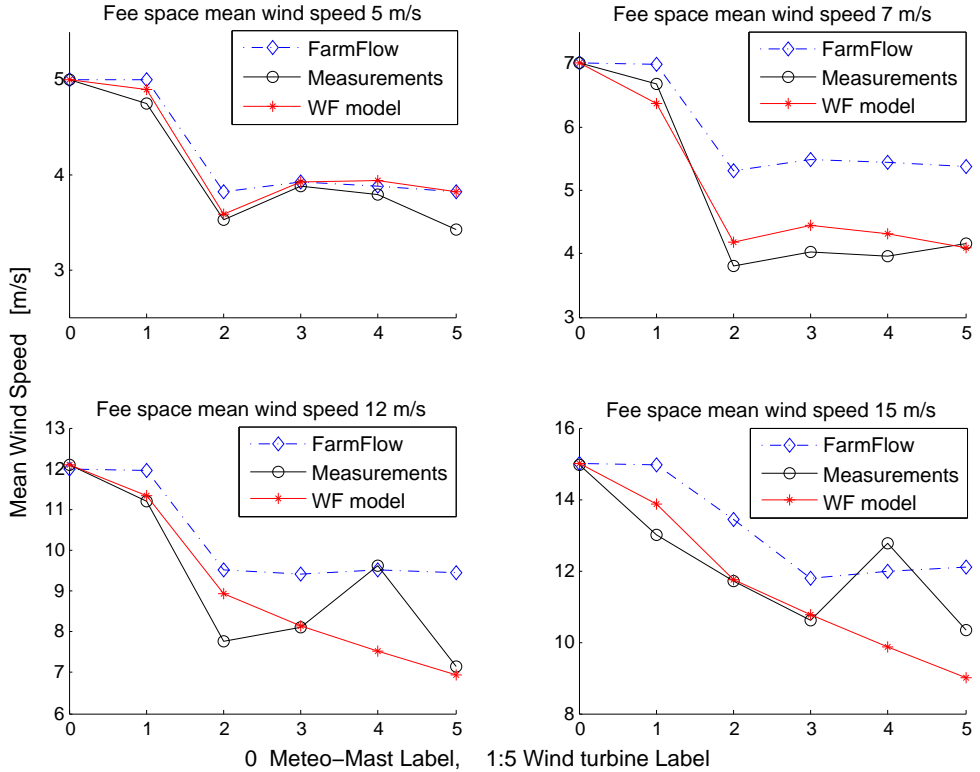
Figure 8.8: Validation of the dynamic wind farm model that calculates the operating points to linearize wind turbine model. The model validated against measurement data from ECNs Wind turbine Test site Wieringermeer (EWTW), and also compared with FARMFLOW software calculations [22].

7   Conclusions

A distributed wind farm controller has been developed in this work using a structured matrix approach. Wind turbines are considered as subsystems and the wind flow and power references as the interactions between them. The controller dynamic (8.43) has been obtained for each subsystem such that the structural load on each turbine is minimized. The control input to each turbine is its individualized power reference signal.

Solving the optimal control problem with constraints on state and input is a bottleneck of this paper. The control method commences with solving the algebraic Riccati equations (ARE) without constraints, and we include them later using the approach explained in Appendix B. Whereas, the constraints on state and control input should be included in the problem formulation in the first place.

Another drawback of this paper is approximating the wind turbine system with a very simple linear model. The uncertainties in the control signals obtained from the linear model are presented in Section 5, and it can be improved by using a more accurate
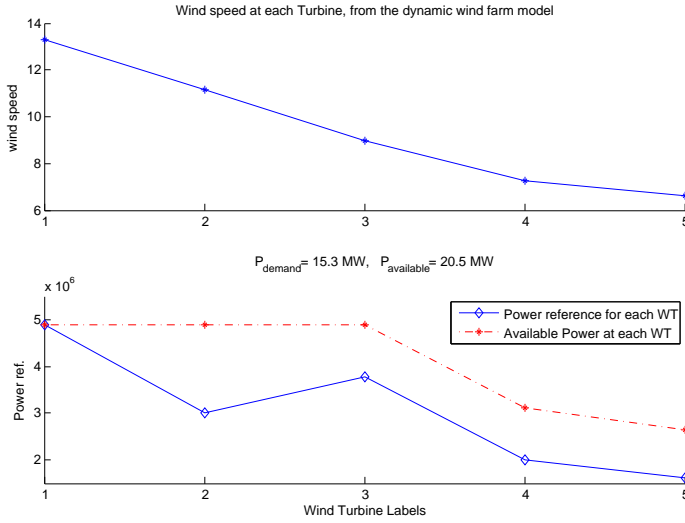
Figure 8.9: Mean wind speed at each wind turbine and the distributed wind farm control solution, which is the mean power reference vector. (wind farm available power 20.5 MW, wind farm demanded power 15 MW)
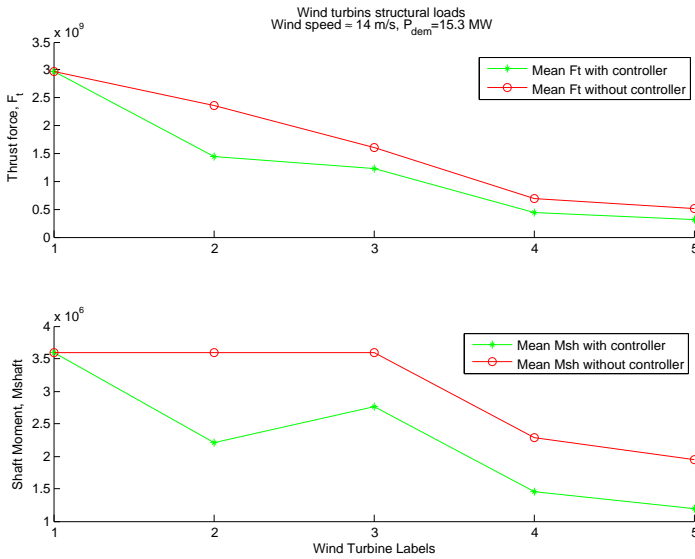

Figure 8.10: Comparing F_t and M_{shaft} with and without controller (mean wind speed as Figure 8.9, wind farm available power 20.5 MW, wind farm demanded power 15 MW)
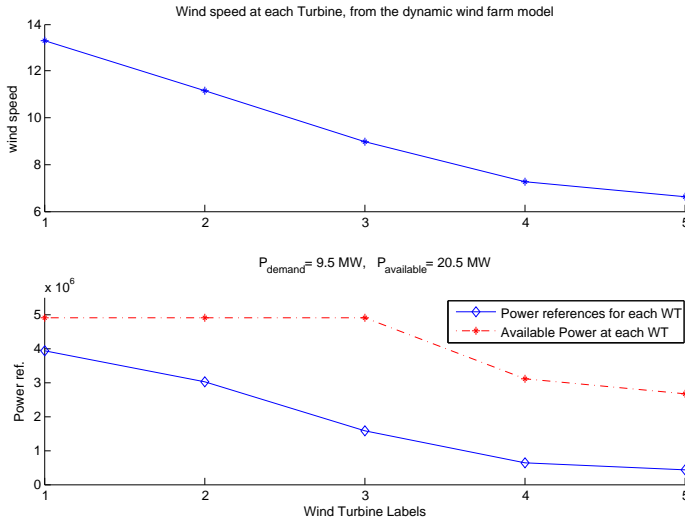
Figure 8.11: Mean wind speed at each wind turbine; and the mean power reference vector. (wind farm available power 20.5 MW, wind farm demanded power 9.5 MW)
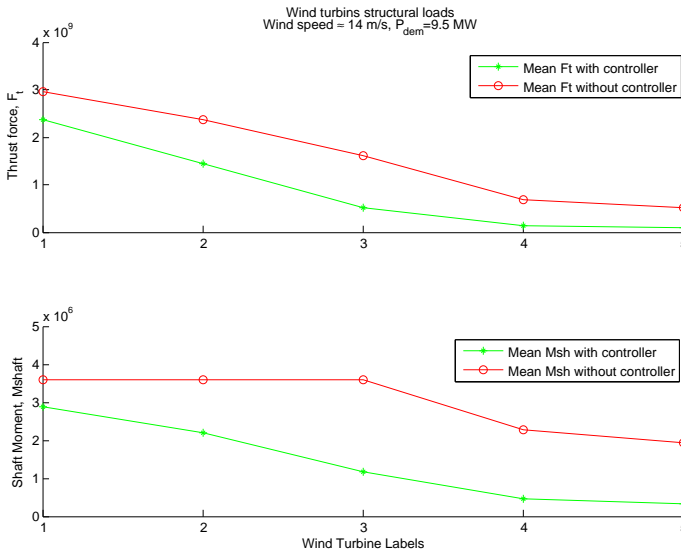

Figure 8.12: Comparing F_t and M_{shaft} with and without controller (mean wind speed as Figure 8.11, wind farm available power 20.5 MW, wind farm demanded power 9.5 MW)
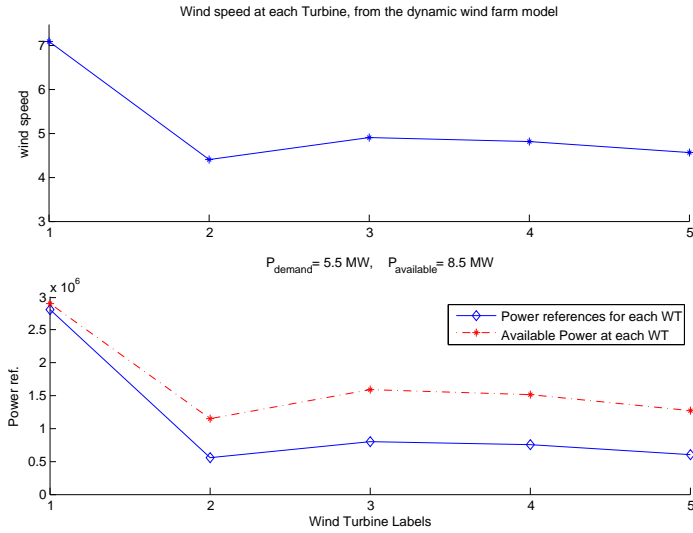
Figure 8.13: Mean wind speed at each wind turbine; and the mean power reference vector. (wind farm available power 8.5 MW, wind farm demanded power 5.5 MW)
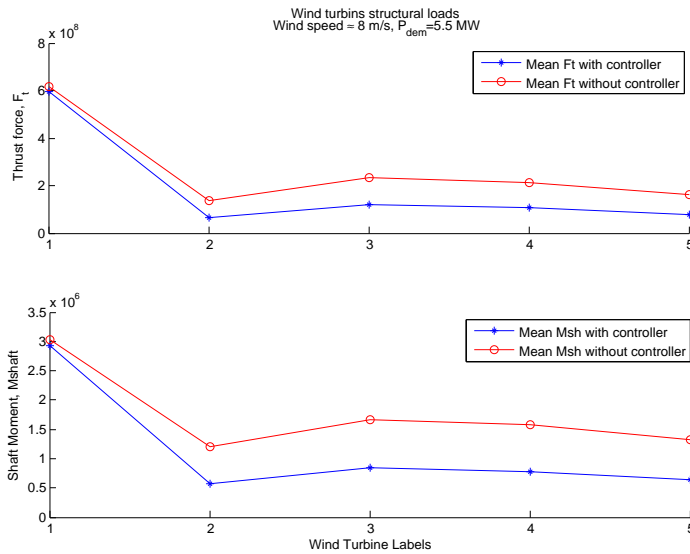

Figure 8.14: Comparing F_t and M_{shaft} with and without controller (mean wind speed as Figure 8.13, wind farm available power 8.5 MW, wind farm demanded power 5.5 MW)
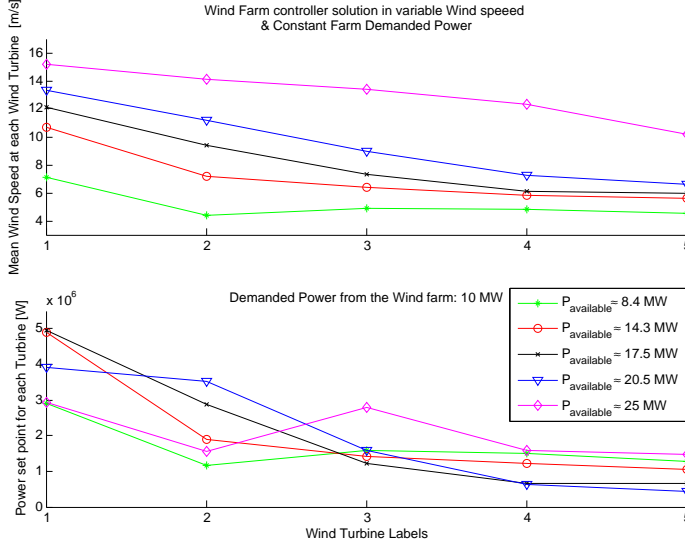
Figure 8.15: Wind farm controller solution in variable wind speed and fixed wind farm demanded power

approximation of the nonlinear system. The nonlinear measured output will be a feedback to the controller, while in this work the only nonlinear feedback to the controller is the wind speed (from the dynamic wind flow model), and the controller gets all the feedbacks from the linear control model.

Appendix A

Linear wind turbine model

The wind turbine system matrices from eq 8.1 are presented in this part. The wind turbine system matrices, for NREL wind turbine in a sample operating point ($W_{op} = 19.6$, $P_{op} = 4.16$ MW), are as follows:

$$A = \begin{bmatrix} 0 & 48.44 & -0.363 \\ -0.026 & -0.278 & 0 \\ 0 & 1.52e+02 & -1.57 \end{bmatrix}, \; B = \begin{bmatrix} 0 \\ -2.07e-08 \\ 0 \end{bmatrix}, \; B_u = \begin{bmatrix} 0 \\ 0.031 \\ 0 \end{bmatrix},$$

$$C = \begin{bmatrix} -7.2e+04 & -7.4e+05 & 0 \\ -1.3e+05 & -1.7e+06 & 0 \end{bmatrix}, \; D = \begin{bmatrix} 0 \\ 0.008 \end{bmatrix}, \; D_u = \begin{bmatrix} 7.6e+04 \\ 1.6e+05 \end{bmatrix},$$

Appendix B

To address both the state and the input constraints, we let $D_{12} = D_{12}\,\gamma = \gamma\,D_{12}$.

Assuming that all the admissible solutions belong to a set $\mathfrak{R}$, we define the following sub level set:

$$\left\{ X \mid X^T P X \leq \alpha \right\} \subseteq \mathfrak{R}, \tag{8.46}$$

where X and P are defined as follows:

$$X = \begin{bmatrix} \hat{x} \\ e \end{bmatrix}, \quad P = \begin{bmatrix} P_l & 0 \\ 0 & P_f \end{bmatrix}, \tag{8.47}$$

in which, $\hat{x}$ is the estimated state and e is the estimation error.

Let X_0 be the initial state, i.e., $(\hat{x}_0, e_0) = (\hat{x}_0(0), e_0(0))$, then

$$X_0^T P X_0 = \alpha, \tag{8.48}$$

it can be shown that for a positive definite matrix P,

$$\overline{\lambda}(P) \, \|X_0\| \geq \alpha, \tag{8.49}$$

where, $\overline{\lambda}(P)$ is the maximum eigen-value of P. Therefore, an admissible value for X_0 is $\alpha / \overline{\lambda}(P)$, which is defined as:

$$\frac{\alpha}{\overline{\lambda}(P)} = \mathfrak{M}. \tag{8.50}$$

Since the differential of $v : X \mapsto X^T P X$ in the direction of the vector field of the closed loop system is negative definite, the norm of solution:

$$\|X(t)\| \leq \mathfrak{M} \text{ for all } t \geq 0. \tag{8.51}$$

On the other hand, if the Matrix D_{12} is tuned with a scalar γ, then $R_l = D_{12}^T D_{12}$ will become:

$$R_l = D_{12}^T D_{12} = \gamma^2 D_{12}^T D_{12}, \tag{8.52}$$

and from (8.37),

$$L = \frac{1}{\gamma^2} \, L. \tag{8.53}$$

Thus, it can be shown that the maximum value for u_c, based on (8.50) and (8.53), is as follows:

$$u_{c_{max}} \leq \gamma \|L\| \mathfrak{M}, \tag{8.54}$$

which the proper value for γ is to be determined to bring the control input inside the constrains.

References

[1] B. M. Adams, "Dynam loads in wind farms ii," Garrad Hassan and Partners Ltd, Tech. Rep. 286/R/1, 1996.

[2] M. Steinbuch, W. de Boer, O. Bosgra, S. Peters, and J. Ploeg, "Optimal control of wind power plants," *Journal of Wind Engineering and Industrial Aerodynamics*, vol. 27, no. 1-3, pp. 237 – 246, 1988.

[3] M. Zhao, Z. Chen, and F. Blaabjerg, "Probabilistic capacity of a grid connected wind farm based on optimization method," *Renewable Energy*, vol. 31, no. 13, pp. 2171 – 2187, 2006.

[4] R. Fernandez, P. Battaiotto, and R. Mantz, "Wind farm non-linear control for damping electromechanical oscillations of power systems," *Renewable Energy*, vol. 33, no. 10, pp. 2258 – 2265, 2008.

[5] J. Rodriguez-Amenedo, S. Arnaltes, and M. Rodriguez, "Operation and coordinated control of fixed and variable speed wind farms," *Renewable Energy*, vol. 33, no. 3, pp. 406 – 414, 2008.

[6] A. Hansen, P. Sørensen, F. Iov, and F. Blaabjerg, "Centralised power control of wind farm with doubly fed induction generators," *Renewable Energy*, vol. 31, no. 7, pp. 935–951, 2006.

[7] M. Soleimanzadeh and R. Wisniewski, "Controller design for a wind farm, considering both power and load aspects," *Mechatronics*, vol. 21, no. 4, pp. 720 – 727, 2011.

[8] M. Mauledoux and V. Shkodyrev, "Distributed multi-objective optimal control for wind farms," in *PHYSCON (Catania, Italy)*, 2009.

[9] D. Madjidian, K. Mårtensson, and A. Rantzer, "A distributed power coordination scheme for fatigue load reduction in wind farms," in *American control conference*, 2011.

[10] J. Rice and M. Verhaegen, "Distributed control: A sequentially semi-separable approach for spatially heterogeneous linear systems," *IEEE Transaction on Automatic Control*, vol. 54, pp. 1270–1283, 2009.

[11] A. Antoulas, *Approximation of large scale dynamical systems*, R. Smith, Ed. SIAM, 2004.

[12] J. Jonkman, S. Butterfield, W. Musial, and G. Scott, "Definition of a 5-mw reference wind turbine for offshore system development," Golden, CO: National Renewable Energy Laboratory, Tech. Rep. NREL/TP-500-38060, 2009.

[13] V. Spudic, M. Jelavic, M. Baotic, and M. Peric, "Hierarchical wind farm control for power/load optimization," in *The Science of making Torque from Wind (Torque2010)*, 2010.

[14] M. Soleimanzadeh, R. Wisniewski, and A. J. Brand, "State-space representation of the flow model for a wind farm," *Wind Energy*, vol. (2nd revision submitted), pp. –, 2012.

[15] M. Soleimanzadeh and R. Wisniewski, "Wind deficit model in a wind farm using finite volume method," in *Proceedings of American Control Conference (ACC)*, 2010.

[16] G. Strang, *Computational science and engineering*. Wellesley, MA: Wellesley-Cambridge Press, 2007.

[17] W. Kress and J. Nilsson, "Boundary conditions and estimates for the linearized navier-stokes equations on staggered grids," *Computers & Fluids*, vol. 32, no. 8, pp. 1093–1112, 2003.

[18] K. A. Hoffmann and S. Chiang, *Computational fluid dynamics*, ., Ed. Austin, TX: Engineering Education System, 1989.

[19] R. Tousain, E. Van der Meché, and O. Bosgra, "Design strategies for iterative learning control based on optimal control," *Selected Topics in Signals, Systems and Control*, vol. 12, p. 8, 2001.

[20] G. Dullerud and F. Paganini, *A course in robust control theory: a convex approach*, ser. Texts in Applied Mathematics. Springer Verlag, 2000, vol. 36.

[21] I. Houtzager and M. Verhaegen, *Sequentially Semi-Separable Matrix Toolbox Version 0.8*, Delft University, 2011. [Online]. Available: http://www.dcsc.tudelft.nl/~datadriven/sss/

[22] P. Eecen and E. Bot, "Improvements to the ecn wind farm optimisation software "farmflow"," in *Presented at the European Wind Energy Conference & Exhibition, Warsaw, Poland*, 20 - 23 April 2010.